INVESTIGATION OF BALLISTIC PERFORMANCE OF CERAMIC ARMORS WITH TESTS AND ANALYSIS WHICH CONTAINS MULTILAYER CERAMIC TILES

ÇOK KATMANLI SERAMİK KARO İÇEREN SERAMİK ZIRHLARIN BALİSTİK PERFORMANSLARININ TEST VE ANALİZLERLE İNCELENMESİ

METEHAN CURA

ASSOC. PROF. DR. BARIŞ SABUNCUOĞLU

Supervisor

ASSIST. PROF. DR. HAMED TANABİ

Co-Supervisor

Submitted to

Graduate School of Science and Engineering of Hacettepe University

as a Partial Fulfillment to the Requirements

for the Award of the Degree of Master of Science

in Mechanical Engineering

2023

to my lovely wife

ABSTRACT

INVESTIGATION OF BALLISTIC PERFORMANCE OF CERAMIC ARMORS WITH TESTS AND ANALYSIS WHICH CONTAINS MULTILAYER CERAMIC TILES

Metehan CURA

Master's Thesis, Department of Mechanical Engineering

Supervisor: Assoc. Prof. Dr. Barış SABUNCUOĞLU

Co-Supervisor: Assist. Prof. Dr. Hamed TANABİ

January 2023, 112 pages

Ceramic armors have been developed to provide high ballistic protection with low density. Ceramic armors consist of three basic components, these are: the ceramic tile, the ductile backing plate, and the adhesive to bond the two together. Ceramic tile has high hardness and high compressive strength and is located in the front of the armor. As the armor piercing bullet tries to penetrate the ceramic tile, the nose of the bullet erodes and becomes blunt due to the high mechanical properties of the ceramic. The blunt and slowed down somewhat bullet core is stopped by the ductile backing plate. During the impact load, the ceramic tile is experienced different type loads. Due to local bending, the strike face of the ceramic tile experiences compressive stress, while the rear face experiences tensile stress. Ceramic tile needs high hardness and compressive strength on the strike face to increase erosion on the bullet. At the same time, it needs high toughness on the rear side to prevent the ceramic tile from breaking easily. However, these two properties

are in conflict with each other and are not usually found at a high level in a material at the same time. In this study, ceramic structures were created by bonding two different ceramics, which one is harder at the strike face and tougher at the rear face, and whether the mentioned requirements would be met or not was investigated by ballistic tests. However, before this examination, a two-layer ceramic structure made of the same material and a monolithic ceramic were compared with ballistic tests in order to examine the effect of the layered ceramic structure. There are conflicting studies in the literature about the effect of layered ceramic structure. In this part of the study, a contribution has been made to the literature about the effect of the layered ceramic structure. In this study, ballistic tests were performed with the Depth of Penetration Method using 7.62 × 51 Armor Piercing bullets. The tested configurations were evaluated using the Ballistic Efficiency formula. In the last part of the study, Finite Element Analysis of ballistic tests were conducted, and the behavior of ceramic structures were examined.

As a result of the study, it was observed that monolithic ceramics provide higher ballistic protection than layered ceramic structures made of the same material. When the layered ceramic structure made of the same material is compared with the layered ceramic structure with harder ceramic placed on the strike face, it has been observed by ballistic tests that harder ceramic increases the ballistic performance. In the Finite Element Analysis, similar behaviors and similar results were observed with ballistic test for both investigations.

Keywords: Ceramic, Layered Ceramics, Depth of Penetration Method, Hydrocode, Ballistic

ÖZET

ÇOK KATMANLI SERAMİK KARO İÇEREN SERAMİK ZIRHLARIN BALİSTİK PERFORMANSLARININ TEST VE ANALİZLERLE İNCELENMESİ

Metehan CURA

Yüksek Lisans, Makina Mühendisliği Bölümü

Tez Danışmanı: Doç. Dr. Barış SABUNCUOĞLU

Yrd. Danışman: Öğr. Üyesi Hamed TANABİ

Ocak 2023, 112 sayfa

Seramik zırhlar düşük öz kütle ile yüksek balistik koruma sağlamak için geliştirilmiştir. Bu zırhlar üç temel bileşenden oluşmaktadır. Bunlar: seramik karo, sünek arka plaka ve bu ikisini birbirine tutturacak yapıştırıcı. Seramik karo yüksek sertliğe ve yüksek basma dayanımına sahiptir ve zırhın ön kısmında yer alır. Zırh delici mermi seramik karoyu delmeye çalışırken, seramiğin yüksek mekanik özelliklerinden dolayı merminin burnu aşınır ve körelir. Körelen ve bir miktar yavaşlayan mermi çekirdeği sünek arka plaka ile durdurulur. Çarpma yükü sırasında seramik karo farklı tip yüklere maruz kalır. Kısmi bükülmeden dolayı seramik karonun ön yüzü basınç gerilmesi hissederken, arka yüzü ise çekme gerilmesi hisseder. Seramik karo mermideki aşınmayı arttırmak için ön yüzünde yüksek sertlik ve basınç dayanımına ihtiyaç duyar. Aynı zamanda seramik karonun kolay kırılmasını önlemek için ise arka yüzünde yüksek tokluğa ihtiyaç duyar. Ancak bu iki özellik birbirleriyle çelişen özelliklerdir ve genelde aynı anda bir malzemede yüksek

seviyede bulunmazlar. Bu çalışmada, önde daha sert, arkada daha tok olan iki farklı seramiğin birbirine yapıştırılmasıyla seramik yapılar oluşturulmuştur ve bahsedilen gereksinimlerin karşılanıp karşılanmayacağı balistik testler ile incelenmiştir. Ancak bu incelemeden önce katmanlı seramik yapının etkisini incelemek için aynı malzemeden oluşan iki katmanlı bir seramik yapı ile tekil bir seramik yapı balistik testler ile karşılaştırılmıştır. Katmanlı seramik yapının etkisi hakkında literatürde birbiri ile çelişen çalışmalar bulunmaktadır. Çalışmanın bu kısmında katmanlı seramik yapının etkisi hakkında literatüre katkı sağlanmıştır. Bu çalışmada 7.62 × 51 Zırh Delici mermi kullanılarak Delme Derinliği Yöntemi ile balistik testler yapılmıştır. Test edilen seçenekler ise Balistik Verim formülü ile değerlendirilmiştir. Çalışmanın son kısmında balistik testlerin Sonlu Elemanlar Analizi yapılmış ve seramik yapıların davranışları incelenmiştir.

Çalışmanın sonucunda tekil seramiklerin, aynı malzemeden oluşturulan katmanlı seramik yapılara göre daha yüksek balistik koruma sağladığı gözlenmiştir. Aynı malzemeden oluşturulan katmanlı seramik yapı ile ön kısmına daha sert seramik yerleştirilen katmanlı seramik yapı karşılaştırıldığında, daha sert seramiğin balistik performansı arttırdığı balistik testlerle gözlenmiştir. Yapılan Sonlu Elemanlar Analizlerinde ise her iki sonuçla uyumlu analiz sonuçları ortaya koyulmuştur.

Anahtar Kelimeler: Seramik, Katmanlı Seramik, Delme Derinliği Yöntemi, Hidrokod, Balistik

ACKNOWLEDGMENTS

I would like to express my gratitude to my supervisor Assoc. Prof. Dr. Barış SABUNCUOĞLU and my co-supervisor Assist. Prof. Dr. Hamed TANABİ for their help and guidance throughout the course of this study.

I would also like to thank my parents, Keziban and Murat CURA, and my sister Nihan CURA for all their love, patience, and encouragement throughout this study.

Many thanks to my colleagues and my managers in Terminal Ballistic Division and Fuze Division at The Scientific and Technological Research Council of Türkiye (TÜBİTAK), Defense Industries Research and Development Institute (SAGE) for supporting this study. I would also like to thank to İbrahim ÇENDEK, Ahmet İLERİ, and Veysel KOCA for helping the test specimens and test table preparation.

I am especially grateful for the support of İhtimam Mert VARDAR for their continuous help throughout my research.

I would like to acknowledge TÜBİTAK SAGE for funding this thesis work.

Finally, very special thanks to my wife Ebru YILDIRIM CURA, for all her encouragement and precious support during the study.

TABLE OF CONTENTS

LIST OF TABLES

LIST OF FIGURES

SYMBOLS AND ABBREVIATION

Symbols

Al_2O_3	Aluminum-Oxide
SiC	Silicon-Carbide
B_4C	Boron-Carbide
Si_3N_4	Silicon-Nitride
TiB_2	Titanium-di-Boride
AlN	Titanium-di-Boride
K_{IC}	Fracture Toughness
η	Ballistic Efficiency Coefficient
ρ_{bac}	Density of the backing plate
ρ_{cer}	Density of the ceramic tile
t	Thickness of the ceramic tile
D_0	DoP of backing plate without ceramic
D_1	DoP of backing plate with ceramic

Abbreviation

AA6061-T6	Aluminum Alloy 6061-T6
Alumina	Aluminum Oxide
AP	Armor Piercing
APDS-T	Armor-Piercing Discarding Sabot with Tracer
DoP	Depth of Penetration
EOS	Equation of State
FEA	Finite Element Analysis
FEM	Finite Element Method
HP	Hot-Presses
JC	Johnson-Cook

L/D	Length to Diameter Ratio
LCS	Layered Ceramic Structure
MIL-STD	Military Standard
MKE	Makine ve Kimya Endüstrisi
NIJ	National Institute of Justice
PS	Pressureless-Sintered
PU	Polyurethane
RB	Reaction-Bonded
RHA	Rolled Homogenous Armor
SJC	Simplified Johnson-Cook
STANAG	Standardization Agreement
TNO	Netherlands Organization for Applied Scientific Research
UHMWPE	Ultra High Molecular Weight Polyethylene
WC	Tungsten Carbide
X-Ray	X-Radiation
Zirconia	Zirconium dioxide

1. DEFINITION OF THE STUDY

1.1. Preliminary Information About Ceramic Armor

Ceramic armor is one of the most widely used armor against kinetic energy threats, which belongs to the passive armor category. Ceramic armor is more protective than similar-weight metallic armor in protection. In other words, it provides the same protection as metallic armor but with less weight. They are generally preferred on platforms with high mobility requirements like body armor, vehicle armor, and aircraft armor.

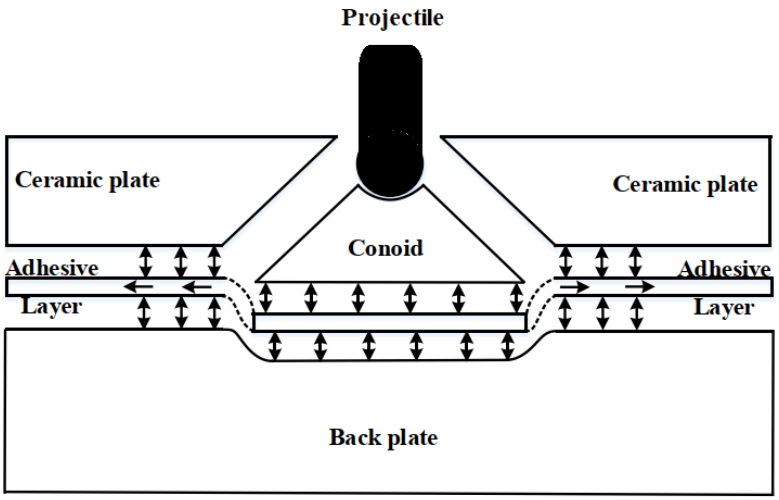

Figure 1. 1. Ceramic armor working principle concept [1].

Ceramic armors are made of three main components. The first one is the ceramic tile that plays a vital role in blunting the bullet's core. The second one is the ductile backing plate that slowdowns and stops the remaining bullet core. The third is the adhesive, which is used for bonding these two (Figure 1. 1). There are a few commercially available armor-grade ceramic tiles worldwide. Some of them are listed with their mechanical properties in Table 1. 1. For the second component, there are different types of ductile materials like metals, fiber-reinforced composites, polymers, etc.

Table 1. 1. Armor grade ceramic properties [2]

Ceramic	**Density [kg/m^3]**	**Hardness [HV]**	**Fracture Toughness [MPa×m$^{1/2}$]**	**Relative Cost**
Aluminum-Oxide 98%	3800	1600	4.5	1.0
Reaction Bonded Silicon-Carbide	3100	1200/2200	4.5	2.5
Sintered Silicon-Carbide	3150	2700	3.2	4.5
Hot Pressed Silicon-Carbide	3220	2200	5.0	9.0
Hot Pressed Boron-Carbide	2520	3200	2.8	16.0

During the bullet impact, both faces of the ceramic tile feel different loads; the strike face feels compressive stress, while the rear face feels tensile loads due to the local bending. Ceramic tile needs high hardness and compressive strength on the strike face to blunt the bullet's core. At the same time, the ceramic needs high toughness on the rear face to prevent the ceramic tile from breaking easily [3]. However, these two properties conflict and are not usually found at a high level in a material. In this study, layered ceramic structures made of different materials are manufactured and tested to provide the strike face and rear face requirements simultaneously. But first, the effect of the layered ceramic structure should be revealed using the same ceramic material. It is necessary here to clarify some terms that are frequently used in the thesis:

- Ceramic Structure: The ceramic part of the ceramic armor.
- Monolithic Ceramic: Single-layer ceramic structure. (Figure 1. 2 (a))
- Layered Ceramic Structure (LCS): A ceramic structure contains two adhesively bonded ceramics.
- Layered Ceramic Structure (LCS) with the same material: Same material ceramics are used in a layered ceramic structure. (Figure 1. 2 (b))
- Layered Ceramic Structure (LCS) with different materials: Different material ceramics are used in a layered ceramic structure (Figure 1. 2 (c))

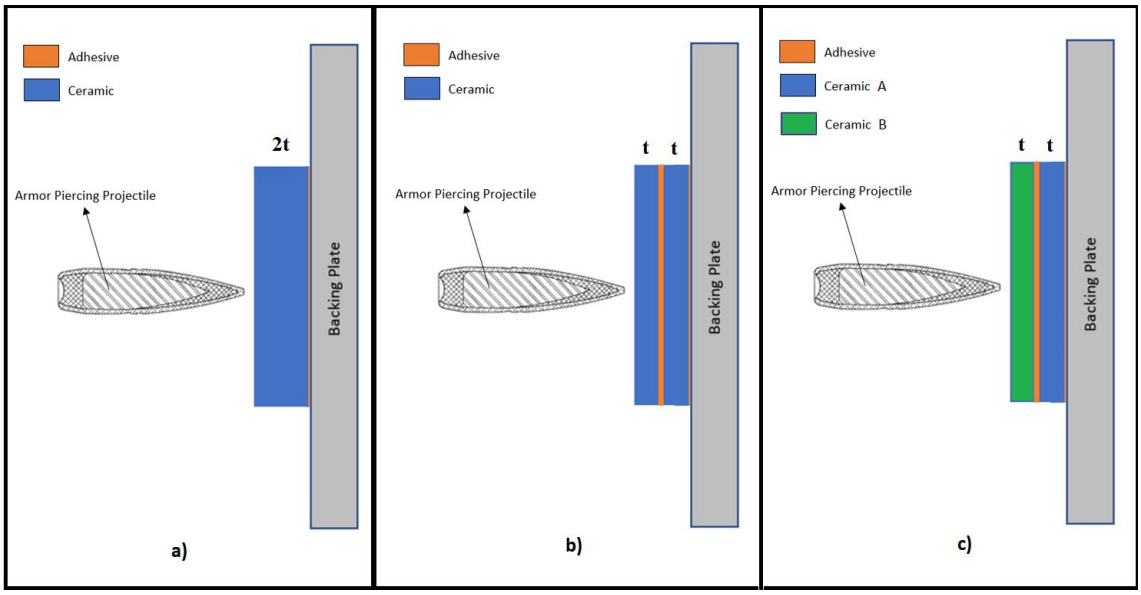

Figure 1. 2. The schematics of the ceramic configurations: a) Monolithic Ceramic b) Layered ceramic structure (LCS) with the same material c) LCS with the different material

1.2. Aims and Objectives of the Study

This study's main aim is to investigate the ballistic protection potential of LCS with different materials by performing ballistic tests. The configurations of the LCS with different materials (Figure 1. 2 (c)) are compared with LCS with the same material (Figure 1. 2 (b)) to see the effect of a different material. There is only one study (Carton et al. [3]) on LCS with different materials in the literature, and this thesis differs from the mentioned study in many ways. The TNO Energy Method is used to compare the configurations in the mentioned study, and this method is hard to perform. Also, the materials that were used in the mentioned study have very similar densities (Silicon-Carbide ($\rho = 3.21$ g/cm^3) and Silicon-Nitride ($\rho = 3.17$ g/cm^3)). In this thesis, the Dept of Penetration (DoP) Method was used, which is a widespread and easy-to-perform method. Also, three different ceramic materials and two types of geometry (hexagonal and square) ceramic tile were used. Ceramic materials are:

- Aluminum-Oxide, ρ=3.85 g/cm^3
- Silicon-Carbide, ρ=3.15 g/cm^3
- Boron-Carbide, ρ=2.50 g/cm^3

Because of the use of different densities, the configurations cannot be compared directly in DoP Method. Therefore, Ballistic Efficiency Coefficients were determined using penetration depth, and these coefficients were compared.

The secondary aim is to investigate the effect of the LCS with the same material on ballistic protection. The LCS with the same material configurations (Figure 1. 2 (b)) were compared with monolithic configurations (Figure 1. 2 (a)). There are numerous studies in the literature on that comparison [1, 4-7]. However, the effect of LCS with the same material on ballistic protection is still controversial. Some studies have found that LCS provides better protection than Monolithic, but others do not. Therefore, to contribute to the literature, this comparison was performed in this study. Also, LCS with different materials compared with monolithic indirectly. Two types of geometry (hexagonal and square) and one ceramic material were used in this study. The DoP Method and Ballistic Efficiency Coefficients were applied for comparison.

The final aim is to develop a calibrated finite element analysis model for predicting other potential layered ceramic structures without a test.

1.3. Limitations of the Study

In layered ceramic structures, ceramics are bonded together with adhesive. The class and thickness of the adhesive are vital for stress wave propagation and ceramic crack initiation. Nevertheless, this thesis does not cover the influence of adhesive class and thickness on layered ceramic structures.

1.4. Research Methodology

The study starts with a detailed literature survey about ceramic armor. Firstly, the underlying mechanism of the bullet-ceramic interaction was investigated. Then armor-level ceramics were introduced. After that, benchmarking methods were searched in the literature. Aluminum-Oxide, Silicon-Carbide, and Boron-Carbide ceramics were used to create the various LCS configurations. The ballistic efficiencies of the configurations were evaluated by the Depth of Penetration (DoP) Method. After that, the layered ceramic

structure phenomena is concluded according to the test results. Lastly FEA model was created and calibrated by DoP tests.

1.5. Outline of the Study

The presented study is made of eight chapters, including this chapter. Each chapter's synopsis is as follows:

Chapter 1, Definition of the Study: The definition of the study and the aim of the study is explained.

Chapter 2, Introduction to Ceramic Armor: The working principle of ceramic armor is introduced. The components of the ceramic armor and their properties are explained.

Chapter 3, Literature Survey About Layered Ceramic Structures: Previous and related studies are investigated.

Chapter 4, Depth of Penetration Method: The DoP method is introduced. The gun, target carrier stand, and shooting range are discussed. The ballistic efficiency calculation and penetration dept measurement method are explained.

Chapter 5, Test Specimen Properties & Configurations: The backing plate dimension and material determination are explained. The adhesive material selection is conducted. The test specimen preparation method is described. Also, the test configurations of the hexagonal and square ceramics are created in this chapter.

Chapter 6, DOP Test Comparisons: Numerous comparisons are generated to understand the layered ceramic structure phenomenon. The DoP test results are conducted, and conclusions are published.

Chapter 7, Finite Element Analysis of DOP Test: Several FE Analysis is performed to observe the ballistic performance of LCS made of the same material and the LCS made of different material.

Chapter 8, General Conclusion & Discussion: A summary of the study is published. Then the conclusion of the ballistic DoP tests are explained. After that, the FE Analysis of DoP tests are investigated. Lastly, the results of this study are compared with the literature studies.

Appendix I – Post-Test Condition of Specimens: Test specimens are published here. The impact location of the bullet and ceramic conditions can be observed.

Appendix II – DOP X-Ray Images: The scaled X-Ray images of the specimens are shared. DoP measurement of specimens can be observed.

2. INTRODUCTION TO CERAMIC ARMOR

Ceramic armor systems have traditionally been used to counter Armor-Piercing (AP) bullets. The AP projectiles are generally made of hardened steel or tungsten carbide cores. Usually, the core is covered with a soft, thin metal jacket for interior ballistic or exterior reasons. The core's properties determine the bullet's penetration performance, and the soft jacket's existence does not influence the bullet's penetration. The projectile's length-to-diameter (L/D) ratio is another vital parameter for penetration performance. The higher L/D can provide higher penetration. The AP projectiles typically have a 3 – 5 L/D ratio [8].

2.1. Ceramic-Armor & Working Principle

The ceramic armor components are shown in Figure 2. 1. The main parts of the ceramic armor are the ceramic tile and the backing plate. According to the working mechanism of ceramic armor, the tile should be positioned on the strike face. Generally, high-strength armor-grade ceramic materials are preferred. The backing plate is typically made of aluminum alloy, steel, polyethylene, or fiber-reinforced polymer, and it supports and stiffens the ceramic tile. These two main components are bonded together with the proper adhesive. Additionally, a cover plate stands on the strike face, protects and confines the ceramic tile, and prevents the ceramic's spalling during the impact.

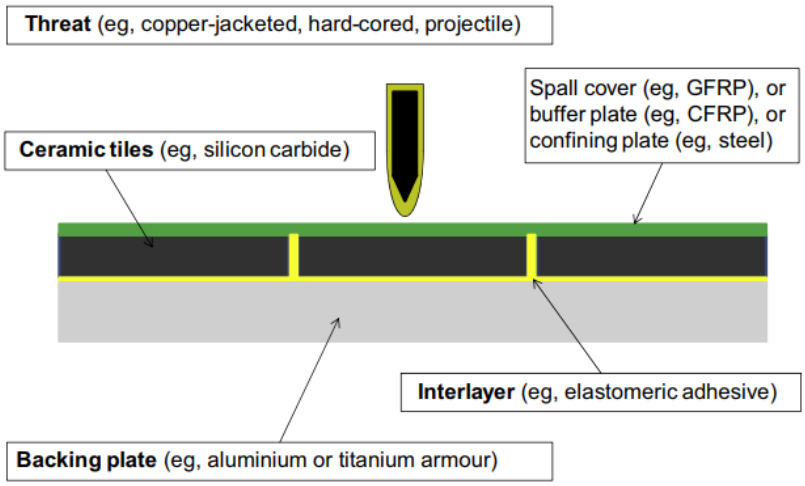

Figure 2. 1. Cross-sectional illustration of a ceramic composite armor [9].

The energy absorbing mechanism and working principle of ceramic armor are explained and displayed in Figure 2. 2 step by step. In this visualization, only two main components of the ceramic armor are demonstrated: the ceramic on the strike face and the supporting material on the back. As mentioned earlier, the AP bullet is made of a hardened steel core and a soft jacket. In the initial stage, the AP bullet comes with a certain velocity to ceramic armor (Figure 2. 2 - 0). The soft jacket nose is stuck between the core and the ceramic surface at the first impact moment. Since the jacket has low strength, it starts to strip away from the impact zone (Figure 2. 2 - 1). While the impact continues, the pointy nose of the brittle hardened core begins to break/erode. This period is called the Dwell Period. During the Dwell Period, the nose of the bullet becomes blunt, and the core loses mass (Figure 2. 2 - 1). After the Dwell Period, damage accumulation occurs on the ceramic tile. During the impact, the compressive stress wave propagates through the ceramic tile, and the compressive stress wave reflects as the tensional stress wave at the end of the ceramic back face. Since the tensional wave and bending of the ceramic tile, Hertzian Cracks start from the point of impact to the back of the ceramic. At the end of this period, a conical fracture happens on the ceramic tile (Figure 2. 2 - 2). Since the conical ceramic fracture increases the contact area with the backing plate, the localized impact stress is distributed on the backing plate. Therefore, the bullet core bulges the backing plate. During this phase, fractured ceramic still contributes to the erosion and deceleration of the bullet core (Figure 2. 2 - 3). At the last stage of the defeat mechanism, the blunt core is decelerated (Figure 2. 2 - 4) and stopped (Figure 2. 2 - 5) by the backing plate.

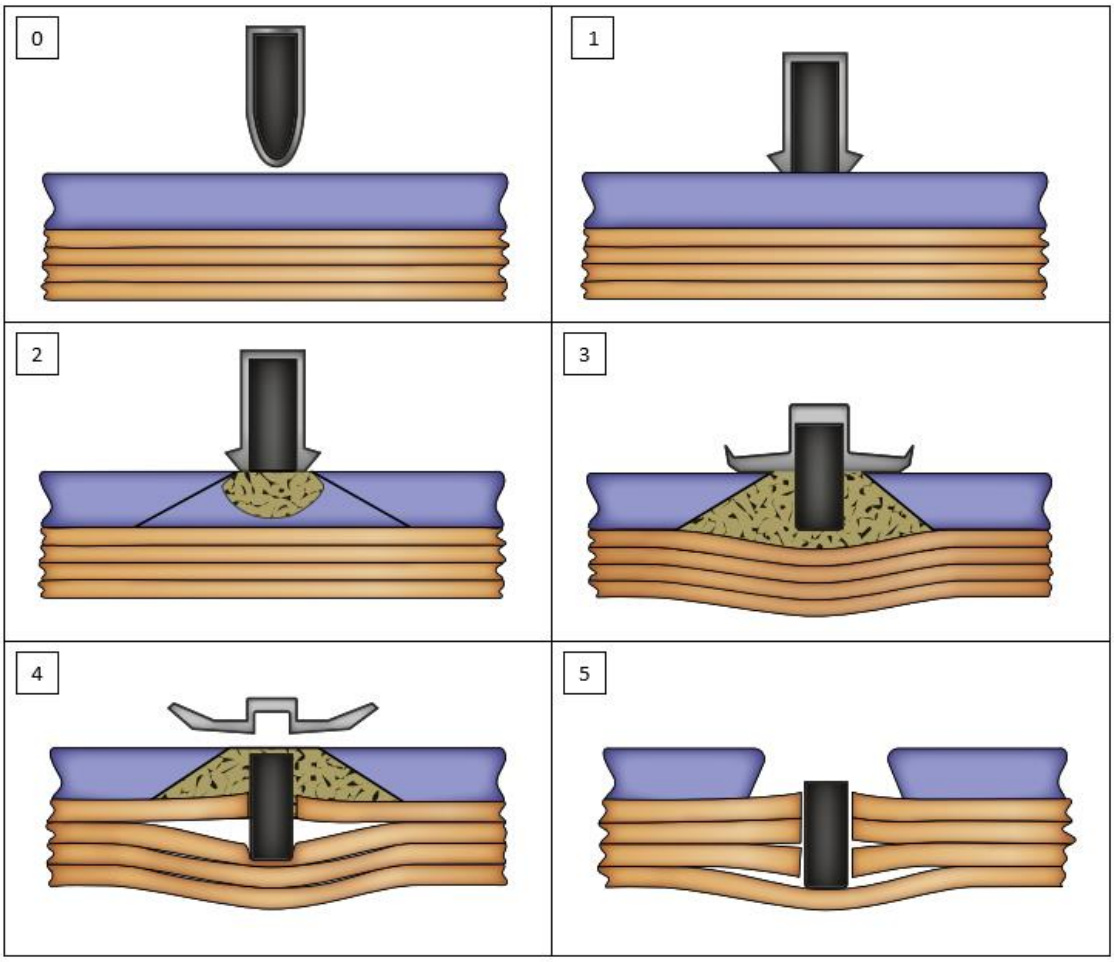

Figure 2. 2. Energy absorbing mechanism and working principle of ceramic armor [9].

2.2. Armor-Grade Ceramic Tiles

Ceramic tiles are the main component of ceramic armor. Various armor-grade ceramic materials are available, and this section explains the most famous ceramics.

i) Aluminum-Oxide

Aluminum-Oxide (Alumina, Al_2O_3) is the least expensive armor-grade ceramic material. It has been the most famous ceramic material for decades due to Alumina's excellent performance/cost ratio. High purity Aluminum-oxide (~99.5%) provides the most weight-efficient ballistic protection (Table 2. 1). The Aluminum-Oxide can be used against calibers ranging from 5.56 to 105 mm. However, it has one significant disadvantage: weight. Al_2O_3 has lower hardness and higher density compared to SiC and B_4C.

Table 2. 1. Variation of Al_2O_3 and their mechanical properties [10].

Al_2O_3 Products	**Al_2O_3 Content [%]**	**Density [g/cm^3]**	**Compressive Strength [MPa]**	**Hardness KNOOP [GPa]**	**Fracture Toughness [MPa×m$^{1/2}$]**
AD-85	85	3.42	1930	9.4	3 - 4
AD-90	90	3.60	2482	10.4	3 - 4
AD-995	99.5	3.90	2600	14.1	4 - 5
PLASMA PURE - UC	99.9	3.92	2700	14.5	4 - 5

ii) Silicon-Carbide

Silicon-Carbide (SiC) is another famous armor–grade ceramic material and has an excellent weight-performance ratio. SiC has higher hardness, compressive strength, and lower density than Al_2O_3. Although B_4C has a better weight–performance ratio, SiC is considered more reliable due to B_4C's shock loading problem [11]. SiC is manufactured commercially in three ways:

- Hot-Presses (HP) SiC
- Pressureless-Sintered (PS) SiC
- Reaction-Bonded (RB) SiC

Hot pressing creates high-performance ceramics for armor application, but it is expensive. Pressureless sintering is a widespread technique, but this technique needs heating temperatures of more than 2000°C. This technique stands between hot-pressed and reaction-bonded in cost and ballistic performance. The RB Silicon-Carbide has lower ballistic performance than hot-pressed and pressureless-sintered. However, RB Silicon-Carbide is the only competitor of Al_2O_3 in terms of price (Figure 2. 3) [12].

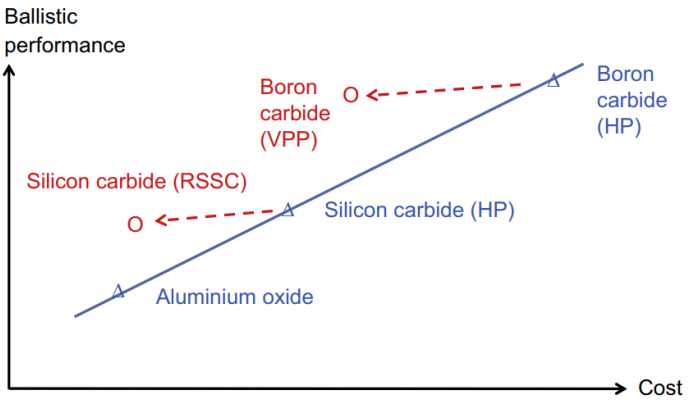

Figure 2. 3. "Ballistic Performance – Cost" relationship of alternative production process [9]

iii) Boron-Carbide

Boron-Carbide (B_4C) is the ultimate armor ceramic, with a density of 2.5 g/cm^3 and a hardness equivalent to SiC. Most Boron-Carbide is hot pressed; however, reaction-bonded B_4C is becoming more widespread [12, 13]. Because of the expensive raw material, vacuum or inert gas requirement, and 2000-2200 °C temperature heating, hot-pressed B_4C is one of the most expensive commercial ballistic ceramic [9].

Despite superior mechanical properties over other ballistic ceramics, B_4C behaves more like a glass manner under the high-velocity impact (high shock loading). This underperformance appears to be caused by shear localization inside the material when it is subjected to shock stress. Boron carbide's shear strength rapidly drops over the Hugoniot Elastic Limit under the high shock loading condition (Figure 2. 4).

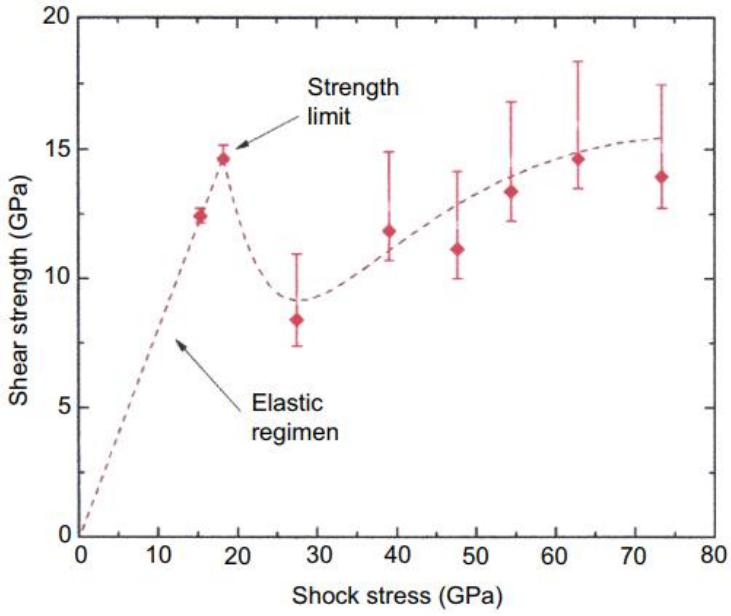

Figure 2. 4. Shear strength of boron carbide as a function of shock stress [11].

iv) Titanium-Di-Boride

Titanium-Di-Boride (TiB_2) is one of the heaviest ballistic ceramic with a density of 4.5 g/cm^3. TiB_2 is a high-performance ballistic material, but it is relatively expensive (the price is approximately two times of the Hot-Presses B_4C) [13].

v) Silicon-Nitride

Like silicon carbide, silicon nitride (Si_3N_4) can be produced by the reaction-bonding process. In spite of this, Si_3N_4 can be sintered or hot pressed and can be used in some niche applications in defeating small arms. Its ballistic efficiency is similar to high-purity Al_2O_3 [13].

2.3. Backing Plates of Ceramic Armor

As mentioned in the working principle, ceramic tiles are effective when they are combined with a ductile backing plate. The choice of the backing plate highly depends on the threat level. The fiber-based composite backing plates may be sufficient for small caliber threats (5.56 – 7.62 mm), while metallic backing plates may be required for high caliber threats (20 – 35 mm) [14]. In this section, some backing plate classes and properties are introduced.

- **Metallic Backing Plate**

Ideally, backing plates need to be as rigid as possible. Therefore, metallic materials are attractive for ceramic armor backing plates [9]. In the early stage of ceramic armor development, RHA steel, aluminum alloys, and titanium alloys were used as backing plates since they have a high Young's Modulus. These metal backing plates were used in many studies. Metallic plates have a high areal density (especially steel) according to composite plates and cannot be shaped easily [9]. On the other hand, they are cheaper and have a longer life cycle than composite plates. Mostly, land vehicles are made of steel or aluminum bodies. The vehicle's body can be used as a natural backing plate when ceramic tiles are bonded on the body (Figure 2. 5).

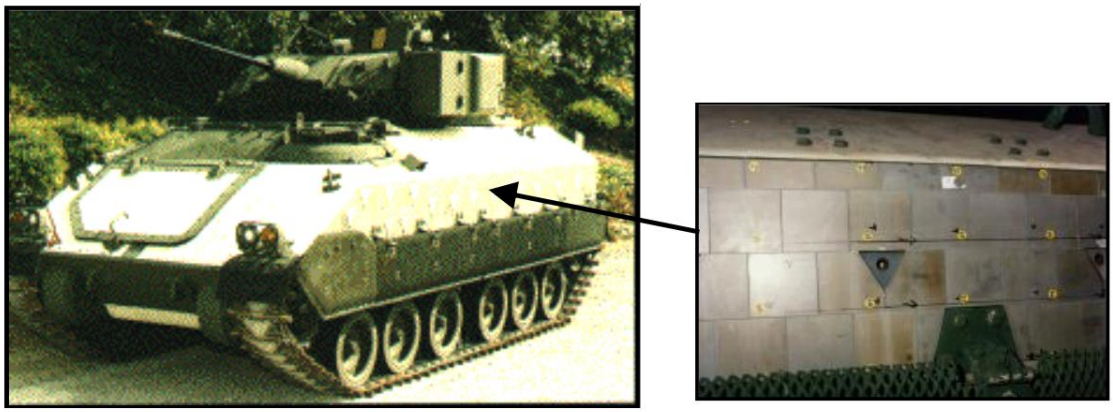

Figure 2. 5. 1st generation CIFV with TiB_2 tiles [8].

- **Woven Aramid Fabric Composite Backing Plate**

Aramid fibers have high mechanical properties. Woven aramid fabrics are good at holding fragments but have difficulty stopping the AP rifle ammunition. Therefore, it is not sufficient to use it alone for ballistic protection against AP rifle ammunition. High mechanical properties, relatively low density, and quite rigidity make it a good option for a backing plate of ceramic armor [14]. Also, anti-trauma behavior is another good property for human body protection. When aramid is selected as the ceramic armor backing plate, the ceramic makes blunt the bullet; and the aramid acts as a fragment retaining mesh (Figure 2. 6).

Figure 2. 6. A ceramic armor with an aramid-based composite backing plate [9]

- **UHMWPE Fiber-Reinforced Composite Backing Plate**

UHMWPE fiber-reinforced composite is made of Ultra High Molecular Weight Polyethylene fibers (Dyneema® / Spectra®) and polymer matrix. UHMWPE fibers are located unidirectional (0/90) layer by layer in the composite (Figure 2. 7). The matrix can be rubber-based resin (soft composite) or Polyurea based resin (rigid composite). UHMWPE fiber-reinforced Polyurea matrix can be a good choice as a backing plate. It has a high stiffness to support ceramic face [14]. Also, the density is relatively lower (~1000 kg/m3). However, this composite has some disadvantages: UHMWPE fiber has low melting temperature and surface energy. Low melting temperature reduces the ballistic performance in high temperatures and long durations (60–80 ºC) [14], so service temperature is limited. Low surface energy causes some boning problems with other armor components like ceramic tile.

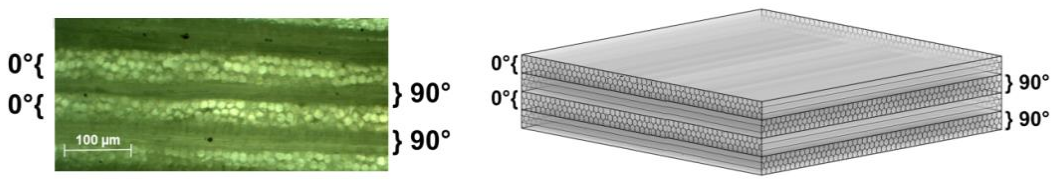

Figure 2. 7. Microsection of DYNEEMA® HB80 plates (Unidirectional 0/90 UHMWPE with Polyurea Resin) [15]

2.4. Bonding of Ceramic Tile and Backing Plate

Since ceramic materials are brittle, bolted fastening can create stress concentration points, which can create cracks and reduce ballistic performance. Ceramic tiles are usually bonded to the back plate with adhesive. However, bonding with adhesive must be resistant to high-impact conditions. In this section, adhesive classes, adhesive thickness, and acoustic impedance effect studies are examined. Also, the effect of the surface treatment on adhesion is mentioned.

In ceramic armor, several adhesive types like Epoxy, Polyurethane, Polyurea, Acrylic, or Ethylene Propylene-based Diene Monomer (EPDM) rubber can be used [16, 17]. However, epoxy and polyurethane are generally preferred. Both adhesives have low density and moduli. Therefore, they have low acoustic impedance relative to ceramic and backing plate. When comparing the two adhesives, epoxy is stiffer and more brittle than polyurethane. For higher ballistic efficiency of ceramic tile, the adhesive must transmit the compressive stress wave from the ceramic tile to the backing plate as fast as possible. Theoretically, the adhesive with the closest acoustic impedance to ceramic should be preferred [18]. However, although epoxy is more efficient for ceramic tile, rubber-based adhesives may be more efficient for armor system (e.g., multi-hit requirement). As seen in Table 2. 2, epoxy has a more similar mechanical impedance than polyurethane to Alumina. However, due to other requirements like multi-hit capability, other adhesives can be an option although their lower mechanical impedance. Ubeyli et al. [17] compared the epoxy and polyurethane with ballistic tests. The results were shown that there is no meaningful ballistic performance between the two adhesives. However, using polyurethane decreases the spalling and debonding of ceramic tiles from the backing plate.

Doherty [19] investigated the soldering bonding technique on ceramic armor, an alternative to adhesive bonding. Soldering material Sn-Ag-Ti has higher moduli and higher density than epoxy. So, the mechanical impedance of Sn-Ag-Ti is more similar to ceramics. In Doherty's study, ballistic tests were performed with epoxy and Sn-Ag-Ti as a bonding technique; however, significant differences were not observed.

Table 2. 2. Mechanical properties of Al_2O_3 and adhesives

Material	**Density [g/cm^3]**	**Young's Modulus [GPa]**	**Longitudinal Elastic Wave Speed [km/s]**	**Acoustic Impedance [kg/(s×m^2)]**	**Reference**
Al_2O_3 95%	3.74	310	9.1	34.0 x 10^6	[18]
Polyurethane	1.15	0.01	0.1	0.1 x 10^6	[18]
Epoxy Resin	1.20	2	1.3	1.6 x 10^6	[18]
Sn-Ag-Ti	7.40	56	2.7	23.0 x 10^6	[19]

2.5. The Key Properties of Ceramic Armor Systems

Various studies have been performed for years to increase the effectiveness of ceramic armor. Some topics that are known to increase ceramic armor's effectiveness have been compiled under this title.

2.5.1 Ceramic Tile Size & Geometrical Effect

Hazell et al. [20] have investigated the influence of the tile size of ceramic on ballistic performance. In this study, two types of SiC (Direct Sintered SiC & Liquid Phase Sintered SiC) and four sizes of ceramics were investigated experimentally and numerically. According to test and analysis results, direct sintered SiC behaves sensitive to the tile size. By contrast, liquid phase sintered SiC is not affected by the tile size differences. As a conclusion of the study, the minimum tile size should be 70 × 70 mm for direct sintered SiC.

2.5.2 Adhesive Thickness

Adhesive layer thickness is another crucial parameter for ballistic performance and bonding ceramic armor components to each other. López-Puente et al. [21] investigated the effect of the thickness of the adhesive layer on ballistic performance through experiments and numerical analysis. In this study, Al_2O_3 (98% purity) and Aluminum were used as ceramic armor components, and they bonded to each other by Hysol EA-9361 epoxy adhesive. Three adhesive layer thicknesses (0.1, 0.5, and 1.1 mm) were investigated by ballistic test. According to the test result, a calibrated FE model has

developed. To better understand the influence of the adhesive thickness, starting from 0.1 to 1.1 with 0.1 mm increment, adhesive layer thickness was investigated by numerical analyses. After all analyses, 0.3 mm adhesive layer thickness was found as optimum. As adhesive thickness increases, energy absorption of the backing plate increases, and debonding of the ceramic fragments is prevented; however, the thicker adhesive allows the ceramic bending, and high adhesive thickness decreases the ceramic efficiency (Figure 2. 8).

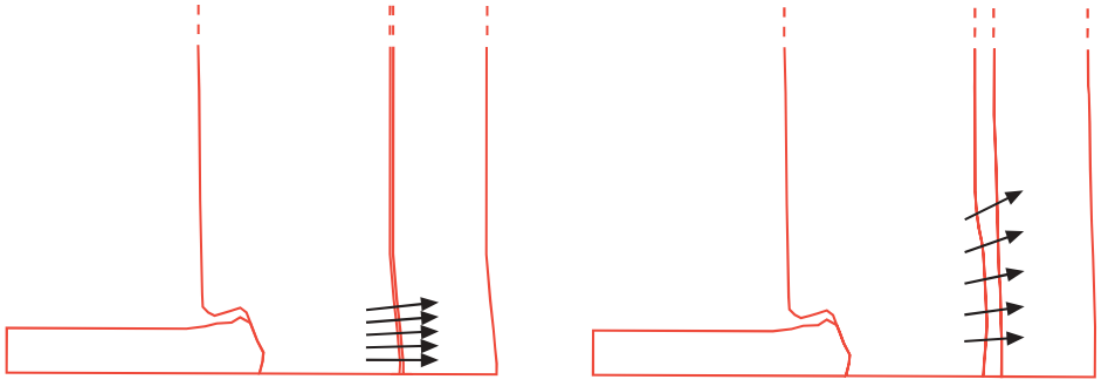

Figure 2. 8. Load distribution on the backing plate with different adhesive thicknesses [21].

Prakash et al. [22] have investigated the influence of the epoxy thickness on Al_2O_3 – Aluminum ceramic armor numerically. Dept of Penetration (DoP) simulations have run for 0.1 – 1.5 mm adhesive thickness by explicit finite element solver AUTODYN. It was observed that the depth of penetration decreased with increasing the epoxy layer thickness.

2.5.3 Surface Treatment of Adherents

In ceramic armor, ceramic and backing plate must be attached considering shock loading. Any weakness caused by adhesive can reduces the protection effectiveness and the multi-hit capability of the armor. There are two main failure modes of the bonding mechanism of adhesive: 1) separation of adherend and adhesive, 2) failure of adhesive [22] (Figure 2. 9), and failure always happens on the weakest one. After the bullet impacts the ceramic, reflected tensional stress waves try to separate the ceramic from the armor system. If the bonding strength of the ceramic-adhesive or backing plate-adhesive is weaker than the

adhesive strength, the separation happens in the early stage of the impact mechanism. Due to this reason, bonding strength must improve as possible.

The bonding strength depends on the surface energy of the adherent and the adhesive properties. As the roughness of the adherent surface increase, the surface energy of the material increases, and because of the high surface energy, a higher bonding strength is provided. As a nature of the materials, some materials (e.g., UHMWPE, SiC) have low surface energy. However, some physical and chemical surface treatment methods exist for surface energy increase. In this section, only the name and some sources of the methods were mentioned:

- Grit-Blast [23] [24],
- Krypton Fluoride Excimer (KrF) Laser [23],
- Etching [24]
- Silane passivation (GBS) [24], [25]
- Open-air plasma (OA) [24], [25]

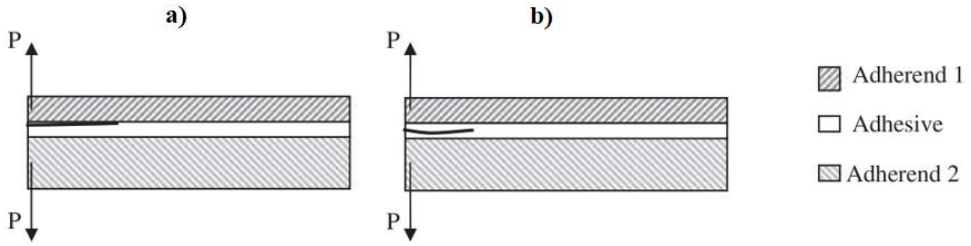

Figure 2. 9. Typical failure modes in adhesive bonds a) bonding strength breaking, b) adhesive failure [22].

2.5.4 Pre-stressed Confinement Effect on Ceramic Tile

Many studies have investigated the ballistic effect of the compressive lateral pre-stress on the ceramic tile during the DoP test (Figure 2. 10). The outcome of most studies shows that the confinement pre-stress has a positive effect on ballistic performance [26-28].

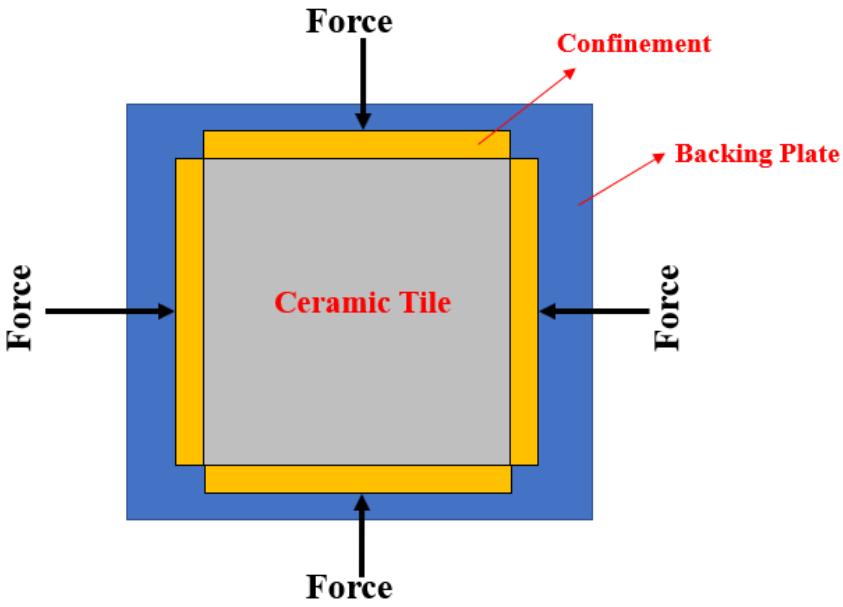

Figure 2. 10. Lateral pre-stress on ceramic tile schematic

Gassman et al. [29] investigated the effect of the pre-stress on Alumina tiles through DoP experiments. Unlike previous studies, they measured the change in the lateral pre-stress level during the DoP test. As seen in Figure 2. 11, lateral stress is stable before the test; then, at the first impact moment, stress increases slightly, and lastly, relaxation is observed.

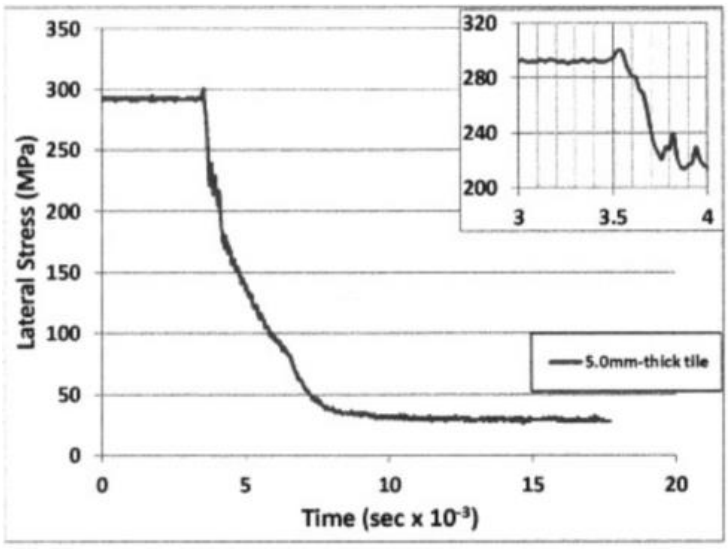

Figure 2. 11. Change of the lateral pre-stress level between ceramic and confinement during ballistic loading [29]

Another study about pre-stress has performed by Chi et al. [30]. They revealed DoP values according to the different pre-stress levels. The outcomes of this study are summarized as follows:

- The lateral pre-stress decreases the DoP values
- As pre-stress increases, the DoP value decrease; however, there is an optimum point
- As the tile thickness increase, the effectiveness of pre-stress also increases
- The damage modes and crack types change when pre-stress level change

2.6. Test Methodologies for Armor Development

Over the decades, various testing techniques have been developed to understand, improve and validate designed armors. Some of these tests have advantages over others (ease, repeatability, low cost, etc.), making them more popular. The testing methods were classified subjectively as phenomenology, armor-material characterization, and armor-design oriented [31].

2.6.1. Phenomenological Experiments

None of the tests under this title are ballistic tests. These tests are used to evaluate ceramic armor components' mechanical properties and behavior under shock loads (Table 2. 3). The evaluated properties and behaviors are used for creating constitutive models or material model parameters for numerical simulation tools [31].

Table 2. 3. Phenomenological experiments [31]

#	**Phenomenological Experiments**
1	Pressure-volume
2	Plate impact (normal, oblique, or multiple impacts-reshock)
3	Split Pressure (Hopkinson or Kolsky) Bar
4	Bar impact (typically bar impacting bar)
5	Tensile or Torsion
6	Quasi-static three- or four-point bending tests
7	Quasi-static indentation

2.6.2. Armor-Material Characterization Experiments

Dynamic impact is used in this category of testing methodologies. These tests are equally phenomenological in origin, but they are used to directly measure or determine features of target resistance or penetration resistance from behavioral models. Although there are differences between testing organizations, these experiments often control the geometry of the test. These tests (Table 2. 4) were designed to analyze, rank, and compare ceramic performance for ballistic armor applications directly or indirectly [31].

Table 2. 4. Armor-material characterization experiments [31]

#	**Armor-Material Characterization Experiments**
1	(CEX) Cavity expansion or cylindrical collapse
2	(DAM) Damage Propagation (edge on impact)
3	(IND) Indentation: dynamic or loading and unloading
4	(NDP) Non-deforming penetration (referred to as rigid penetration)
5	(PEN)Semi-infinite penetration vs. velocity time histories
6	(DOP) Depth-of-penetration experiments
7	(DWE) Complete dwell (for damage onset and for structural response)
8	(DPT) Dwell/penetration transition (concerns about shock mitigation)

2.6.3. Armor Design-Oriented Ballistic Experiments

This group of experimental methodologies (Table 2. 5) is applicable to armor system applications and so can be used to refer to the direct evaluation of material in a specific application. However, they are the most complex test procedures to employ in order to obtain knowledge about how to optimize the material's performance. Additionally, due to the probabilistic nature of these tests, a significant number of tests must be run. This is why more straightforward screening experiments such as those mentioned above have been created [31].

Table 2. 5. Armor design-oriented (ballistic) experiments and methodologies [31]

#	**Armor Design-Oriented (Ballistic) Experiments and Methodologies**
1	(FTG) Fixed geometry (e.g., 1-4-3 thicknesses at 60-deg obliquity)
2	(TCA) Tandem configurations (MTL/BRL patent)
3	(VBL) Ballistic Limit Velocity tests (V50 or perforation test data)
4	(BAD) Behind Armor Debris
5	(TAD) Minimum Target Areal Density (different for each material combination)

2.7. Test Standards for Armor Verification

Some countries and some relevant organizations create some test standards. These standards require armors to be qualified using the test methods mentioned above. Test standards and specifications are vital for the armor designer, manufacturer, and purchaser. Fine-tuning of these test methods and new test techniques continues to evolve, as well as the materials themselves. However, the most popular of these methods is the V50 test, and many standards use this test. Some of the test standards are listed in Table 2. 6.

Table 2. 6. Standards and specifications for lightweight ballistic materials [14]

Standard Name	**The Scope of the Test Method**
MIL-STD-662F	Standard for V50 ballistic test
NIJ - 0101.04	Standard for personal body armor
STANAG 2920	Standard for personal armor
NIJ standard, 0106.01	Standard for ballistic helmets
NIJ 0108.01	Standard for ballistic protective materials
STANAG 4569	Standard for armored land vehicles

3. LITERATURE SURVEY ABOUT LAYERED CERAMIC STRUCTURES

Several studies have been published about the layered ceramic structure in recent years. In these studies, the advantages and disadvantages of LCS over monolithic ceramic have been investigated. However, most studies used the same ceramic material in layers. In between these studies, some concluded that LCS with the same materials has better ballistic protection than monolithic ones, and others concluded the opposite. Apart from these, one study was found about LCS with different materials in the literature. In this chapter, previous studies on LCS with the same material and LCS with different materials were described. Unless otherwise specified, the term LCS defines the LCS with the same material.

Yadav and Ravichandran were the first researchers to investigate Layered Ceramic Structure (2001) [5]. They manufactured and tested three configurations to investigate the LCS ballistic protection using Aluminum-Nitride (AlN) ceramic tiles. The created ceramic structures are 1 × 38.1 mm and 3 × 12.7 mm; the total ceramic thickness equals 38.1 mm. Yadav and Ravichandran used the Depth of Penetration (DoP) Method to compare the configurations. The schematic of the DoP test of the 3 × 12.7 mm configuration is shown in Figure 3. 1. Yadav and Ravichandran concluded that the 3 × 12.7 mm layered ceramic structure has less penetration depth; in other words, LCS has better ballistic protection than monolithic ceramic tile.

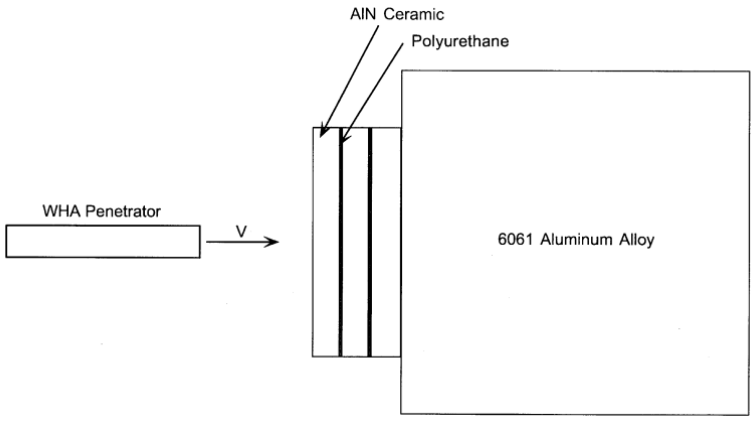

Figure 3. 1. Yadav and Ravichandran's study, a DoP test configuration (3 × 12.7 mm) [5]

Weiss et al. (2017) [4] performed an experimental and numerical study involving layered ceramic structures using large caliber 25 mm APDS-T. In the mentioned study, a monolithic 40 mm Al_2O_3 tile and a (3 × 14 mm) 42 mm layered ceramic structure Alumina were compared with DoP tests. The results of Weiss et al.'s study are consistent with Yadav and Ravichandran's study. The study was shown that layered ceramic structures perform better than monolithic one. Depending on the polymer layer thickness between the ceramics, penetration depth decreases (ballistic protection increases) up to 20%. Thin adhesive layer modeling between ceramic layers in FEA is problematic; however, according to the FEA results, layered ceramic structures performed better by up to 9%. Consistent results were obtained by Ls-Dyna finite element analysis. It can be seen in Figure 3. 2 that the LCS has less penetration depth.

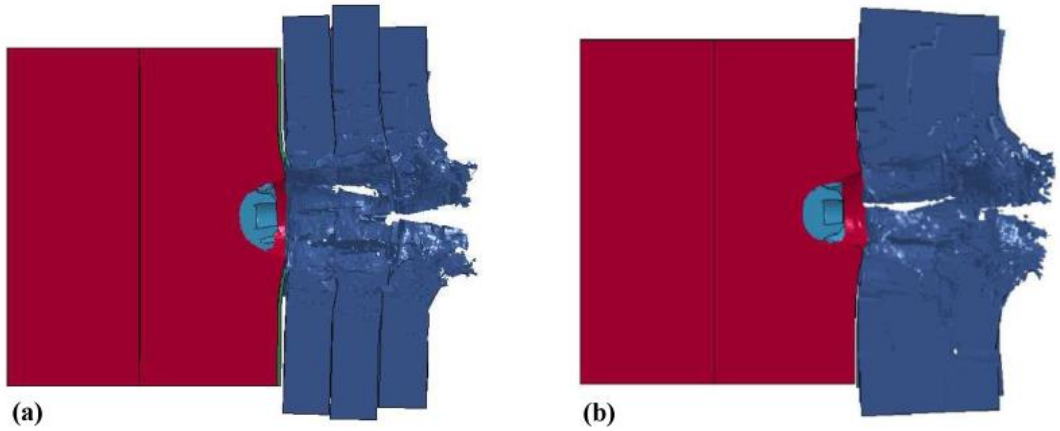

Figure 3. 2. Comparison of analysis results, (a) layered structure (b) monolithic [4]

Gao et al.'s study (2017) [1] is another study that has a consistent conclusion with the first two studies. They compared the 1 × 10 mm monolithic and 2 × 5mm LCS configurations by the DoP method and numerical analysis. Also, they investigated the effect of the adhesive layer thickness (0.5, 1.0, 1.5, and 2.0 mm) in between the ceramic layers. In the study, sintered TiB_2-B_4C based ceramic tiles were used as ceramic, and the aluminum alloy was used as a backing plate. A test specimen of the study can be seen in Figure 3. 3. According to the experiments and analyses result, better ballistic protection was observed when LCS was used instead of monolithic. The study also concluded that the penetration depth decreases (protection increases) with the increase of the adhesive layer thickness.

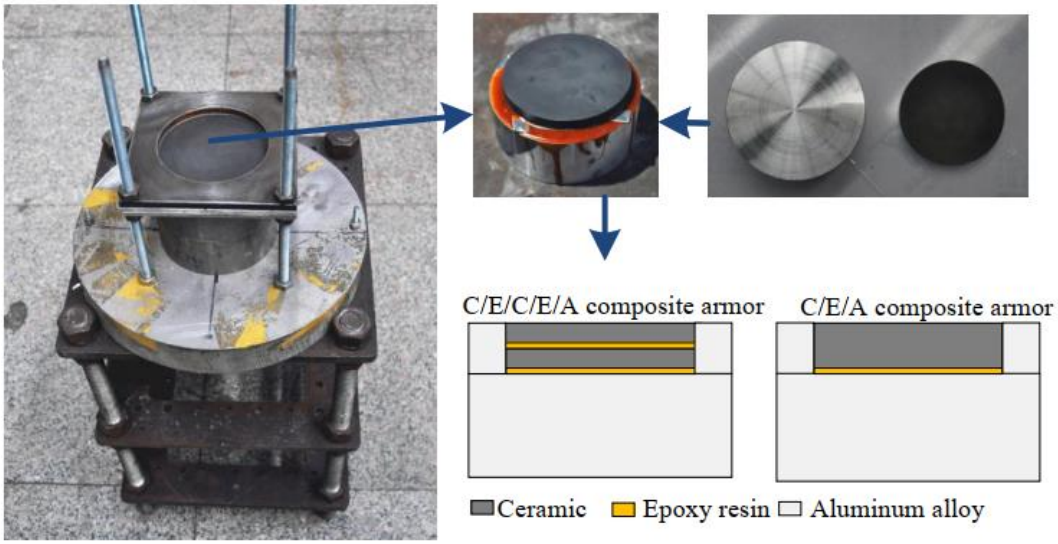

Figure 3. 3. Test configurations of the Gao et al. study [1]

Contrary to the described first three studies, some studies concluded that monolithic ceramic has better protection than LCS. The study of Yadav and Ravichandran was mentioned above; they also investigated the 6 × 6.35 mm configuration and compared it with 1 × 38.1 mm and 3 × 12.7 mm in the same study [5]. According to the DoP test results, even monolithic ceramic performs better than a 6 x 6.35 mm configuration. The penetration depth of the configurations can be seen in Figure 3. 4.

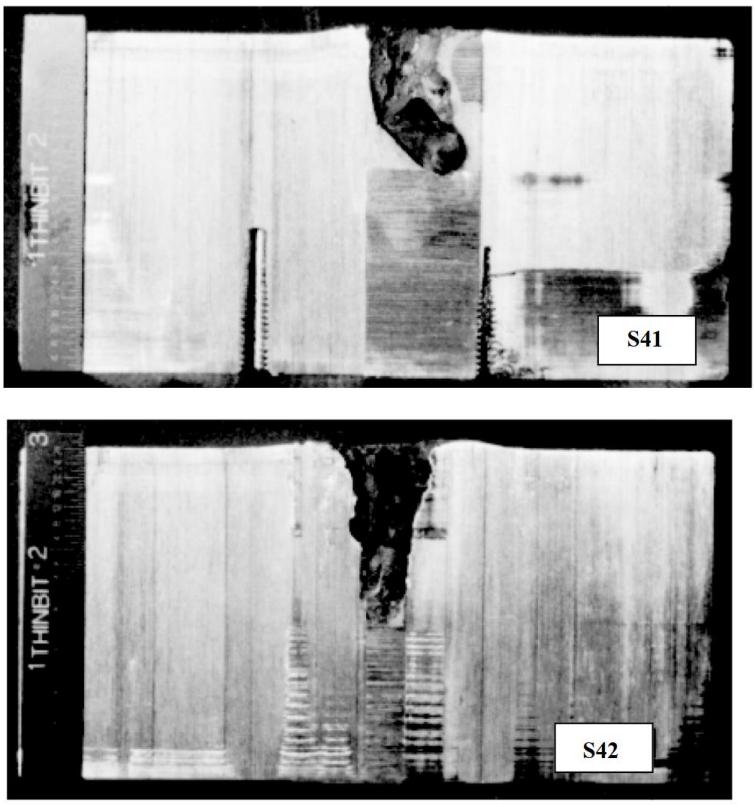

Figure 3. 4. Yadav and Ravichandran's study [5], penetration depth comparison a) 1 × 38.1 mm, b) 6 × 6.35 mm.

Another study was conducted by Carton et al. [3] in 2016, and they compared LCS and monolithic with two total thicknesses (7 and 10 mm). The compared configurations can be seen in Table 3. 1. Carton et al. used TNO Energy Method for comparing the ceramics. This method is hard to perform and needs initial and residual mass & velocity to calculate kinetic energy loss during the ceramic perforation. In that study, the comparisons were conducted in terms of dwell time. The higher dwell time represents relatively better ballistic protection. The test results are shown in Figure 3. 5. The monolithic ceramics performed better protection than LCS.

Table 3. 1. Carton et al.'s study [3], Monolithic and LCS comparisons

Comparisons	**Monolithic Configuration**	**LCS Configuration**
#1	7 mm SiC	3.5 mm SiC + 3.5 mm SiC
#2	10 mm SiC	7 mm SiC + 3.5 mm SiC*

* There is no information about which ceramic is on the strike face.

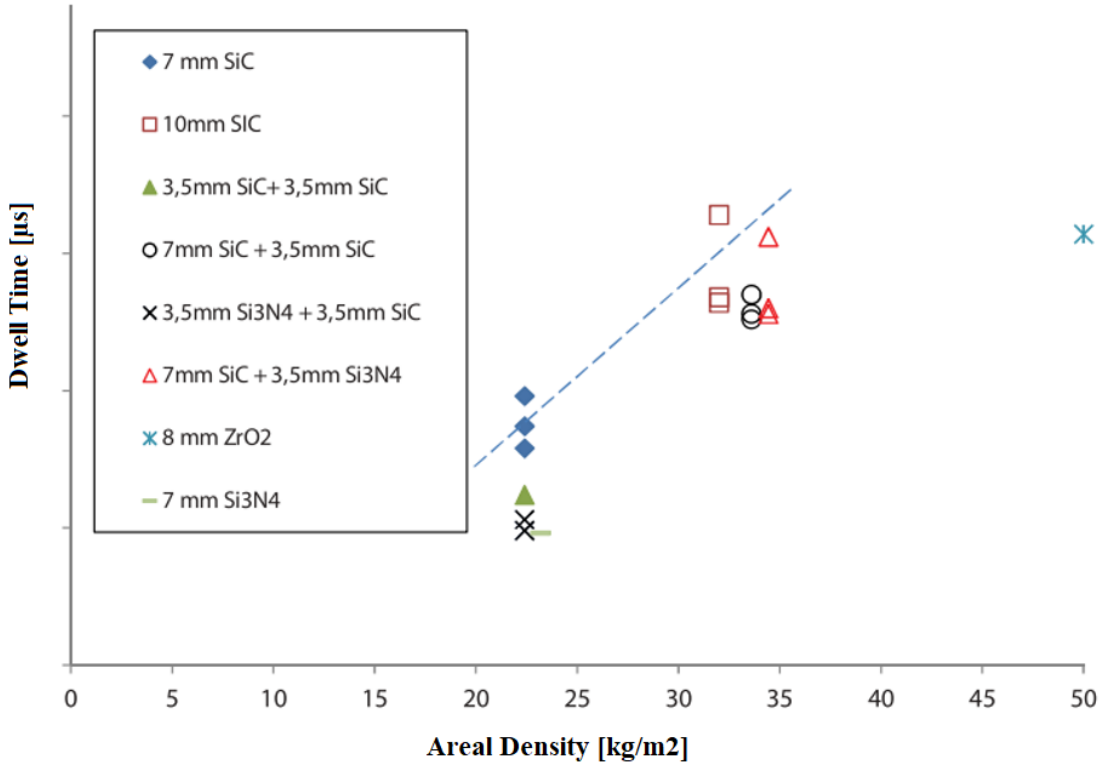

Figure 3. 5. Dwell time versus areal density for monolithic and layered ceramic structures against 7.62 APM2 at 830m/s [3]

Polla et al. (2019) also investigated the layered ceramic structure made of the same material with DoP tests [7]. The tested configurations can be seen in Table 3. 2. The DoP tests of this study have been conducted with a 7.62 × 51 mm Armor-Piercing bullet. According to the DoP test results, monolithic Al_2O_3 performed better ballistic protection than 2 × 3 mm Al_2O_3 and 3 × 2 mm Al_2O_3.

Table 3. 2. The tested configurations in Polla et al.'s study [7]

Monolithic Configuration	**LCS Configuration 1**	**LCS Configuration 2**
6 mm Al_2O_3	2 × 3 mm Al_2O_3	3 × 2 mm Al_2O_3

The study of Carton et al. [3] was mentioned above. In the same study, they also investigated the LCS with different materials. Silicon-Carbide (SiC) and Silicon-Nitride (Si_3N_4) have been used for the investigation of LCS with different materials. Si_3N_4 is much tougher than SiC; however, the hardness of Si_3N_4 is relatively low (close to the Alumina). Since SiC and Si_3N_4 have similar densities (respectively, 3.21 g/cm^3 and 3.17

g/cm^3), the tested configurations can be compared directly. The tested configurations can be seen in Table 3. 3. In Figure 3. 5, the results can be seen in terms of dwell time. Carton et al. concluded that LCS with the same material and LCS with different materials perform ballistic protection equal or worse than monolithic.

Table 3. 3. Carton et al.'s study [3], LCS with the same material and different materials comparisons

Total Thickness	**LCS Configuration**	**LCS with Different Material Configuration**
7 mm	3.5 mm SiC + 3.5 mm SiC	3.5 mm SiC + 3.5 mm Si_3N_4
10.5 mm	7 mm SiC + 3.5 mm SiC*	7 mm SiC + 3.5 mm Si_3N_4 *

* There is no information about which ceramic is on the strike face.

The main purpose of the study, investigate the ballistic protection potential of LCS with different materials by performing ballistic tests. The configurations of the LCS with different materials were compared with LCS with the same material to see the effect of a different material. There is only one study (Carton et al. [3]) on LCS with different materials in the literature, and this thesis differs from the mentioned study in many ways. In the mentioned study, a non-common method was used (TNO Energy Method) to compare the configurations, which is hard to perform. Also, the materials that were used in the mentioned study have very similar densities (Silicon-Carbide (ρ = 3.21 g/cm^3) and Silicon-Nitride (ρ = 3.17 g/cm^3)). In this thesis, the Dept of Penetration (DoP) Method was used, which is a widespread and easy-to-perform method. Also, three dissimilar ceramic materials (Al_2O_3, SiC, and B_4C) and two types of geometry (hexagonal and square) ceramic tile were used. The compared configurations have different areal densities; therefore Ballistic Efficient Coefficient of each configuration was determined with penetration depth. The comparisons were conducted in terms of Ballistic Efficiency.

The secondary aim is to investigate the effect of the LCS with the same material on ballistic protection. The LCS with the same material configurations were compared with monolithic configurations. As mentioned above, numerous studies exist on that comparison [1, 4-7]. However, the effect of LCS with the same material on ballistic

protection is still controversial. Some studies have found that LCS provides better protection than Monolithic, but others do not. Therefore, to contribute to the literature, this comparison was performed in this study. Also, LCS with different materials compared with monolithic indirectly.

The final aim is to develop a calibrated finite element analysis model for predicting other potential layered ceramic structures without a test.

4. DEPTH OF PENETRATION METHOD

The Depth of Penetration (DoP) method is a ballistic test method that is used to compare the protection of armor materials. Since it is an easy and inexpensive method, it has been frequently used in studies in the literature. Most studies described in Chapter 3 have used this method. The ceramics examined in this study were tested with this method. This chapter explains the DoP method, test setup, and ballistic efficiency formulas.

For many years, the Depth of Penetration (DoP)) test has been used to compare the protectiveness of armor materials, especially ceramics [32-34]. The DoP test measures the ballistic effectiveness of the ceramic material by looking at the penetration depth in the ductile semi-infinite backing material [9, 35, 36]. A projectile is impacted on a protected (Figure 4. 1(b)) or unprotected semi-infinite backing plate (Figure 4. 1(a)), and the penetration depths are compared. The DoP test is highly guiding in the selection of ceramic materials. However, it is well acknowledged that DOP testing does not provide the ultimate answer to determining the optimum armor design.

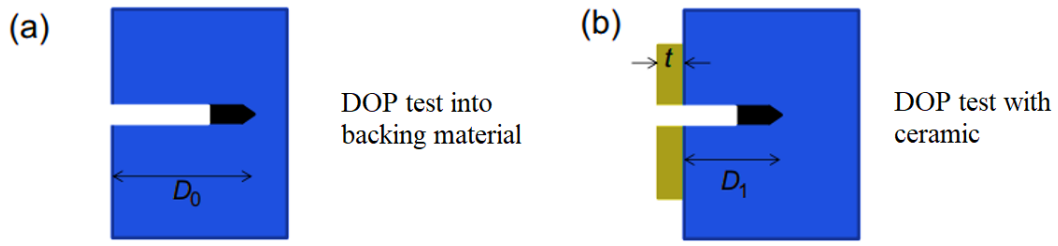

Figure 4. 1. Depth of penetration schematic

4.1. Test Setup

In order to perform the DoP test, the projectile must impact the target at a certain angle and velocity. A suitable test setup was prepared to provide desired velocity and impact angle in the DoP tests. The test setup schematic is shown in Figure 4. 2, which includes a gun, gun stand, target, and target carrier table. DoP tests were performed at the MKE Gazi Fişek Factory's shooting range. The gun and gun stand are shown in Figure 4. 3. The gun is equipped with a special barrel for reducing the deviation of bullets.

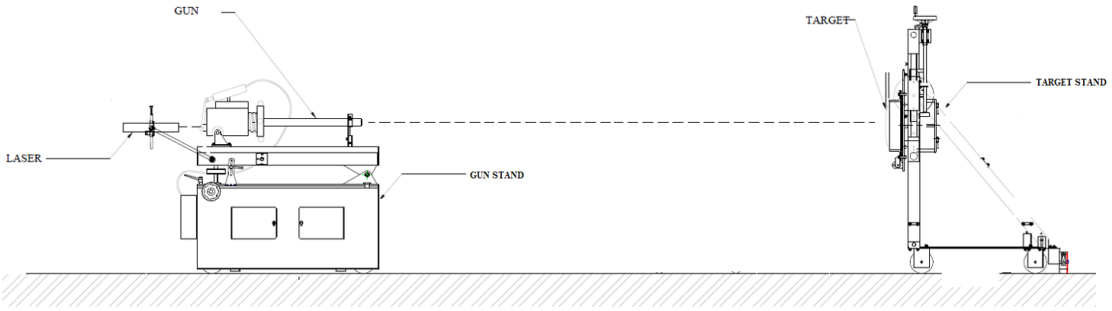

Figure 4. 2. Schematic of the test setup

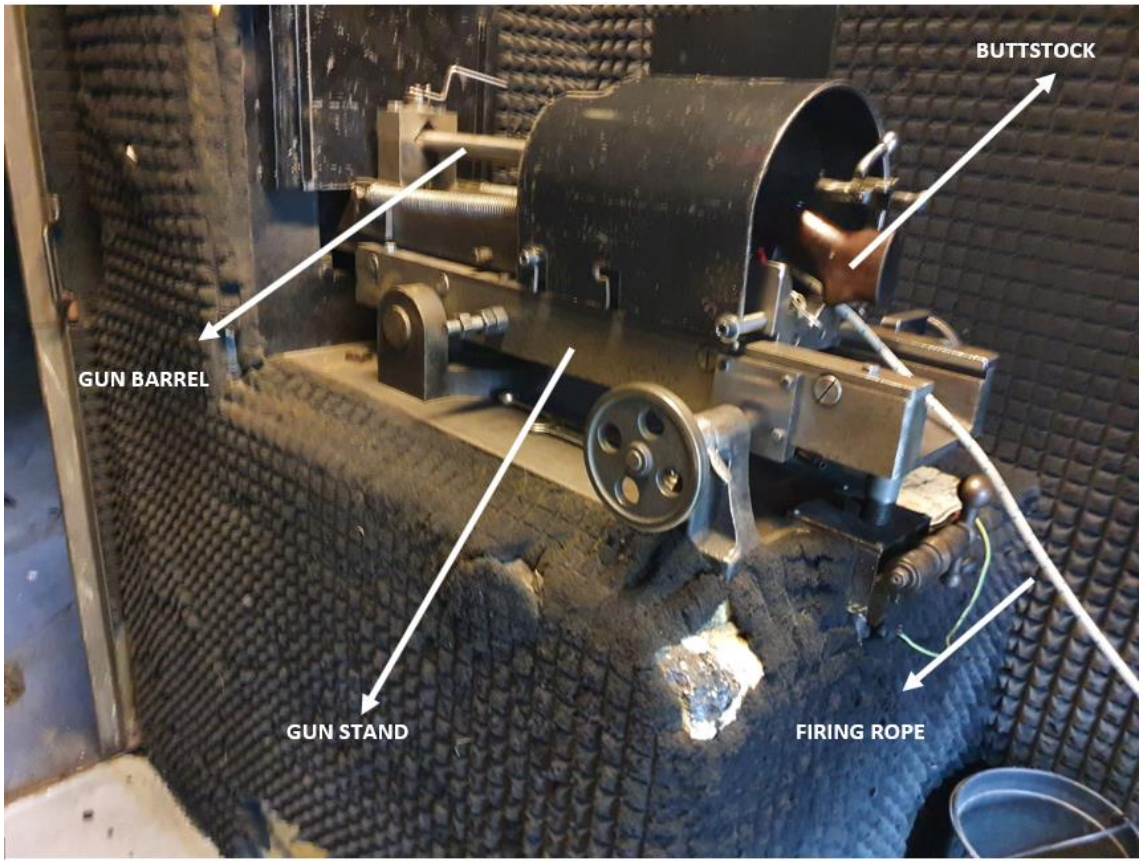

Figure 4. 3. Gun stand and mounted gun.

A suitable target carrier stand is designed and manufactured after the geometry and dimensions of the target are determined. A V-shaped bed is mounted on the stand to carry the cylindrical target. Then an apparatus is designed and manufactured to hold the target tight to the stand. The apparatus presses the target from the top so it cannot move in any direction during impact. The designed target carrier stand and apparatus are shown in Figure 4. 4 and Figure 4. 5, respectively.

Figure 4. 4. Target carrier stand with cylindrical block a) isometric view, b) side view

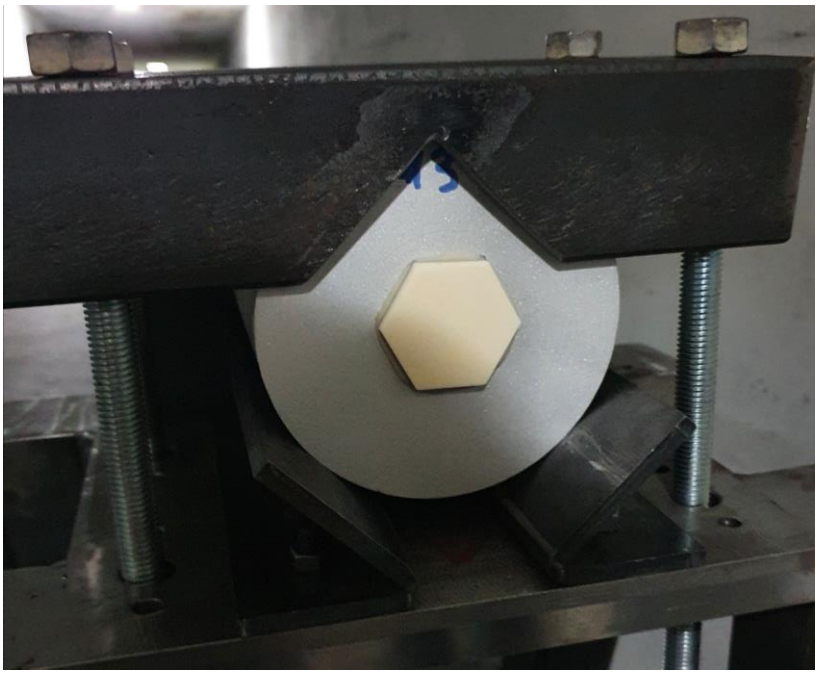

Figure 4. 5. Mounted target on the target carrier stand with the apparatus

In DoP tests, NATO M61 7,62 × 51 mm Armor Piercing (AP) bullets were used. This bullet contains a brass jacket, lead filler, and hardened steel core, as shown in Figure 4. 6. According to MKE quality policy, the cartridges must provide ±9 m/s muzzle velocity tolerance for M61. Therefore, any velocity measurement system was not used for

projectiles. In DoP tests, MKE-made same-batch cartridges were performed. MKE's external ballistic calculations show that the M61 bullet reaches ~833 m/s at ~20 m. For this reason, the target carrier stand is positioned 20 m ahead of the gun.

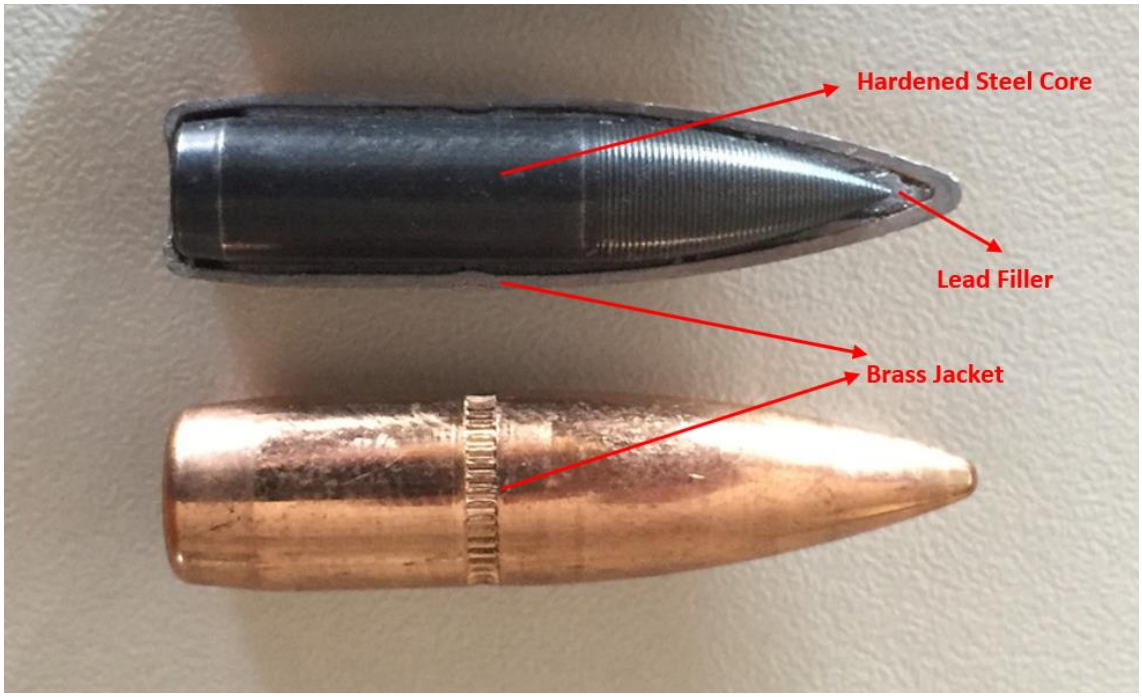

Figure 4. 6. View of the NATO M61 7,62 × 51 mm Armor Piercing Bullet

The bullets used in the DoP tests were shot from the grooved gun barrel. These bullets are spin-stabilized. The bullet's motion is illustrated in Figure 4. 7. The velocity vector is Vector-2, and the nose of the bullet follows Path-3. Therefore, there is always an angle of attack, but it is variable.

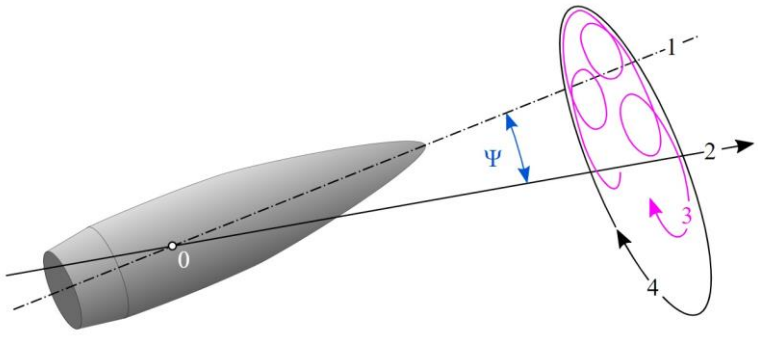

Figure 4. 7. Bullet's nose motion along the travel [37].

4.2. Ballistic Efficiency Calculation

If the areal densities of the compared ceramics are similar, they can be compared directly using DoP. However, if not, comparing the ceramic materials based only on DoP can be misleading. For this reason, some methods for calculating the efficiency of ceramics have been developed [38]. Since the efficiency calculations include the density and thickness properties of the ceramic, it offers the opportunity to compare different types of ceramic. Murat et al. [39] have developed a method for comparing the ceramic's ballistic effectiveness that is called "Ballistic Efficiency Coefficient (η)". In this study, total thicknesses were kept constant instead of areal density. Therefore, the comparisons between tested configurations were performed by Ballistic Efficiency Coefficient.

The Ballistic Efficiency Coefficient (η) is derived using areal density equivalence. The areal density is the mass per unit area, calculated by "density × thickness". The areal density equivalence and η calculation are explained step by step with the help of Figure 4. 1. In Figure 4. 1 (a) projectile penetrates the semi-infinite backing plate. All kinetic energy of the projectile is consumed by the density of the backing plate along the D_0 length. In Figure 4. 1 (b), the same projectile first perforates the ceramic and then penetrates the backing plate. The same kinetic energy is consumed by the density of the ceramic along the ceramic thickness "t" and the density of the backing plate along the D_1 length. The method claims that as the consumed kinetic energies are the same, the penetration total areal density must be the same. The areal density equivalence and ballistic efficiency coefficient calculation is shown by equation (1) and (2), respectively.

$$D_0 \times \rho_{bac} = (\eta \times \rho_{cer}\, x\, t + D_1 \times \rho_{bac}) \quad (1)$$

$$\eta = \frac{\rho_{bac}(D_0 - D_1)}{\rho_{cer} t_{cer}} \quad (2)$$

ρ_{bac} = Density of the backing plate

ρ_{cer} = Density of the ceramic tile

t = Thickness of the ceramic tile

η = Ballistic efficiency coefficient

D_0 = DOP of backing plate without ceramic

D_1 = DOP of backing plate with ceramic

4.3. Penetration Depth Determination

There are several methods for measuring the penetration depth (D_0, D_1) in the backing plate. Cutting the backing plate along the penetration hole is a standard solution. Choosing a transparent backing plate material is another option to determine penetration depth. However, in this study, the non-destructive X-Ray imaging method is selected.

At the DoP tests, the bullet's core may not travel perpendicular to the impact face of the backing plate during the penetration. The main reasons for that are the impact angle and angle of attack of the bullet, the ceramic's failure mechanism, and the deformation of the bullet's core. Taking only one X-Ray image can be misleading for maximum penetration depth measurement. For this reason, several X-Ray images were taken with different angles to determine the maximum DoP for every specimen (Figure 4. 8). Before the DoP measurement, a small procedure must be performed. Using raw images may give wrong measurements; therefore, a scale operation is performed. The aluminum backing plate diameter is known as 120 mm; according to this dimension, the X-Ray images were scaled. After the scaling procedure, penetration depths were measured on X-Ray images. Then the maximum DoP of each specimen was used to determine the ballistic efficiency of the ceramic tile configuration.

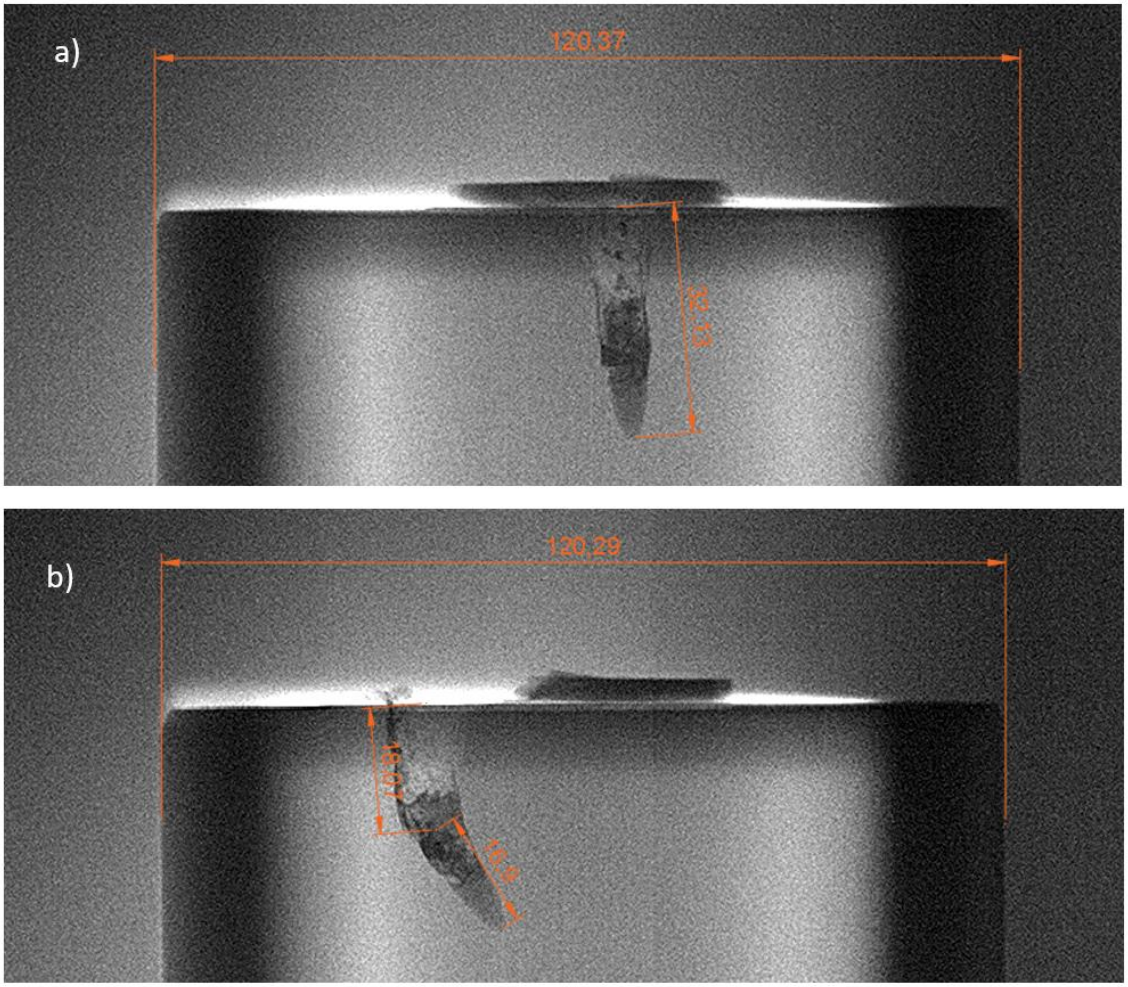

Figure 4. 8. Two X-Ray images of a DoP specimen (a) 0° position image, (b) 90° position image

4.4. Evaluation of the DoP Test

As mentioned before, the spin-stabilized bullets become more stable as they travel. In spite of their great accuracy, since the bullet hits the target before they become fully stable (20 m away), it hits the target with minor deviations. Since the surface area of ceramics is relatively small, minor deviations change the location of impact on the ceramic. Therefore, hitting the ceramic from the center could not be achieved most of the time. The observed impact locations are defined in Figure 4. 9. These are Center Impact, Non-Center Impact, Near the Edge Impact, and Edge Impact. The impact locations significantly affect the DoP results. Some of Near the Edge and all Edge Impact tests were accepted as invalid. The influence of Impact Location on the DoP results was discussed in Chapter 6. An example of each Impact Location can be seen in Figure 4. 10.

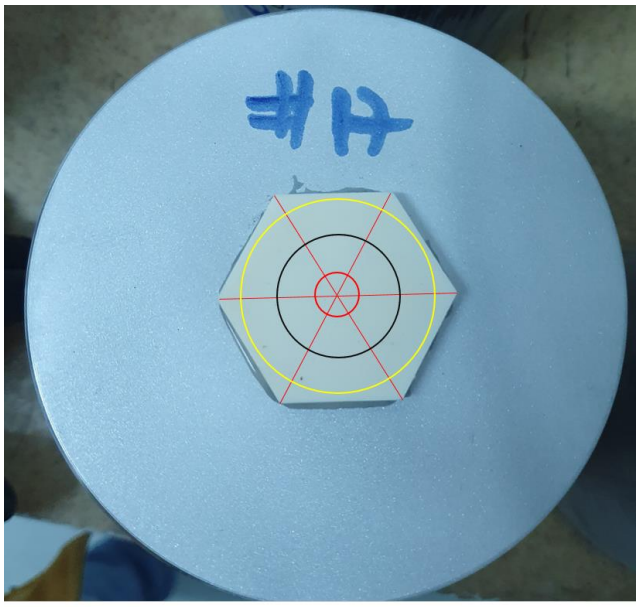

Inside of the red circle	Ø0 mm ≤ Center Impact < Ø10 mm
Between the black and red circle	Ø10 mm ≤ Non-Center Impact < Ø20 mm
Between the yellow and black circle	Ø20 mm ≤ Near the Edge Impact < Ø35 mm
Outside of the yellow circle	Ø35 mm ≤ Edge Impact

Figure 4. 9. Impact location definition on a hexagonal ceramic tile

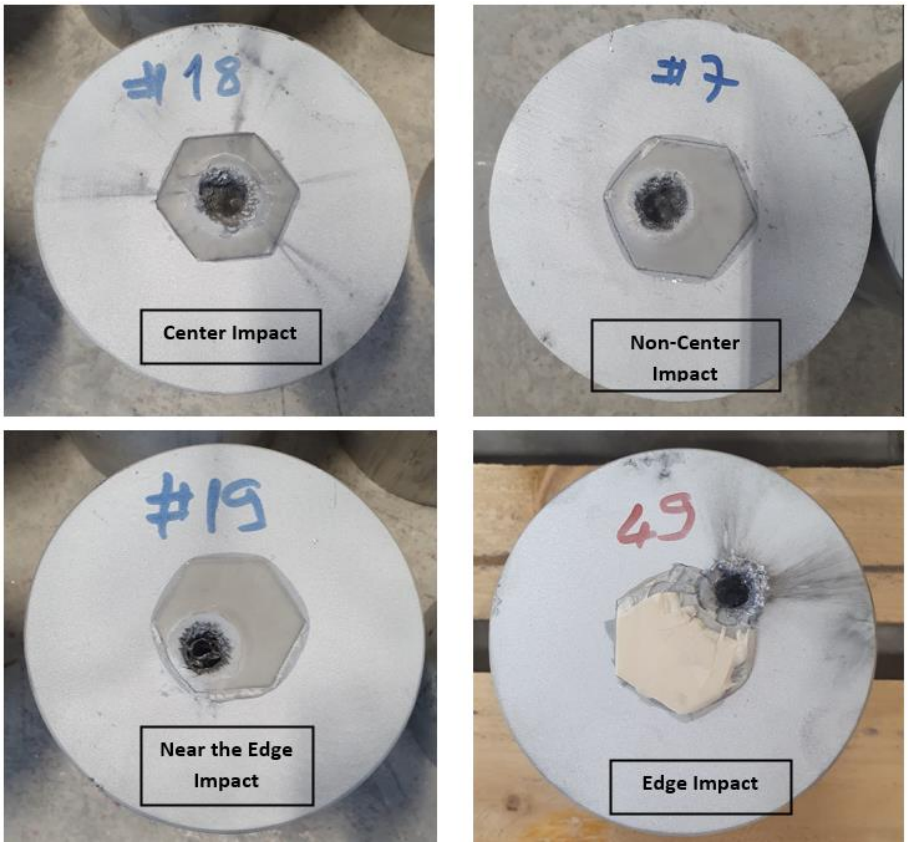

Figure 4. 10. Impact locations of the DoP Test

5. TEST SPECIMEN PROPERTIES & CONFIGURATIONS

The DoP test specimen consists of a semi-infinite backing plate, the ceramic to be tested, and the adhesive to bond the two together. The schematic of the DoP test specimen is shown in Figure 5. 1. This section explains the material, geometry, and other details of the test specimen components.

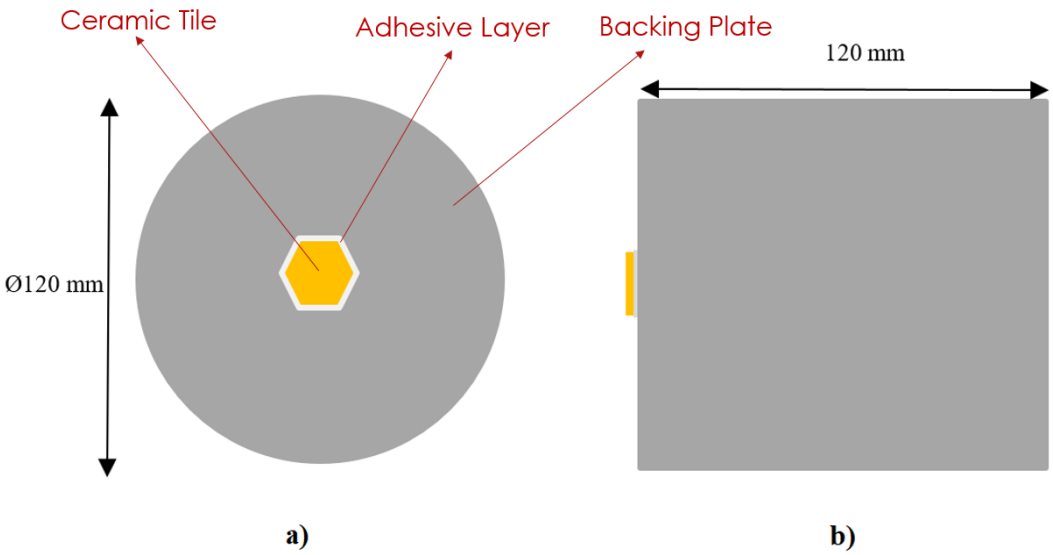

Figure 5. 1. The schematic of the DoP specimen a) front view, b) side view

5.1. Backing Plate Material and Dimension Determination

Generally, RHA steels are used as a semi-infinite backing plate in DoP tests for large caliber projectiles because penetration resolution is fair enough. Also, the target of the large caliber projectiles is generally land vehicles made of RHA steel. Therefore, it gives intuition to armor designers about vehicle protection [35, 40]. However, for small-caliber projectiles, the RHA steel backing plate is not proper. Due to the high density and strength of the RHA steels, very low DoP is observed when small-caliber projectiles are performed. A relatively low-density backing material, such as aluminum, is suggested to improve DoP measurement resolution for better differentiation of the data [35, 36]. Due to this reason, AA6061-T6 material is selected for the backing plate.

A preliminary finite element analysis was done to determine the thickness and diameter of the AA6061-T6 backing plate. In pre-FE analysis, a 7.62 × 51 mm AP projectile is

penetrated into AA6061-T6 material without any ceramic. Due to the analysis result, the Ø120 × 120 mm cylinder block (Figure 5. 1) was found to be enough for a semi-infinite backing plate. The penetration hole is sufficiently far from the ends in all directions.

The backing material has a substantial impact on the ballistic efficiency calculations. The inconsistencies in the properties of the backing material have a significant impact on the ballistic efficiency calculation. Due to this reason, the same batch of the AA6061-T6 backing plate is used during the DoP tests.

5.2. Ceramic Tiles

Various ceramics have been purchased to investigate the ballistic efficiency of layered ceramic structures. These are the most commercially available armor-grade Al_2O_3, SiC, and B_4C ceramics. The shapes, geometric dimensions, and materials of the purchased ceramics are shown in Figure 5. 2. The ceramic's mechanical properties are shown in Table 5. 1.

a)

Hexagon Height: 40 mm	Al2O3	SiC	B4C
Thickness	-	2 mm	2 mm
	3 mm	3 mm	3 mm
	5 mm	5 mm	-

b)

Square 50 x 50 mm	Al2O3	SiC
Thickness	3 mm	3 mm
	5 mm	5 mm
	7 mm	7 mm
	-	8 mm
	-	9 mm

Figure 5. 2. Purchased armor-grade ceramics

Table 5. 1. Purchased ceramic's mechanical properties

Ceramic	**Density [kg/m^3]**	**Hardness (HV)**	**Fracture Toughness K_{ic} [MPa×m$^{1/2}$]**	**Flexural Strength (GPa)**
99% Al_2O_3	>3850	1600	4.5	375
Sintered SiC	>3150	2700	3.2	570
HP B_4C	>2500	3200	4	410

5.3. Adhesive Material Selection and Thickness Determination

As mentioned in the introduction part of the study, several adhesive types can be used in bonding ceramic tile and backing plate. Polyurethane (PU) based and Epoxy-based adhesives are the most popular ones. PU-based adhesives are generally preferred to satisfy multiple impact criteria in armor systems, but in the DoP test, the specimen experience only one impact. Epoxy has a relatively close acoustic impedance to ceramic than PU (Table 2. 2); thus, Epoxy-based adhesive was selected as the adhesive type. Araldite® 2015 is a strong epoxy adhesive generally used for structural bonding. Also, the mechanical properties of the Araldite® 2015 can be found in the literature. Therefore, Araldite® 2015 was selected for ceramic-ceramic and ceramic-backing plate bonding.

López-Puente et al. [21] studied the effect of the thickness of the adhesive layer on ballistic performance, and according to the results, 0.3 mm thickness is found to be the best for ballistic performance. Based on this study, ~0.3 mm adhesive is applied to the ceramic-ceramic bonding and ceramic-backing plate bonding. A prepared DoP specimen is shown in Figure 5. 3.

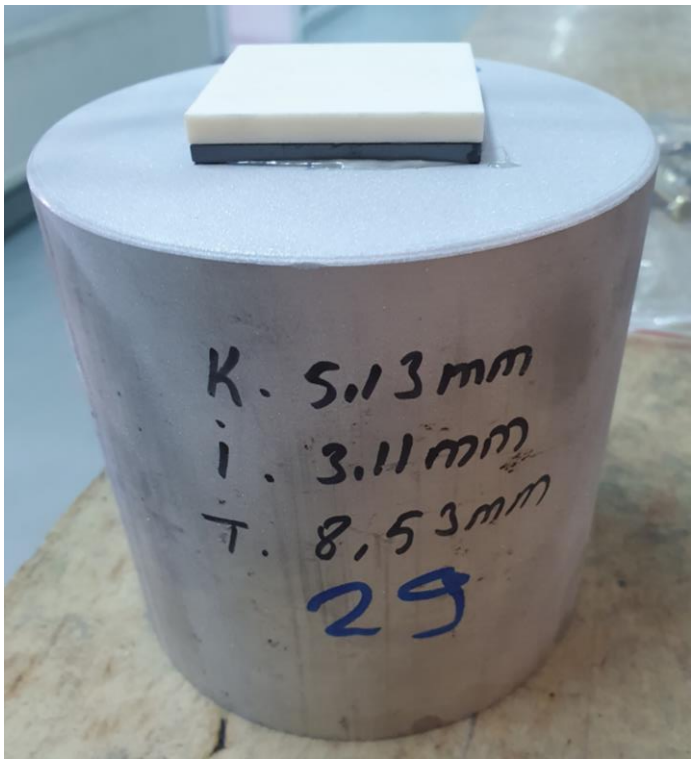

Figure 5. 3. A DoP test specimen

5.4. Sample Preparation

To maintain the consistency of sample preparation, a method was followed.

1) Aluminum 6061-T6 bars (120 Ø × 3000 mm) were purchased,
2) 120 Ø × 120 mm Aluminum blocks were cut from the bar,
3) Grit-blasting surface treatments were applied to the bonding surface of the Aluminum blocks,
4) Surface cleaning of aluminum blocks was performed with proper chemicals (e.g., Isopropyl Alcohol, etc.),
5) To avoid external cracks, visually inspected ceramic tiles were selected,
6) To avoid internal cracks, X-Ray photography of the selected ceramic tiles was taken (Figure 5. 4),
7) Surface cleaning of ceramic tiles was performed with proper chemicals,
8) Some Araldite® 2015 was applied between ceramic and aluminum block,
9) 2 kg weight was put on the ceramic during curing time. This weight maintains the approximately 0.3 mm adhesive thickness. With the help of weight, excess adhesive overflows from the sides of the ceramic tile,
10) The adhesive was cured at room temperature for at least 48 hours,

11) If there was a second ceramic tile for bonding, some Araldite® 2015 was applied between ceramic tiles and repeated the 9th and 10th processes.

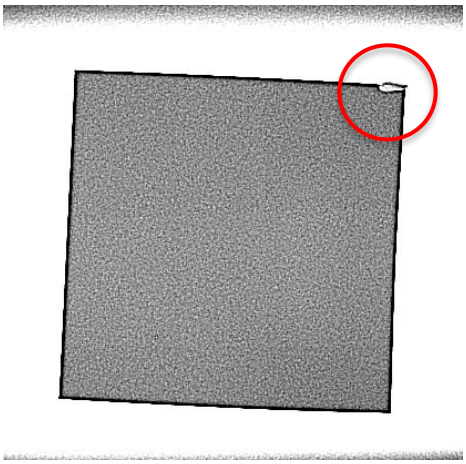

Figure 5. 4. X-Ray image of a square ceramic tile (an external on crack right-top corner)

5.5. DoP Test Configurations

Various test configurations were manufactured to investigate LCS with different materials and LCS with the same materials by the DoP method. In this study, two types of geometry (hexagonal and square (Figure 5. 2)) and three types of ceramic material (Al_2O_3, SiC, and B_4C) were used. The hexagonal test configurations are shown in Table 5. 2; the square test configurations are shown in Table 5. 3. The configurations are represented with a code name; Alu, SiC, and BC prefixes represent the Aluminum-Oxide, Silicon-Carbide, and Boron-Carbide, respectively. The number that comes after the prefix represents the ceramic tile's thickness. For instance, Configuration #1 has a hexagonal, 5 mm thickness Silicon-Carbide ceramic tile.

Hazel et al. showed that the ceramic tile size and geometry notably affect ballistic protection [20]. Therefore, the hexagonal and square ceramics are compared within themselves to eliminate the geometrical effects of the ceramics. The hexagonal ceramic tiles with a total thickness of 5 mm and 6 mm and square ceramic tiles with a total thickness of 6 mm and 8 mm were examined.

Table 5. 2. Hexagonal DoP test configurations

Configuration Number	Configuration Code		Total Ceramic Thickness	Geometry
	Strike Face Ceramic	Backing Face Ceramic		
#0	(Only Backing Plate)			No Ceramic
#1	SiC5	-	5 mm	Hexagonal
#2	SiC3	SiC2		
#3	SiC2	SiC3		
#4	BC3	SiC2		
#5	Alu3	SiC2		
#6	BC3	SiC3	6 mm	
#7	SiC3	Alu3		
#8	BC3	Alu3		

Table 5. 3. Square DoP test configurations

Configuration Number	Configuration Code		Total Ceramic Thickness	Geometry
	Strike Face Ceramic	Backing Face Ceramic		
#9	SiC8	-	8 mm	Square
#10	SiC5	SiC3		
#11	SiC3	SiC5		
#12	SiC5	Alu3		
#13	Alu5	Alu3		
#14	SiC3	SiC3	6 mm	
#15	SiC3	Alu3		
#16	Alu3	Alu3		

6. DOP TEST COMPARISONS

In this chapter, LCS with the same material and LCS with different materials were examined using Ballistic Efficiency Coefficients that were calculated using DoP. The ballistic performance of LCS with the same material was investigated by comparing it with monolithic ceramic. This comparison revealed the influence of the LCS with the same material. The LCS with different materials was investigated by comparing it with LCS with the same material. This comparison revealed the influence of the different strike face materials.

6.1. DoP Test Without Ceramic

Ballistic Efficiency Coefficient (η) calculations were shown in Equations 1 & 2. For this calculation DoP of the backing plate without ceramic value (D_0) is needed. Therefore, initially, the backing plates without ceramic were tested (Figure 6. 1). Two shots were fired to the backing plate, and the DoP results of the tests can be seen in Table 6. 1. When DoP results were compared, consistent penetration depth values were observed. While making Ballistic Efficiency Coefficient calculations, 50.81 mm penetration depth is taken as a $D_{0,}$ which is the average value of these two shots. The X-Ray measurements can be seen in Appendix II.

Table 6. 1. Penetration depth of the ceramic-free backing plate

Config. No.	Specimen No.	Ceramic Code	Strike Face Ceramic Thickness [mm]	Rear Face Ceramic Thickness [mm]	Ceramic Areal Density [kg/m2]	Test No.	DoP [mm]	Ballistic Efficiency Coefficient	Impact Location
#0	1	-	-	-	-	1	51,85	-	-
	2					2	49,77		

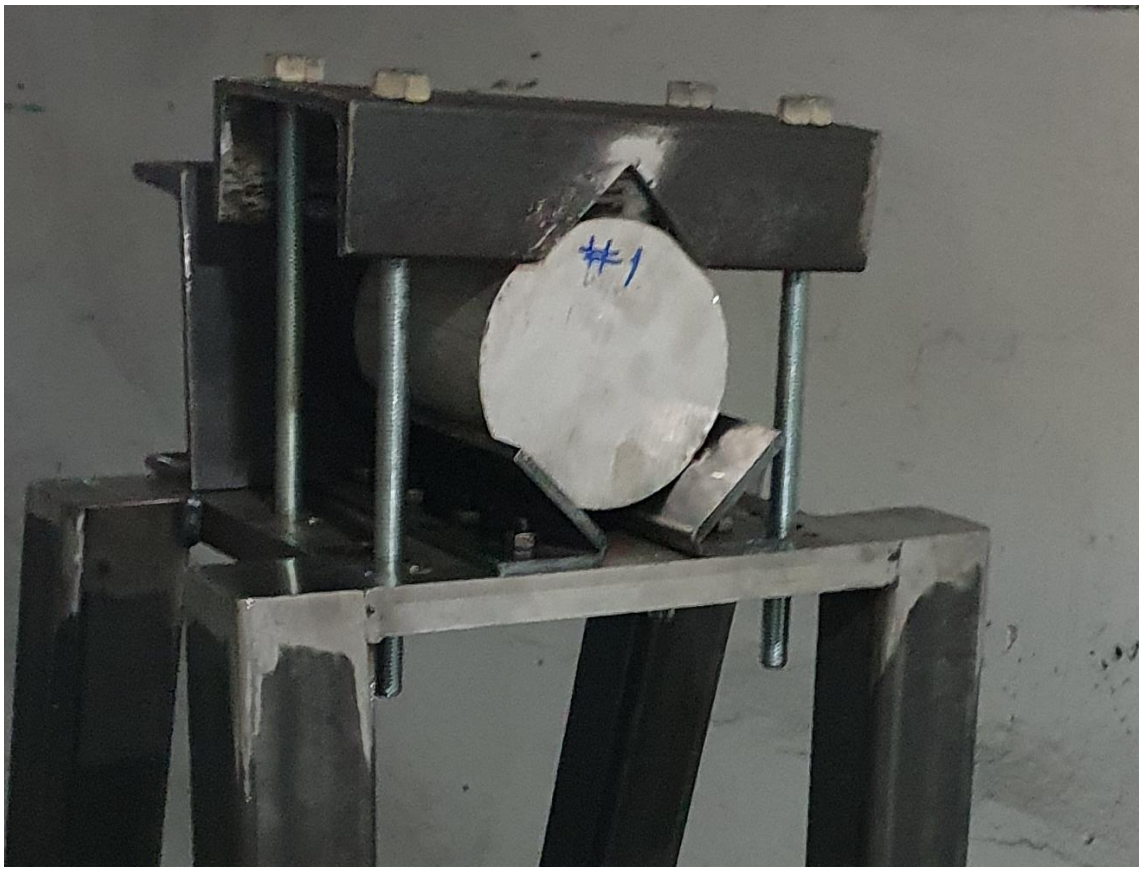

Figure 6. 1. Test Specimen #1: DoP test without ceramic

6.2. Hexagonal Ceramic Tiles DoP Tests

In this section, LCS with the same material and LCS with different materials were investigated by hexagonal ceramic tiles. The layered ceramic structures were created with a 5 and 6 mm total thickness.

6.2.1. 5 mm Total Ceramic Tile Thickness

With available hexagonal ceramic tiles, five configurations with a total thickness of 5 mm were created. The created configurations are shown in Table 5. 2 (Config. #1 to #5). Two comparisons were generated from these five configurations to understand the layered ceramic structure phenomena. These comparisons are shown in Table 6. 2.

Table 6. 2. Comparison table of the hexagonal 5 mm total ceramic tile thickness configurations

Comparison No.	Config. Code	Config. Code	Config. Code
1	SiC5	SiC3+SiC2	SiC2+SiC3
2	SiC3+SiC2	BC3+SiC2	Alu3+SiC2

Comparison #1 is made between monolithic and LCS with the same material. This comparison examines the difference between a single layer and two layers. While creating the layered 5 mm thick ceramic structure, 3 mm and 2 mm ceramics were used. For this reason, two configurations were created using 3 mm and 2 mm thick ceramics on the strike face. Comparison #2 is made between LCS with the same material and LCS with different materials. In this comparison, the rear ceramic of SiC3+SiC2 was kept, and the strike face ceramic was changed to BC3 and Alu3. The DoP tests were performed with these test specimens; the test results are shown in Table 6. 3. The post-test condition of specimens can be seen in Appendix I, and the X-Ray images of all specimens can be seen in Appendix II.

Table 6. 3. DoP configurations of hexagonal 5 mm total ceramic tile thickness

Config. No.	Specimen No.	Config. Code	Strike Face Ceramic Thickness [mm]	Rear Face Ceramic Thickness [mm]	Ceramic Areal Density [kg/m2]	Test No.	DoP [mm]	Ballistic Efficiency Coefficient	Impact Location
1	5	SiC5	5.20	-	16.59	1	7.55	7.04	Center
	6		5.14	-	16.4	2	19.08	5.22	Near the Edge
	18		5.10	-	16.27	3	11.14	6.58	Center
2	7	SiC3+SiC2	3.10	2.15	16.75	1	16.21	5.58	Non-Center
	8		3.10	2.16	16.78	2	16.51	5.52	Non-Center
	19		3.11	2.18	16.88	3	19.57	5	Near the Edge
3	9	SiC2+SiC3	2.10	3.13	16.68	1	21.9	4.68	Non-Center
	10		2.14	3.15	16.88	2	22.74	4.49	Near the Edge
4	40	BC3+SiC2	3.20	2.14	14.86	1	25.77	4.55	Non-Center
	41		3.12	2.17	14.75	2	28.16	4.15	Non-Center
5	42	Alu3+SiC2	3.15	2.13	19.1	1	20.99	4.22	Non-Center
	43		3.07	2.15	18.85	2	25.18	3.67	Near the Edge

Some test results have large deviations in terms of Ballistic Efficiency Coefficient in repeated tests. It was detected that the only difference was the impact location of the bullet. Then the test results were investigated considering the impact location, and it was revealed that Ballistic Efficiency decreases as the impact location shifts from the center to the edge. Center and Non-Center impact location's test results are similar and consistent. However, Near-the-Edge or Edge impact location's test results generally have lower Ballistic Efficiency. All Edge impact conditions and some Near-the-Edge impact conditions (%15 or move deviate from Center or Non-Center impact conditions) were accepted as invalid tests. Therefore, Specimen #6 was excluded from the evaluation. The Ballistic Efficiencies of the hexagonal 5 mm total ceramic tile and impact locations were visualized in Figure 6. 2, and the invalid test was marked by a red circle.

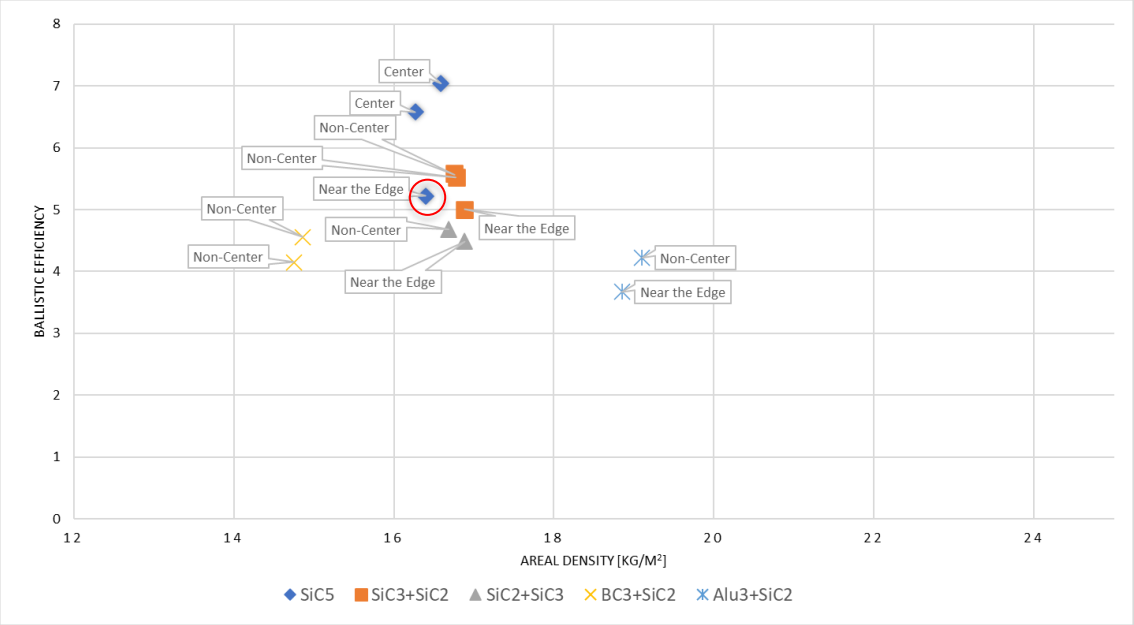

Figure 6. 2. Areal Density vs. Ballistic Efficiency of hexagonal 5 mm total ceramic tile

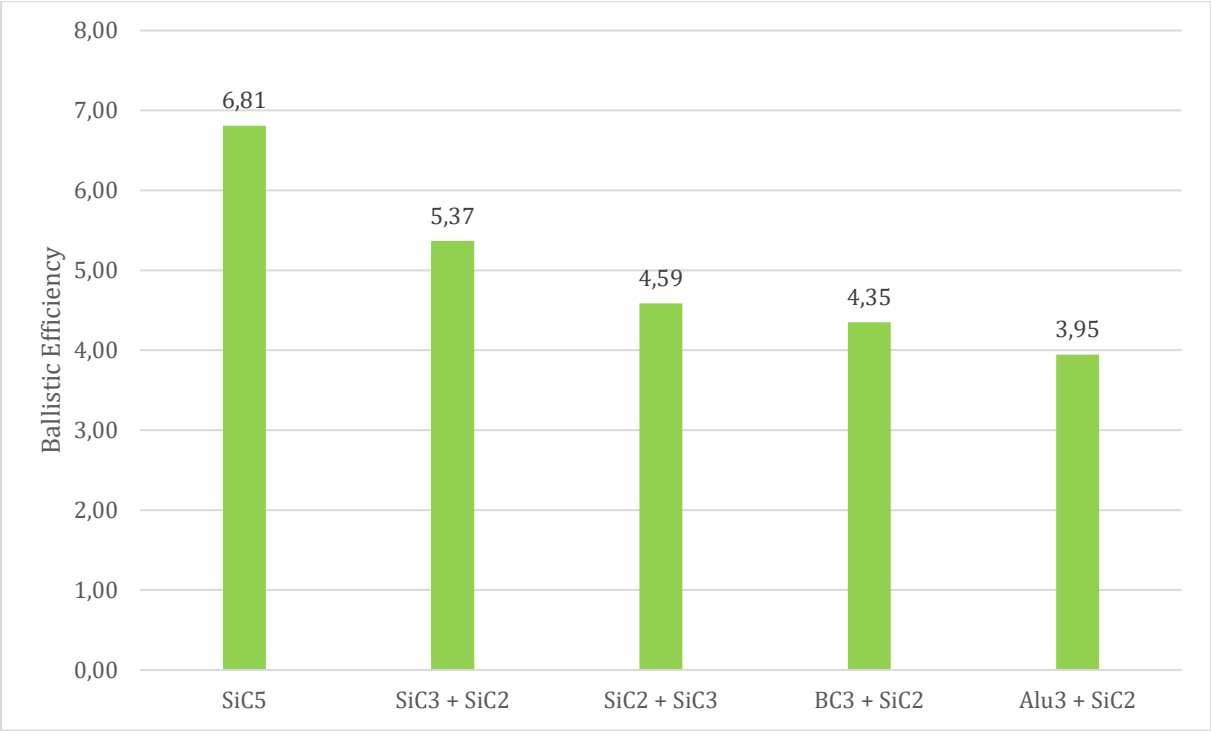

Figure 6. 3. Average results of the Ballistic Efficiencies of 5 mm hexagonal ceramic tiles

The average Ballistic Efficiency results were summarized in Figure 6. 3. For Comparison #1; monolithic SiC5 ceramic has higher Ballistic Efficiency than SiC3+SiC2 and SiC2+SiC3 layered ceramic structures. While LCS with the same material were compared within themselves, it is observed that SiC3+SiC2 provides better ballistic protection than SiC2+SiC3. If the Ballistic Efficiency of SiC5 is accepted as 100%, SiC3+SiC2 has 79%, and SiC2+SiC3 has 67% Ballistic Efficiency. As a result of Comparison #1, two main conclusions were revealed. The first conclusion is that monolithic ceramic provides the relatively best ballistic protection. The second conclusion is that when the thicker ceramic is positioned on the strike face in LCS, the Ballistic Efficiency is relatively high. Therefore, in the following tests, the thicker ceramic is positioned on the strike face of the LCS.

For Comparison #2, the average Ballistic Efficiency (Figure 6. 3) results of Configuration #2, #4, and #5 were investigated. It was observed that the SiC3+SiC2 layered ceramic structure provides relatively higher Ballistic Efficiency between them. When LCS with different materials were compared, BC3+SiC2 provided slightly better protection than Alu3+SiC2. If the average ballistic efficiency of SiC3+SiC2 is accepted as 100%, BC3+SiC2 has 81%, and Alu3+SiC2 has 74% Ballistic Efficiency.

6.2.2. 6 mm Total Ceramic Tile Thickness

With available hexagonal ceramic tiles, three configurations (SiC3+Alu3, BC3+Alu3, and BC3+SiC3) with a total thickness of 6 mm were created. Two comparisons (Comparison #3 and #4) were created with these three configurations to understand the LCS with different materials phenomena. These comparisons are shown in Table 6. 4.

Table 6. 4. Comparison table of the hexagonal 6 mm total ceramic tile thickness configurations

Comparison No.	**Config. Code**	**Config. Code**
3	SiC3+Alu3	BC3+Alu3
4	BC3+SiC3	BC3+Alu3

In these configurations, relatively hard ceramic is positioned on the strike face. In Comparison #3, the effect of the strike-face ceramic material was studied by keeping the rear ceramic the same. In Comparison #4, the effect of the rear ceramic material was examined by keeping the strike-face ceramic the same. The DoP tests were performed with these test specimens; the test results are shown in Table 6. 5. The post-test condition of specimens can be seen in Appendix I, and the X-Ray images of all specimens can be seen in Appendix II.

Table 6. 5. DoP configurations of hexagonal 6 mm total ceramic tile thickness

Config. No.	Specimen No.	Config. Code	Strike Face Ceramic Thickness [mm]	Rear Face Ceramic Thickness [mm]	Ceramic Areal Density [kg/m2]	Test No.	DoP [mm]	Ballistic Efficiency	Impact Location
6	47	BC3+SiC3	3.09	3.28	18.22	1	26.24	3.64	Near the Edge
	48		3.1	3.12	17.73	2	15.19	5.42	Non-Center
7	49	SiC3+Alu3	3.16	3.09	22.15	1	34.97	2.01	Edge
	50		3.14	3.14	22.28	2	10.98	4.83	Non-Center
8	51	BC3+Alu3	3.06	3.2	20.18	1	15.79	4.69	Non-Center
	52		3.06	3.1	19.79	2	11.17	5.41	Center

As mentioned, the tests with Edge and some Near-the-Edge impact locations were excluded from the evaluation. Therefore, Specimen #47 and #49 were excluded. Due to the exclusion of these tests, BC3+SiC3 and SiC3+Alu3 configurations were evaluated with only one test. The Ballistic Efficiencies of the hexagonal 6 mm total ceramic tile and impact locations were visualized in Figure 6. 4, and the invalid test was marked by red circles.

The average Ballistic Efficiency results are summarized in Figure 6. 5. In Comparison #3; it was expected that the BC3+Alu3 configuration would have a higher ballistic efficiency because the Boron-Carbide is relatively harder. The test results showed that BC3+Alu3 has ~5% higher average Ballistic Efficiency than SiC3+Alu3. The expectation was satisfied.

In Comparison #4, it was expected that the BC3+Alu3 configuration would have a higher ballistic efficiency because the Alumina is relatively tougher. The test results showed that BC3+SiC3 has ~7% higher average ballistic efficiency than BC3+Alu3. The BC3+SiC3 performed slightly higher ballistic efficiency; therefore, the expectation was not satisfied. As mentioned in Table 5. 1, the Al_2O_3 has higher fracture toughness than SiC, but SiC has higher hardness than Al_2O_3. Comparison #4 was shown that not only toughness but also hardness is vital in rear ceramics.

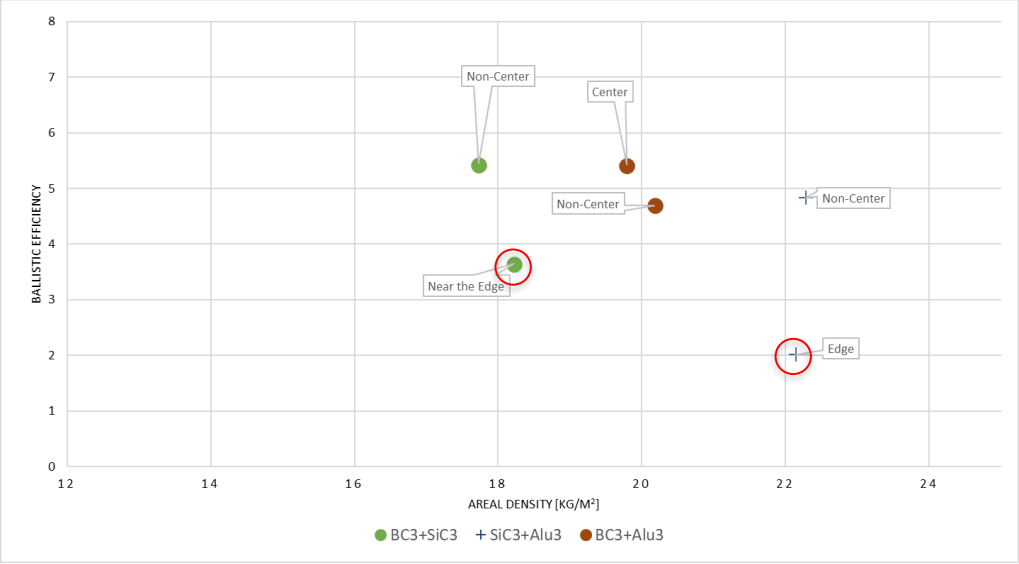

Figure 6. 4. Areal Density vs. Ballistic Efficiency of hexagonal 6 mm total ceramic tile

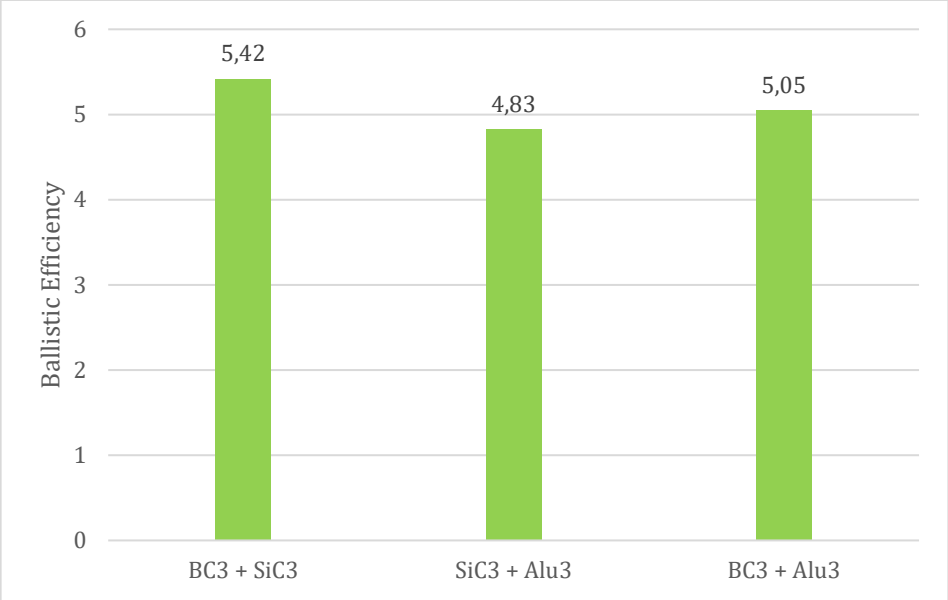

Figure 6. 5. Average results of the Ballistic Efficiency of 6 mm hexagonal ceramic tiles

6.3. Square Ceramic Tiles DoP Tests

In this section, LCS with the same material and LCS with different materials were investigated by square ceramic tiles. The layered ceramic structures were created with an 8 and 6 mm total thickness.

6.3.1. 8 mm Total Ceramic Tile Thickness

With available square ceramic tiles, six configurations with a total thickness of 8 mm were created. The created configurations are shown in Table 5. 3 (Config. #9 to #13). Two comparisons were generated with these six configurations to understand the LCS with the same material and LCS with different materials phenomena. These comparisons are shown in Table 6. 6. The post-test condition of specimens can be seen in Appendix I.

Table 6. 6. Comparison table of the square 8 mm total ceramic tile thickness configurations

Comparison No.	Config. Code	Config. Code	Config. Code
5	SiC8	SiC5+SiC3	SiC3+SiC5
6	SiC5+SiC3	Alu5+Alu3	SiC5+Alu3

Comparison #5 is made between monolithic and LCS with the same material. This comparison examines the difference between a single layer and two layers, as in Comparison #1. While creating the layered 8 mm thick ceramic structure, 5 mm and 3 mm ceramics were used. For this reason, two configurations were created using 5 mm and 3 mm thick ceramics on the strike face. Comparison #6 is made between LCS with the same material and LCS with different materials. In Comparison #6, there are two LCS with the same material (SiC5+SiC3, Alu5+Alu3) and one LCS with different materials (SiC5+Alu3). The DoP tests were performed with these test specimens; the test results are shown in Table 6. 7.

Table 6. 7. DoP configurations of square 8 mm total ceramic tile thickness

Config. No.	Specimen No.	Config. Code	Strike Face Ceramic Thickness [mm]	Rear Face Ceramic Thickness [mm]	Ceramic Areal Density [kg/m2]	Test No.	DoP [mm]	Ballistic Efficiency	Impact Location
9	11	SiC8	8.15	-	26.00	1	0	-	Non-Center
	12		8.12	-	25.90	2	0	-	Non-Center
10	13	SiC5+SiC3	5.12	3.13	26.32	1	0	-	Center
	14		5.18	3.12	26.48	2	0	-	Non-Center
11	15	SiC3+SiC5	3.13	5.16	26.45	1	0	-	Non-Center
	16		3.16	5.15	26.51	2	0	-	Non-Center
12	27	SiC5+Alu3	5.13	3.05	28.27	1	0	-	Non-Center
	28		5.13	3.1	28.47	2	0	-	Non-Center
13	31	Alu5+Alu3	5.09	3.09	31.94	1	0	-	Center
	32		5.13	3.07	32.02	2	0	-	Non-Center

DoP tests were performed for square 8 mm total thickness ceramic tiles, and penetration depth was not observed in any test. Only small crater formations were observed on the backing plates. Therefore, the Ballistic Efficiencies cannot be calculated.

SiC8, SiC5+SiC3, and SiC3+SiC5 configurations have similar areal densities; therefore, they can be compared without the Ballistic Efficiency calculation. Some comments could be made about the test results by visual inspection. As shown in Figure 6. 6, the three similar areal density configurations were investigated. According to visual inspection, the SiC8 configuration has the least damaged zone and crater depth. SiC5+SiC3

configuration has a relatively wider damaged zone; however, crater depth is similar to SiC8. SiC3+SiC5 configuration has some scars which belong to the bullet's hardened core. The damaged zone is relatively narrow than SiC5+SiC3; however, crater depth is relatively higher. Based on these comments, protection levels can be evaluated as SiC8 has the relatively best protection, SiC5+SiC3 has relatively second-best protection, and SiC3+SiC5 has the relatively worst protection. These results are consistent with Comparison #1 (Hexagonal LCS with the same material) tests.

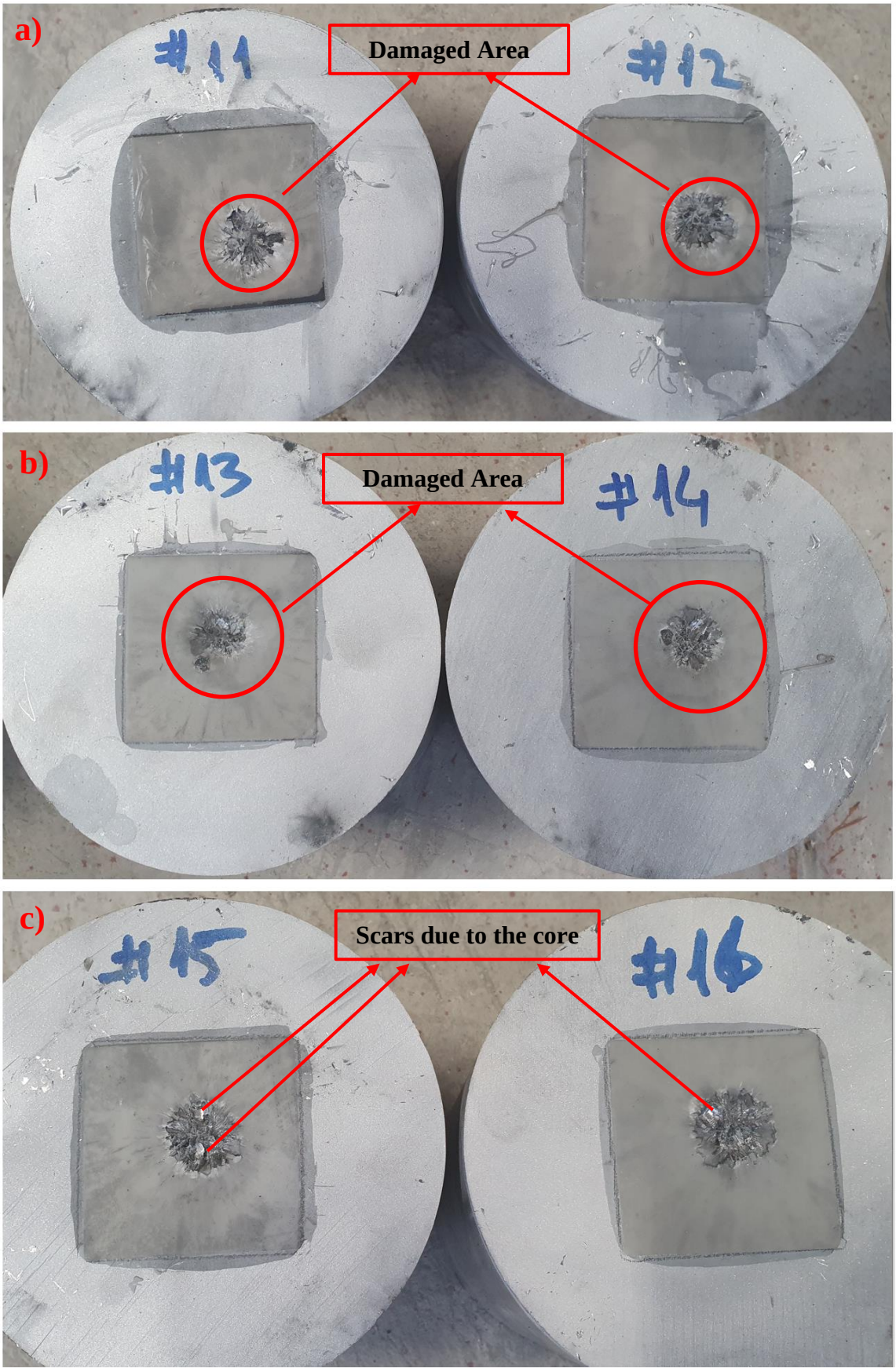

Figure 6. 6. Visual inspection of similar areal density configurations: a) SiC8, b) SiC5+SiC3, c) SiC3+SiC5 configurations

6.3.2. 6 mm Total Ceramic Tile Thickness

With available square ceramic tiles, three configurations with a total thickness of 6 mm were created. The created configurations are shown in Table 5. 3 (Config. #14 to #16). Comparison #7 was generated from these four configurations to understand the LCS with different materials phenomena. These comparisons are shown in Table 6. 8. The post-test condition of specimens can be seen in Appendix I, and the X-Ray images of all specimens can be seen in Appendix II.

Table 6. 8. Comparison table of the square 6 mm total ceramic tile thickness configurations

Comparison No.	Config. Code	Config. Code	Config. Code
7	SiC3+SiC3	Alu3+Alu3	SiC3+Alu3

Comparison #7 was made between LCS with the same material and LCS with different materials. In this comparison, all ceramic thicknesses are equal. The DoP tests were performed with these test specimens; the test results are shown in Table 6. 9.

Table 6. 9. DoP configurations of square 6 mm total ceramic tile thickness

Config. No.	Specimen No.	Config. Code	Strike Face Ceramic Thickness [mm]	Backing Face Ceramic Thickness [mm]	Ceramic Areal Density [kg/m2]	Test No.	DoP [mm]	Ballistic Eff.	Impact Location
14	53	SiC3+SiC3	3.16	3.16	20.16	1	8.34	5.69	Center
	54		3.15	3.17	20.16	2	11.85	5.22	Near the Edge
15	55	SiC3+Alu3	3.15	3.11	22.19	1	9.01	5.09	Non-Center
	56		3.18	2.97	21.74	2	16.83	4.22	Near the Edge
16	57	Alu3+Alu3	3	3.06	23.66	1	10.55	4.59	Non-Center
	58		3.06	3.12	24.13	2	10.17	4.55	Non-Center

As mentioned, the tests with Edge and some Near-the-Edge impact locations were excluded from the evaluation. Therefore, Specimen #56 was excluded. Due to the exclusion of Specimen #56, the SiC3+Alu3 configuration was evaluated with only one test. The Ballistic Efficiencies of the square 6 mm total ceramic tile and impact locations were visualized in Figure 6. 7, and the invalid test was marked by a red circle.

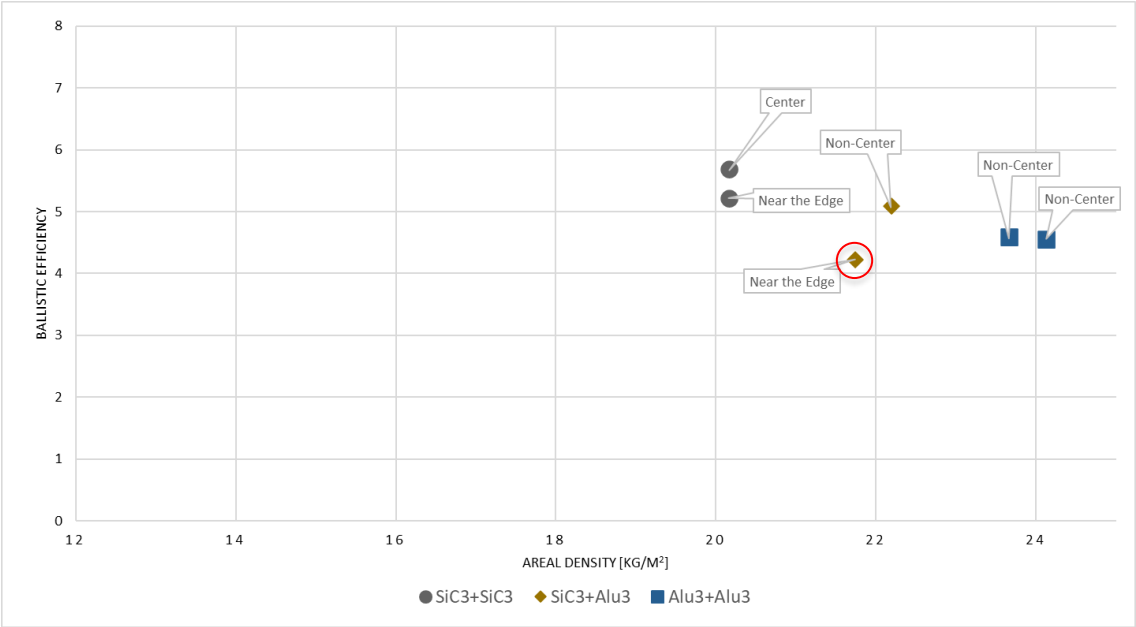

Figure 6. 7. Areal Density vs. Ballistic Efficiency of square 6 mm total ceramic tile

Average efficiency results are summarized in Figure 6. 8. The SiC3+SiC3 configuration provides the relatively best protection between them. If the average ballistic efficiency of SiC3+SiC3 is accepted as 100%, SiC3+Alu3 has 93%, and Alu3+Alu3 has 84% ballistic efficiency. This means that the ballistic efficiency of the SiC3+Alu3 is closer to SiC3+SiC3 than Alu3+Alu3.

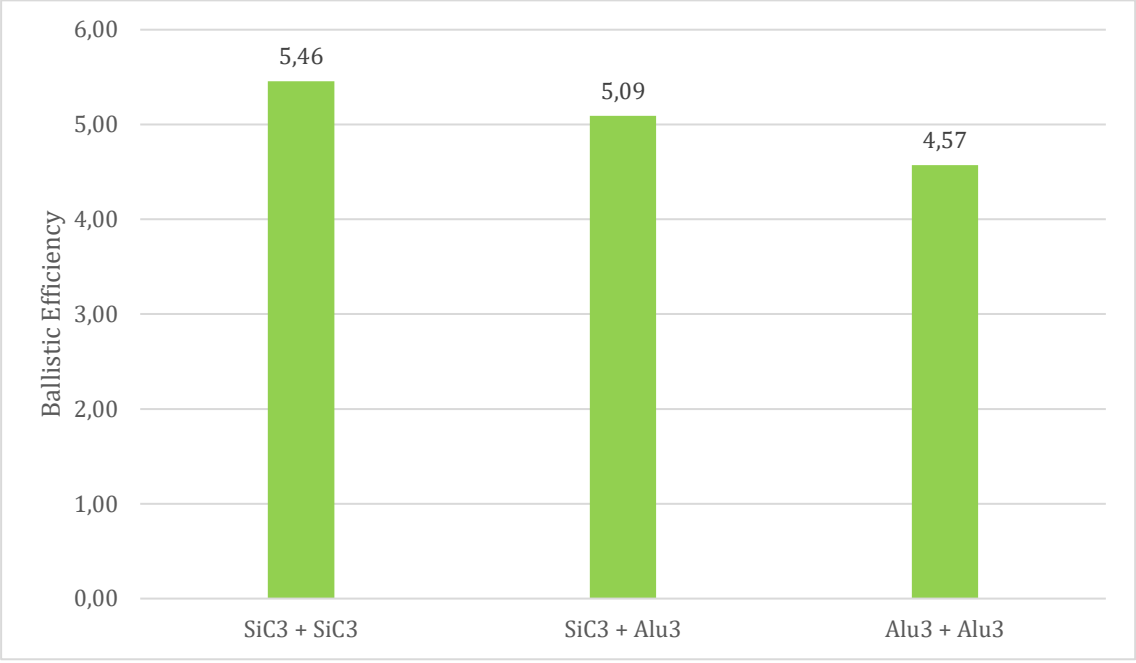

Figure 6. 8. Average results of the Ballistic Efficiency of 6 mm square ceramic tiles

6.4. Conclusion of the DoP Test Results

Monolithic ceramic structures, LCS with the same material, and LCS with different materials were investigated by Depth of Penetration Tests and compared by Ballistic Efficiency Coefficient. Hazel et al. showed that the ceramic tile size and geometry notably affect ballistic protection [20]. Therefore, each geometry is compared within itself in this study to avoid the geometrical effects on the results.

6.4.1. Layered Ceramic Structure with the Same Material

The layered ceramic structures were investigated by using 5 mm Hexagonal and 8 mm Square ceramics. Two comparisons were conducted and shown in Table 6. 10. The table shows the configurations and results of the tests. In Comparison #1, Ballistic Efficiency Coefficients clearly are shown that monolithic ceramic provides better ballistic performance than two-layered configurations. Also, Comparison #5 supports the same argument. In Comparison #5 tests, ballistic efficiency could not be calculated. However, by visual inspection, it can be clearly said that monolithic ceramic provides better protection than layered ceramics. These conclusions are consistent with studies of Carton et al.'s [3] and Polla et al.'s [7].

Table 6. 10. Summary of the LCS with the same material results.

	Config. Code (Average Ball. Efficiency)	**Config. Code (Average Ball. Efficiency)**	**Config. Code (Average Ball. Efficiency)**
Comparison #1 (Hexagonal)	SiC5 (6.81)	SiC3+SiC2 (5.37)	SiC2+SiC3 (4.49)
Comparison #5 (Square)	SiC8 (Visually Best)	SiC5+SiC3 (Visually Better)	SiC3+SiC5 (Visually Worse)

6.4.2. The Thickness of the Strike Face Ceramic of LCS

In this study, the ceramic layers have different thicknesses. The LCS of 5 mm total thickness is made of 2 mm and 3 mm layers. The LCS of 8 mm total thickness is made of 3 mm and 5 mm layers. Due to the different thicknesses, the LCS can be constructed in two ways. The first way is the thicker ceramic located in the strike face and the thinner ceramic located in the rear face; the second way is vice-versa. While comparing

monolithic and the LCS with the same material, the strike face ceramic's thickness was investigated. As shown in Table 6. 10, the thicker ceramic on the strike face performed better protection than the thinner ceramic. SiC3+SiC2 has higher Ballistic Efficiency than SiC2+SiC3. Also, better protection was observed by visual inspection from SiC5+SiC3 than SiC3+SiC5. All previous studies in the literature used the same ceramic thickness. This is the first study in the literature that investigates the effect of ceramic thickness on the strike face in the layered ceramic structure.

6.4.3. Layered Ceramic Structure with Different Materials

The LCS with different materials were compared with LCS with the same materials for investigating the effect of the different material layers. Two comparisons were conducted and shown in Table 6. 11. The table shows the configurations and results of the tests. In Comparison #2, SiC3+SiC2 is the control configuration, and BC3+SiC2 and Alu3+SiC2 were compared with SiC3+SiC2. It was known that from the literature, the B_4C is the most efficient, Al_2O_3 is the least efficient material in terms of ballistic protection/density, and SiC is positioned between them. Therefore, the BC3+SiC2 configuration was expected to protect better than SiC3+SiC2, and the Alu3+SiC2 configuration was expected to protect worse than SiC3+SiC2. When average Ballistic Efficiency Coefficients were considered, it can be seen clearly that Alu3+SiC2 efficiency was lower than SiC3+SiC2. However, there is a surprising result here, BC3+SiC2 efficiency is also lower than SiC3+SiC2. In Carton et al.'s study, it was shown that there is a critical areal density for ceramics. When the areal density decrease below the critical value, the protection ability of ceramic decreases dramatically. The SiC3+SiC2 configuration has ~16.8 kg/m^2 areal density, and the BC3+SiC2 configuration has ~13.67 kg/m^2 areal density. The reason for the unexpected Ballistic Efficiency results of the BC3+SiC2 can be critical areal density.

In Comparison #7, SiC3+SiC3 and Alu3+Alu3 are both control configurations. The SiC3+Alu3 configuration was compared with these two. As mentioned, it is known from the literature SiC is more efficient than Al_2O_3. As expected, Alu3+Alu3 has the relatively lowest Average Ballistic Efficiency, and SiC3+SiC3 has the relatively highest. SiC3+Alu3 configuration's efficiency is in between them. According to these efficiency results, it can be said that if a more efficient ceramic (SiC3) with coupled with a ceramic

(Alu3), the total efficiency (SiC3+Alu3) is higher than two coupled ceramic (Alu3+Alu3).

Table 6. 11. Summary of the LCS with the same material and LCS with different materials results.

	Config. Code (Average Ball. Efficiency)	**Config. Code (Average Ball. Efficiency)**	**Config. Code (Average Ball. Efficiency)**	**Total Ceramic Thickness**
Comparison #2 (Hexagonal)	SiC3+SiC2 (5.37)	BC3+SiC2 (4.35)	Alu3+SiC2 (3.95)	5 mm
Comparison #7 (Square)	SiC3+SiC3 (5.46)	SiC3+Alu3 (5.09)	Alu3+Alu3 (4.57)	6 mm

The effect of the strike face and rear face ceramic material on the LCS with different materials were investigated. These investigations were discussed in Comparison #3 and #4. The comparisons and average Ballistic Efficiency Coefficients can be seen in Table 6. 12. In Comparison #3; the strike face ceramic material difference was investigated by keeping the rear face ceramic. As expected, the BC3+Alu3 configuration has higher Ballistic Efficiency. In Comparison #4, the rear face ceramic material difference was investigated by keeping the strike face ceramic. Table 6. 12 shows that the BC3+SiC3 configuration has higher efficiency than BC3+Alu3. As mentioned, Al_2O_3 has higher toughness than SiC. However, overall, SiC has high Ballistic Efficiency than Al_2O_3. So, these results are consistent with other LCS with different materials results.

Table 6. 12. Summary of the LCS with different materials results.

	Config. Code (Average Ballistic Efficiency)	**Config. Code (Average Ballistic Efficiency)**	**Total Ceramic Thickness**
Comparison #3 (Hexagonal)	SiC3+Alu3 (4.83)	BC3+Alu3 (5.35)	6 mm
Comparison #4 (Hexagonal)	BC3+SiC3 (5.79)	BC3+Alu3 (5.35)	6 mm

To sum up, except for the BC3+SiC2's Ballistic Efficiency result (the possible reason was explained above), all comparisons were shown that when rear face ceramic was combined with a more efficient strike face ceramic, the total efficiency was increased. This means LCS with different materials (proper combinations) have better ballistic protection than LCS with the same materials. This conclusion does not match with Carton et al.'s study. However, it can be said that the monolithic ceramic performed better ballistic protection than LCS with the same material. This conclusion is consistent with Carton et al.'s [3] and Polla et al.'s [7] studies.

7. FINITE ELEMENT ANALYSIS OF DOP TEST

Finite Element Analysis can be performed for several problem areas, which are structural analysis, heat transfer, fluid flow, mass transport, and electromagnetic [41]. Fast-occurring high-intensity loading, like impact, explosion, etc., are defined as high strain rate events [42], and in this study, an impact phenomenon was performed. The explicit finite element solvers are able to solve time-dependent, non-linear (high-strain rate) problems, and they are called Hydrocode. There are several commercial hydrocode software, and some of them are AUTODYN, ABAQUS, IMPETUS, RADIOSS, and LS-DYNA. In this study, Ls-Dyna Solver is selected for modeling and simulating the DoP tests.

7.1. Introduction to Ls-Dyna

LS-DYNA is a general-purpose hydrocode used to simulate the non-linear response of structures, specifically high deformations using an explicit finite element solver. LS-DYNA is able to perform more than 250 material models [43, 44]. Contact-impact algorithms utilize both constraint and penalty-based methods to satisfy many contact conditions, which allows for difficult contact problems to be analyzed. Preprocessing inputs can be defined by its keyword interface LS-PRESPOST or a text editor [9, 44, 45].

Before the start of the calibration of the DoP test, two analysis methods were performed, and one of them was selected. The performed analysis are:

- 3D-Lagrangian,
- 2D-Axisymmetric Lagrangian,

As explained in Chapter 4, the spin-stabilized bullets travel with variable angle of attack. The angle of attack of the bullet must be considered to make a better simulation. Although 2D-Axisymmetric Lagrangian analysis is proper for DoP test analysis, this method was not selected for calibration. The main reason is the lack of modeling angle of attack in the 2D-Axisymmetric method.

The 3D-Lagrangian method was selected for calibration. This method is straightforward and well-suited for high strain rates and large deformation problems. In half-symmetric condition, the angle of attack of the bullet can be modeled. Therefore, the DoP test was modeled as half-symmetric to save computational time. The half-symmetric model can

be seen in Figure 7. 1. For a complete understanding of the analysis model, a reflected view of the model is shown in Figure 7. 2. The similarity between the actual DoP specimen and the modeled specimen can be seen in Figure 7. 3.

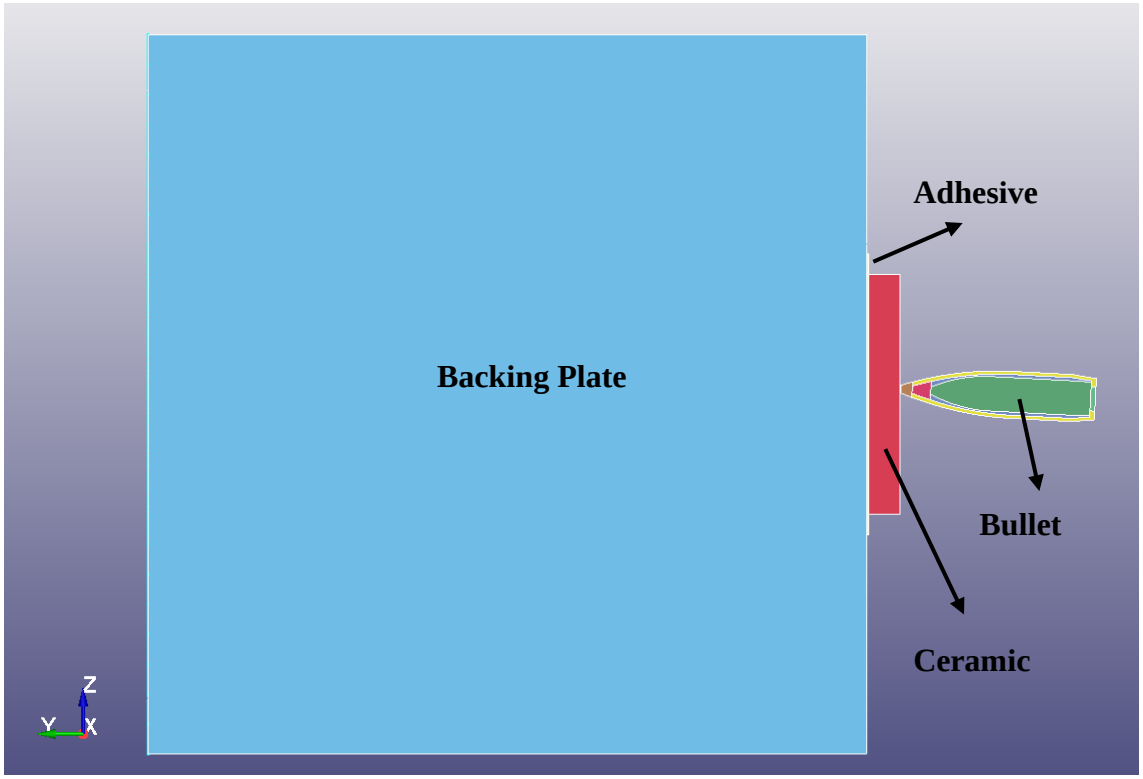

Figure 7. 1. Half-symmetric Ls-Dyna model of DoP test

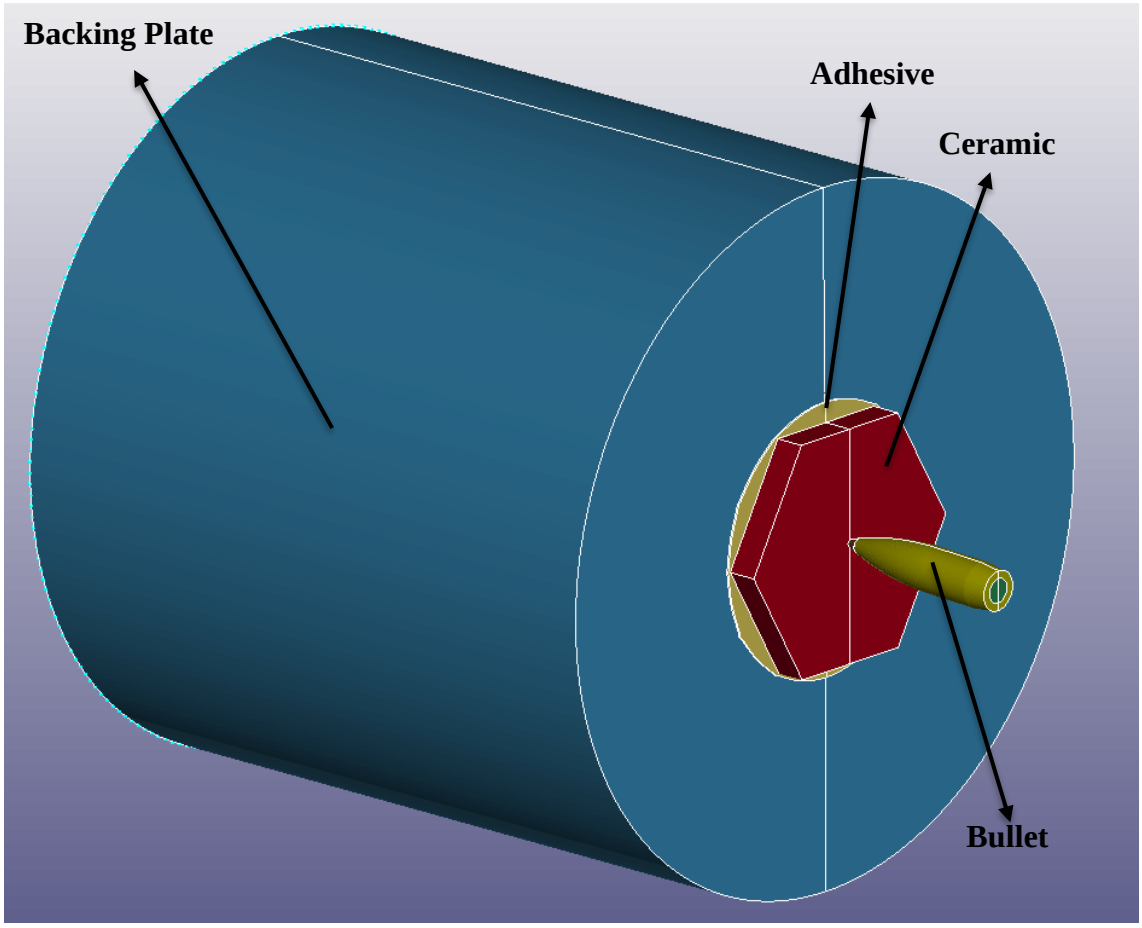

Figure 7. 2. The reflected view of the half-symmetric model

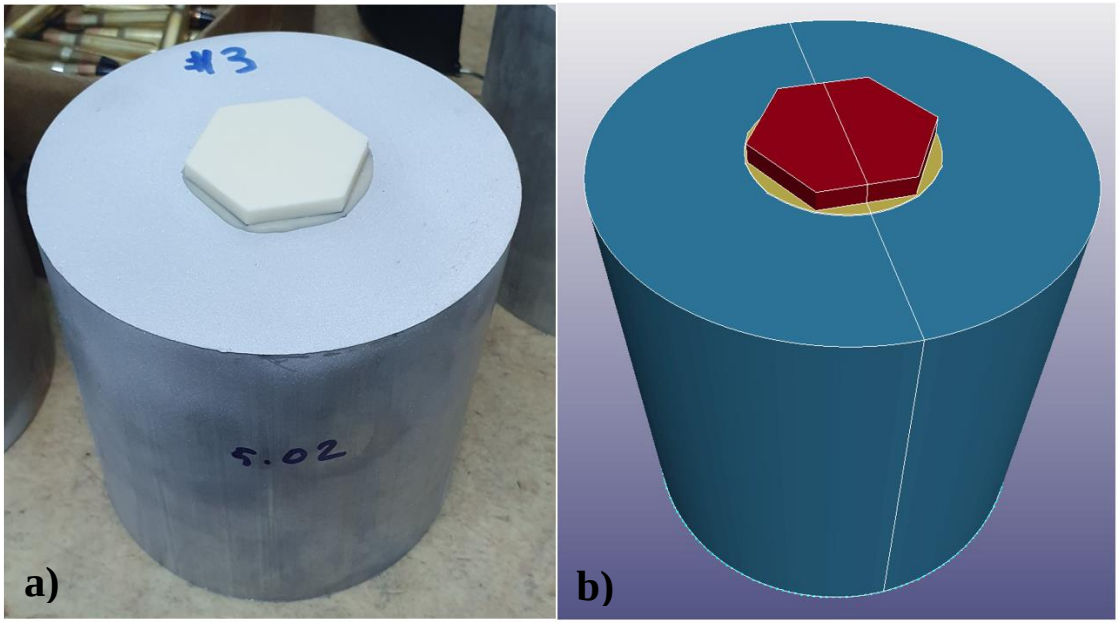

Figure 7. 3. a) a DoP specimen, b) DoP specimen model (reflected view).

7.2. Meshing

Initially, the projectile and target geometry was modeled by computer-aided design (CAD) software. In order to get quality elements (mesh), the modeled parts have been modified. The small surfaces, small holes, and small radius round faces have been removed from solid parts. Then prepared solid parts were imported to ANSYS Workbench / Ls-Dyna, Modelling section, and they have meshed carefully. The mesh type and mesh quality are critical parameters for analysis. Meshing a part fully with hexahedron elements is difficult, especially if there are small faces. However, it is known that hexahedron mesh is more efficient than other mesh types because it can fill the same volume with fewer nodes. Also, hexahedron mesh is more proper for large deformation problems. In the Type A analysis, fully hexahedron mesh is used.

7.2.1. Backing Plate Meshing

While meshing the backing plate, a variable mesh size was used. In this analysis, an important region is the impact zone. To save computational time, only the impact zone meshed fine, and the other regions meshed coarser. When DoP tests were investigated, the maximum penetration depth was observed as ~50 mm. This value was obtained from a test without ceramic (#0 Configuration). Although the maximum depth is determined as 50 mm, the fine zone depth is determined by 70 mm with some factor of safety. Also, the fine zone diameter is determined from the ceramic's dimensions as 50 mm. The average mesh size of the fine zone is 0.8 mm. The meshed backing plate is shown in Figure 7. 4.

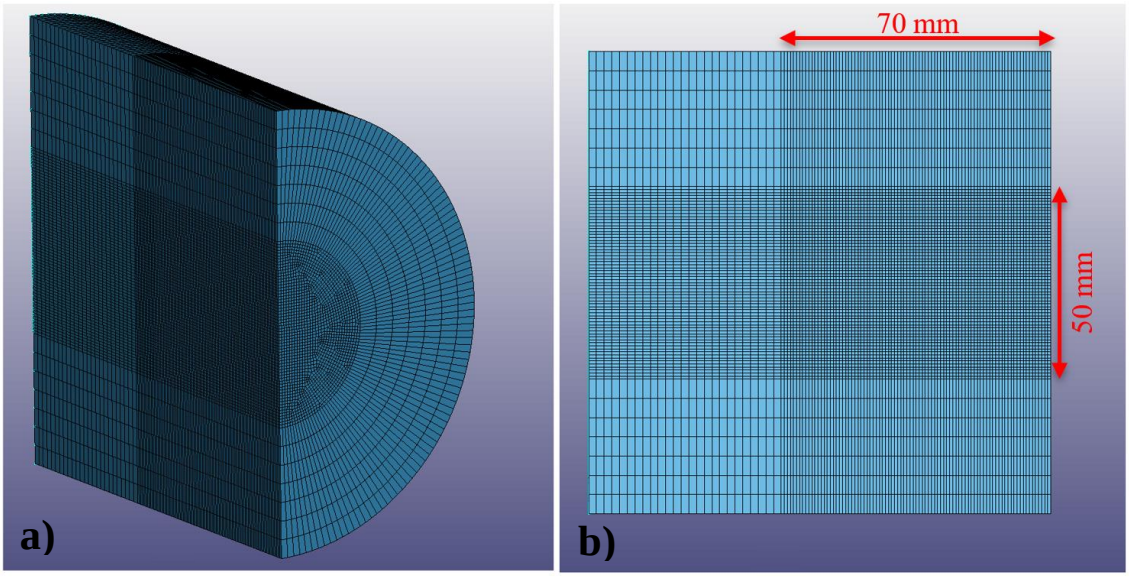

Figure 7. 4. Meshed backing plate, a) isometric view, b) side-view.

7.2.2. Ceramics and Adhesive Meshing

The strength, fracture, and other properties are important for ceramic; therefore, ceramic has meshed fully fine mesh. The meshed hexagonal ceramic is shown in Figure 7. 5. The average mesh size of the ceramic is 0.5 mm.

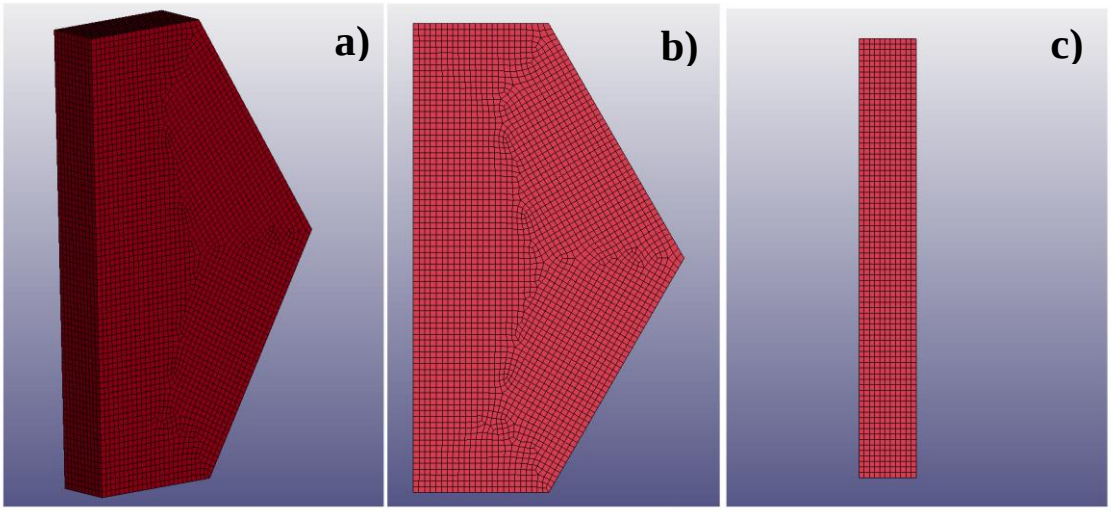

Figure 7. 5. Meshed hexagonal ceramic, a) isometric, b) front, c) side view.

In the DoP specimen, the ceramic and backing plate is bonded together with adhesive. It is known from the literature survey that adhesive thickness is an important parameter for ballistic problems. During the DoP specimen preparation, ~0.3 mm adhesive was applied

between the ceramic and the backing plate. In the analysis, 0.3 mm thick adhesive is modeled, and along the thickness, the two-layer mesh is applied. At least a two-layer mesh is important for the quality of the analysis. Single-layer 8 nodes hexahedron mesh may lead to instabilities and wrong deformations. Adhesive meshes have a poor aspect ratio; the average mesh dimensions are 0.8 × 0.8 × 0.015 mm. The meshed ceramic, adhesive, and backing plate parts can be seen in Figure 7. 6.

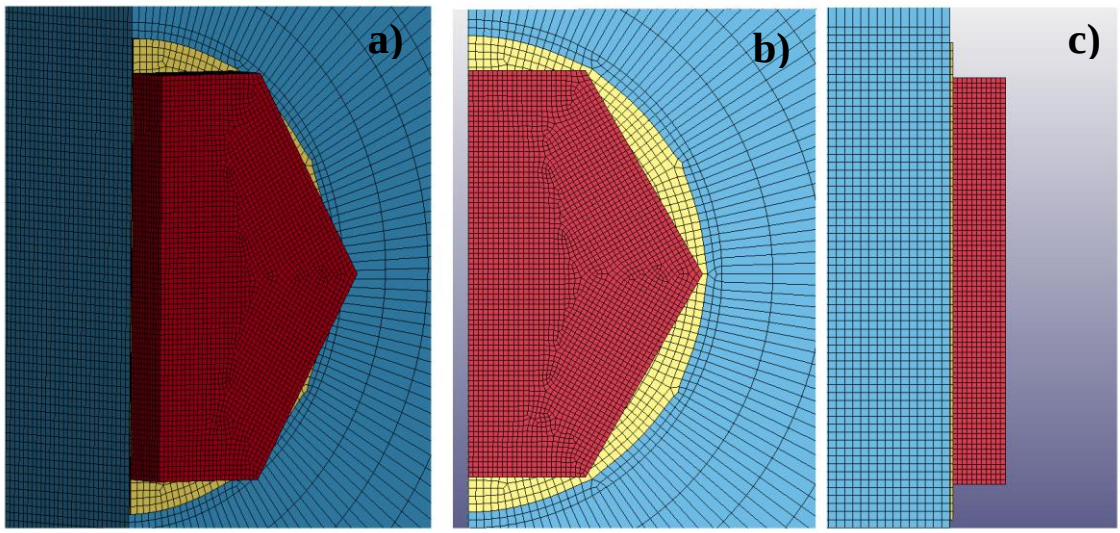

Figure 7. 6. Meshed ceramic, adhesive, and backing plate; a) isometric, b) front, c) side view

The layered ceramic structure is another configuration that is modeled in Ls-Dyna. This specimen is made of ceramic-adhesive-ceramic-adhesive layers and a backing plate. The meshed layered ceramic structure is shown in Figure 7. 7.

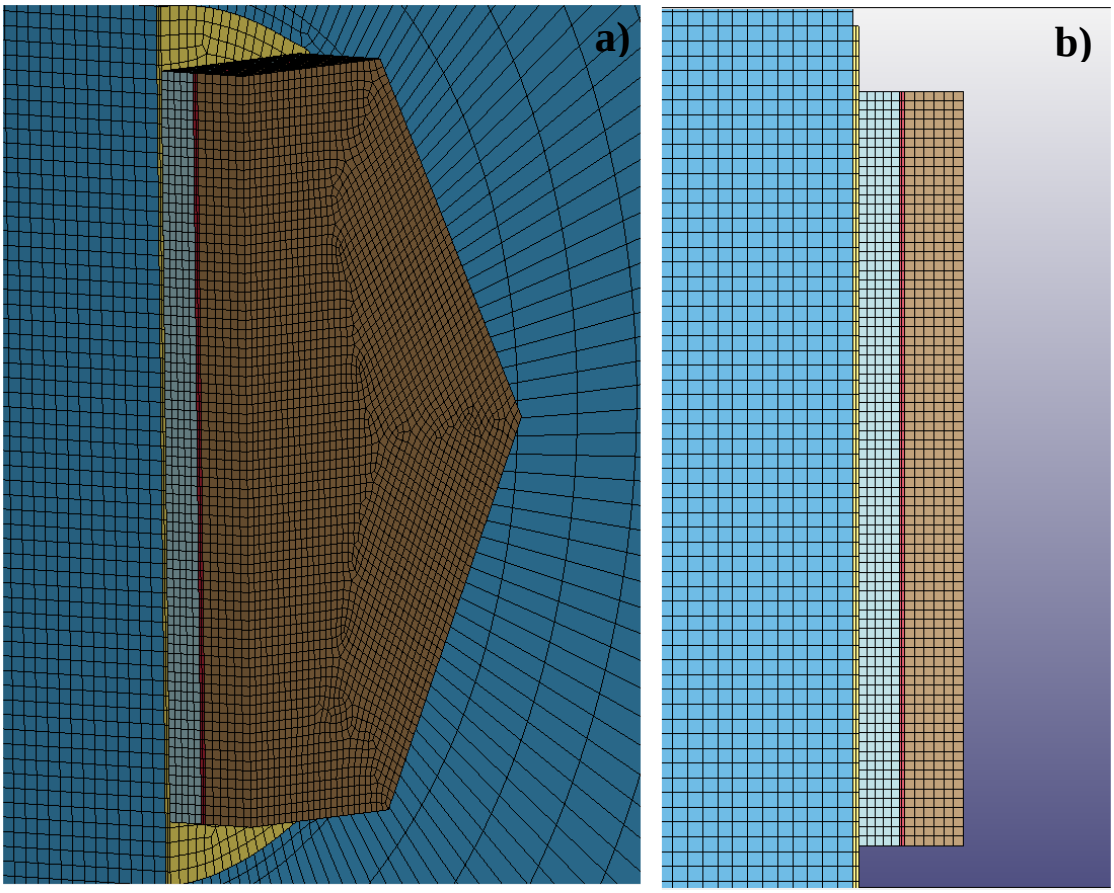

Figure 7. 7. Meshed layered ceramic structure; a) Isometric, b) Side view.

7.2.3. Bullet Meshing

The bullet is the last part of the test. 7.62 × 51 mm Armor-Piercing M61 bullet has meshed fully hexahedron. The bullet is made of three components which are the core, jacket, and filler. Firstly, the bullet has meshed, as shown in Figure 7. 8, to provide a continuous and good-quality mesh (aspect ratio ≈ 1). At the nose of the bullet, the average mesh size drops to 0.006 mm. In the first trial with this bullet, several contact problems were observed; also, this mesh dramatically decreased the time step size of the analysis. Therefore, new meshing was performed for the bullet. To solve the contact problem and time step decrease, the nose of the jacket and fillet were split into two parts. Then coarser meshes were applied to all the bullet's parts. The split parts of the jacket and filler were bonded with the Tied_Contact card before the analysis started. The meshed bullet that was used in the analysis is shown in Figure 7. 9. The average mesh size of the jacket and filler was increased to ~0.15 mm. Also, the core's nose has a similar mesh size. The average mesh size of the middle and back of the core is ~0.25 mm.

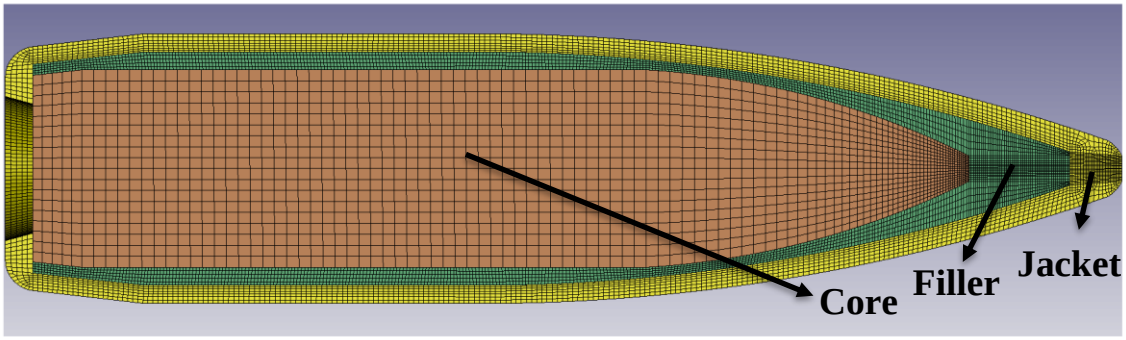

Figure 7. 8. First meshing trial for the bullet

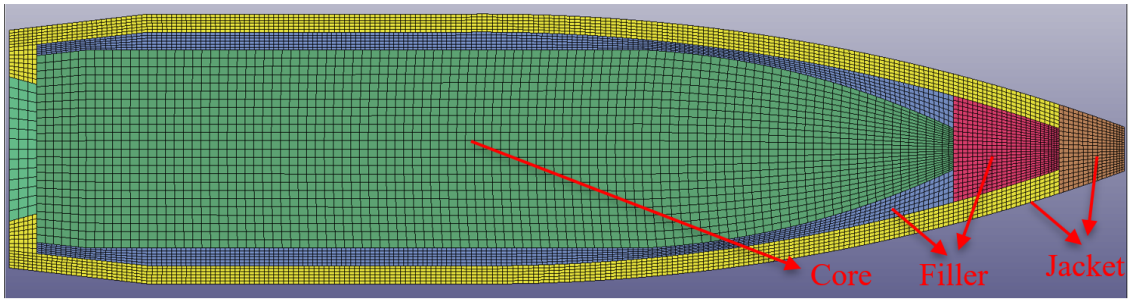

Figure 7. 9. Final meshed bullet.

7.3. Material Models and Parameters

The impact phenomenon is a high strain-rate event. For modeling this phenomenon, strain rate sensitive and proper to highly plastic deformation material models must be used. For metallic materials, Johnson-Cook (JC) model; for ceramic materials Johnson-Holmquist model and for adhesive Elastic-Plastic-Hydro model is selected. At the first iterations of the analysis calibration, the JC model was used; however, it was experienced that JC sometimes causes negative volume errors. Then Simplified-Johnson-Cook (SJC) model is used instead of Johnson-Cook in the analysis. The Simplified JC model is very similar to JC; only thermal effect and thermal damage are ignored in this model. The material models used in the analysis were explained briefly then material parameters were shown.

7.3.1. Simplified Johnson Cook Model

This model represents metallic materials' high strains and high strain rates. An individual term is constructed for each phenomenon (strain hardening and strain rate hardening), and flow stress is produced by multiplying these terms. In contrast to the full Johnson-Cook

model, this model does not calculate thermal softening, which is 50% faster than the full Johnson-Cook model. The yield stress can be calculated as follows:

$$\sigma_y = \left[A + B\bar{\varepsilon}_p^n\right][1 + C\ln(\dot{\varepsilon}^*)]$$

$$\dot{\varepsilon}^* = \frac{\dot{\bar{\varepsilon}}_p}{\dot{\varepsilon}_0}$$

Where *A* is the initial yield stress, *B* is the strain hardening coefficient, and n is the strain hardening exponent, $\bar{\varepsilon}_p$ is the effective plastic strain, $\dot{\bar{\varepsilon}}_p$ is the effective plastic strain rate, $\dot{\varepsilon}_0$ is the user-selected reference strain rate (often 1.0 s^{-1}) and *C* is the strain rate coefficient [43]. The required material parameters are shown in Table 7. 1.

Table 7. 1. Metallic materials parameters

MAT_98_SIMPLIFIED_JOHNSON_COOK [m/kg/s]				
	Filler–Lead [46]	**Jacket-Brass [46]**	**Core-Steel [46]**	**AA6061-T6[47]**
RO	1.07E+04	8525	7850	2700
E	1.00E+09	1.15E+11	2.10E+11	7.60E+10
PR	0.42	0.31	0.295	0.33
A	1.40E+07	2.06E+08	1.20E+09	3.24E+08
B	3.00E+08	5.05E+08	5.00E+10	1.14E+08
N	1	0.42	1	0.42
C	0.1	0.01	0	0.002
PSFAIL	1.921	1.7	0.35*	0.75*
SIGMAX	5.00E+07*	4.00E+08*	0.00E+00	6.00E+08*
SIGSAT	6.00E+07*	5.00E+08*	0.00E+00	8.00E+08*
EPSO	5.00E-04	5.00E-04	5.00E-04	1

*These values are determined after calibration.

7.3.2. Elastic-Plastic-Hydro Material Model & Gruneisen Equation of State

The Elastic-Plastic-Hydro model is a general-purpose material model, and Araldite® 2015 is modeled with it. This model allows the modeling of an elastic-plastic hydrodynamic material and requires an equation of state. In addition, the incorporation of an equation of state permits accurate modeling of a variety of different materials [43]. The required material parameters are shown in Table 7. 2.

Table 7. 2. Adhesive material parameters.

Araldite® 2015 [m/kg/s]						
ELASTIC_PLASTIC_HYDRO [48]				**EOS_GRUNEISEN [49]**		
RO	**G**	**SIGY**	**FS**	**C**	**S1**	**GAMA0**
1400	5.60E+08	1.26E+07	0.43	3234	1.255	1.13

7.3.3. Johnson-Holmquist Ceramic Material Model

Johnson and Holmquist developed one of the first strain rate-dependent constitutive models for ceramics. It is known as the JH1 equation in the literature. A few years later, this model was developed and updated as the JH2 material model. The gradual softening of the ceramic from 'intact' to 'failed' and a gradual increase in the bulking pressure until full damage was added to the JH2 model. This model includes the strength model, damage model, and equation of states together. In the Analysis, only SiC and B4C ceramics were used. The required material parameters are shown in Table 7. 3.

Table 7. 3. Ceramic materials parameters

JOHNSON_HOLMQUIST_CERAMIC [m/kg/s]		
	Silicon-Carbide [50]	**Boron-Carbide [50]**
RO	3163	2510
G	1.83E+11	1.97E+11
A	0.96	0.927
B	0.6*	0.7
C	0	0.005
M	1	0.85
N	0.65	0.67
EPSI	1	1
T	3.70E+08	2.60E+08
SFMAX	0.8	0.2
HEL	1.46E+10	1.90E+10
PHEL	5.90E+09	8.70E+09
BETA	1	1
D1	0.2*	0.001
D2	0.48	0.5
K1	2.05E+11	2.33E+11
K2	0	-5.93E+11
K3	0	2.80E+12
FS	3*	2**

*These values are taken from another study [9]

**These values are determined after calibration

7.4. Boundary & Initial Conditions

This DoP test simulation model was created as half-symmetric, and the Y-Z plane is the symmetry plane. Therefore, this simulation has 3 degrees of freedom. The parts can

translate along the Y-axis and Z-axis and also, and they can rotate around X-axis (directions can be seen in Figure 7. 1).

The DoP test specimen was fixed on the target carrier stand. It was observed that the target carrier stand and specimen were moved slightly back together when the DoP test was performed. Therefore, applying the fixed condition to the backing plate in six DoF is unrealistic in analysis. When the DoP test was performed, the bullet's kinetic energy and momentum were transferred to the backing plate, and target carrier stand. In analysis, the target carrier's mass was added to the rear face nodes of the backing plate to simulate realistic conditions. The target carrier is ~30 kg; however, the simulation is half-symmetric; therefore, 15 kg mass is added.

According to the MKE's exterior ballistic calculation, the bullet's velocity is 833±9 m/s at 20 m away from the muzzle. The specimen was located 20 m away in DoP tests. Therefore, 833 m/s velocity is applied to the bullet as an impact velocity in the simulation. As explained in Chapter 4, the spin-stabilized bullets fly with a variable angle of attack. For this reason, to better simulate the DoP test, a 2° angle of attack is applied to the bullet.

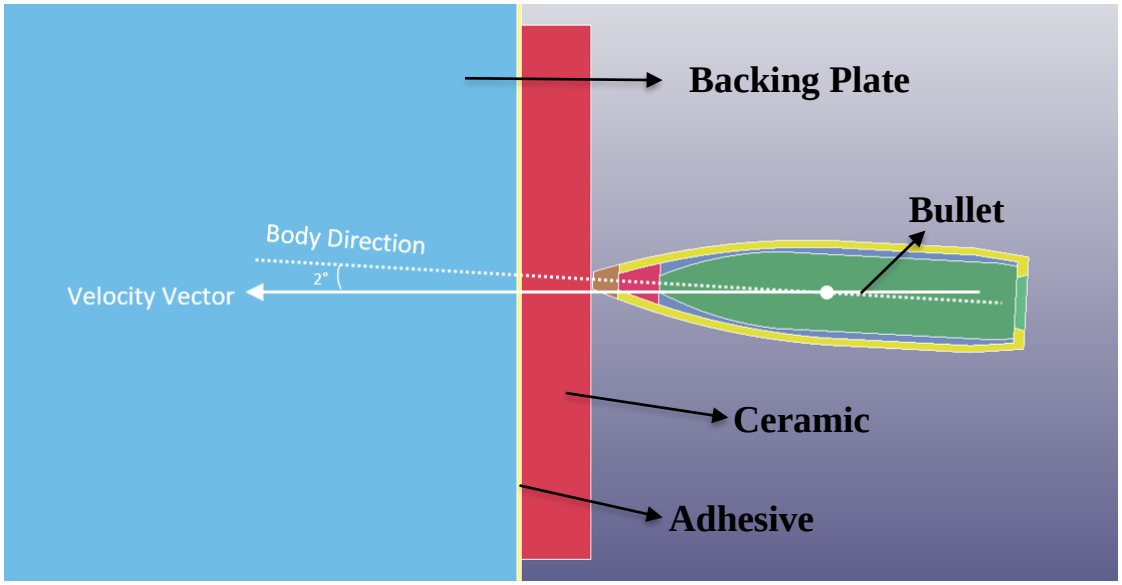

Figure 7. 10. The angle of attack of the bullet

7.5. Other Settings

7.5.1. Contacts

Two types of contact are defined in the analysis. These are:

- CONTACT_ERODING_SINGLE_SURFACE

This contact is an Automatic Contact, and this contact maintains the interaction of the parts with each other. In this contact card, slave and master surfaces are defined by themselves according to the properties of the parts. Also, this contact card can automatically define new interaction surfaces that occur due to the erosion of parts.

- CONTACT_TIED_SURFACE_TO_SURFACE

This contact type is used for bonding two parts. This contact card was applied between two parts of the brass jacket and lead filler of the bullet, as mentioned in Figure 7. 9. Also, this contact was applied between the backing plate – adhesive and adhesive – ceramic.

7.5.2. Element Formulation

Eight node hexahedron elements are used in the analysis. There are several element formulations for different problems. Constant stress solid element (default element type) was used. This formulation is proper for large deformations; also, it is cost-efficient; however, the hourglass is the main problem of the reduced element formulations.

SECTION_SOLID, ELFORM=1

7.5.3. Hourglass

As mentioned, the hourglass is the main weakness of the constant stress solid element. Therefore, to control the hourglass energy, the CONTROL_HOURGLASS card is activated. The stiffness form of the Flanagan-Belytschko formulation is selected, and the hourglass coefficient is used as 0.05.

CONTROL_HOURGLASS, IHQ=4, QH=0.05

7.5.4. Timestep

The time step is automatically determined by the LS-DYNA solver. However, sometimes in high strain rate problems, complex sound speed error occurs when the time step is higher. There is a time step scale factor in the analysis settings; this setting multiplies the

initial time step with a factor that is smaller than 1 to drop to timestep. In this analysis time step scale factor was determined by 0.67.

CONTROL_TIMESTEP, TSSFAC = 0.67

7.6. Post-Process of the Analysis

Once an analysis is run and the problem is solved, the resulting information related to deformations, stress, strain, temperatures, velocities, accelerations, forces, moments, energies, etc., can be obtained either graphically or quantitatively in numbers. This entire process of inferring or obtaining the results from the solver is called post-processing. For this study, LS-PrePost software was used for post-processing.

7.7. Calibration of Analysis and Comparison with Ballistic Test

7.7.1. Calibration Methodology of DOP Tests

The last aim of this study is to calibrate an FEA model to see the other LCS configurations. Until this section, the key points of the FEA were discussed (meshes, material models, material parameters, boundary conditions, initial conditions, and analysis options). The analysis calibration method was explained in this section, and the six FE Analyses (from Analysis #0 to #5) were discussed. The analyzed configurations and analysis names are shown in Table 7. 4.

Table 7. 4. The analyzed configurations and analysis names.

Configuration Name	Configuration No:	Analysis Name
DoP Without Ceramic	#0	Analysis #0
SiC5	#1	Analysis #1
SiC3+SiC2	#2	Analysis #2
SiC2+SiC3	#3	Analysis #3
BC3+BC2	-	Analysis #4
BC3+SiC2	#4	Analysis #5

For calibrating the DoP test analysis, a method was followed:

a) Analysis #0: In the beginning, the DoP test without any ceramic (#0 Configuration) was simulated. In this analysis, the backing plate's and bullet's

material parameters were calibrated. The initial condition of Analysis #0 is shown in Figure 7. 11.

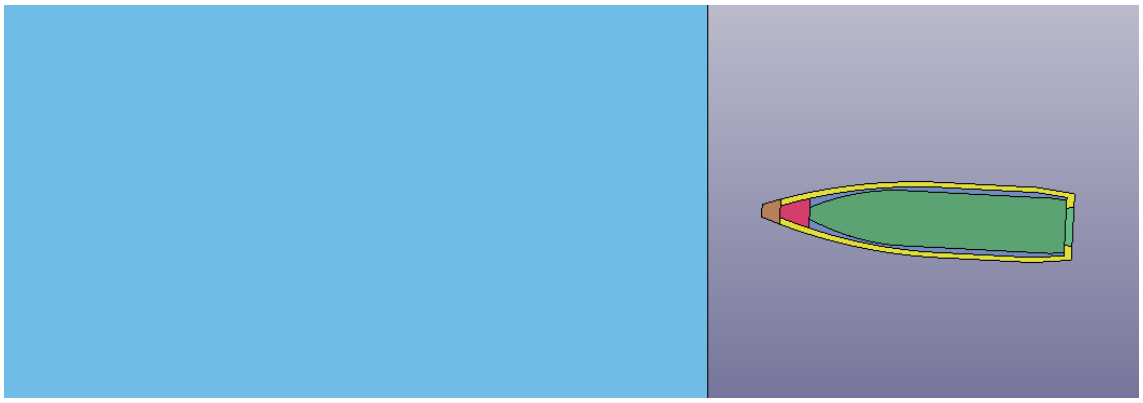

Figure 7. 11. Initial condition of Analysis #0

b) Analysis #1: The core and backing plate were calibrated in Analysis #0. In Analysis #1, a hexagonal monolithic 5 mm SiC ceramic is added with adhesive. The initial condition of Analysis #1 is shown in Figure 7. 12.

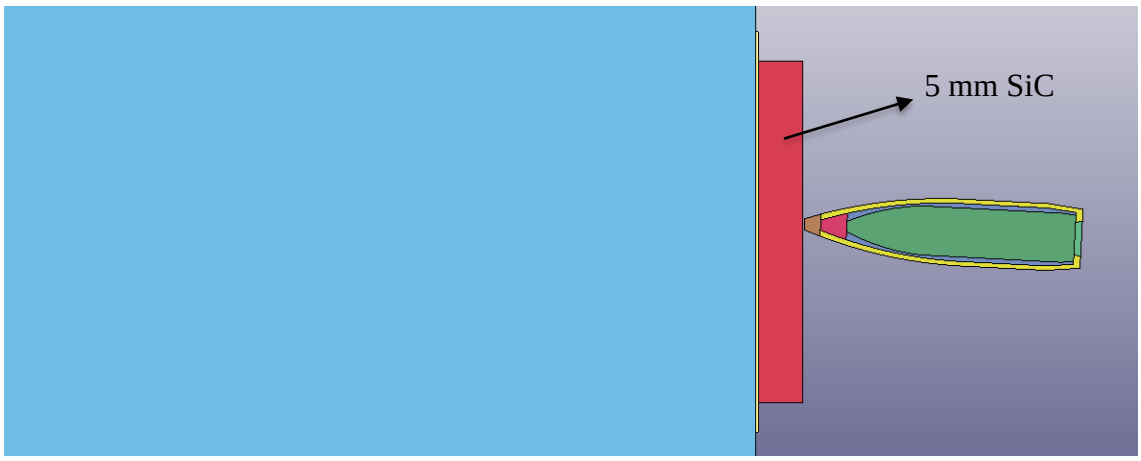

Figure 7. 12. Initial condition of Analysis #1

c) Analysis #2 & Analysis #3: The monolithic SiC5 configuration was analyzed in Analysis #1. Then LCS with the same material configurations (hexagonal SiC3+SiC2 and SiC2+SiC3) were simulated. Until here, monolithic and LCS with the same material comparison are investigated with FEA. The initial conditions of Analysis #2 and #3 are shown in Figure 7. 13 and Figure 7. 14.

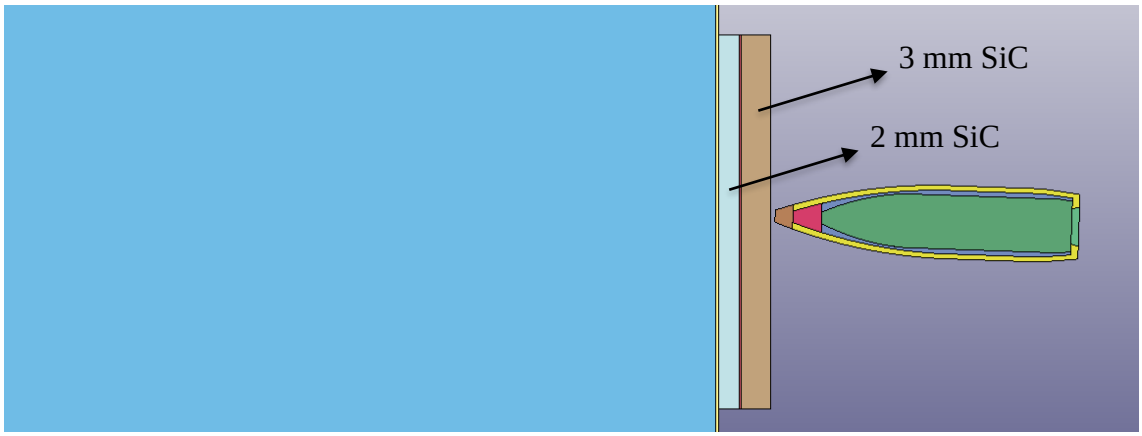

Figure 7. 13. Initial condition of Analysis #2

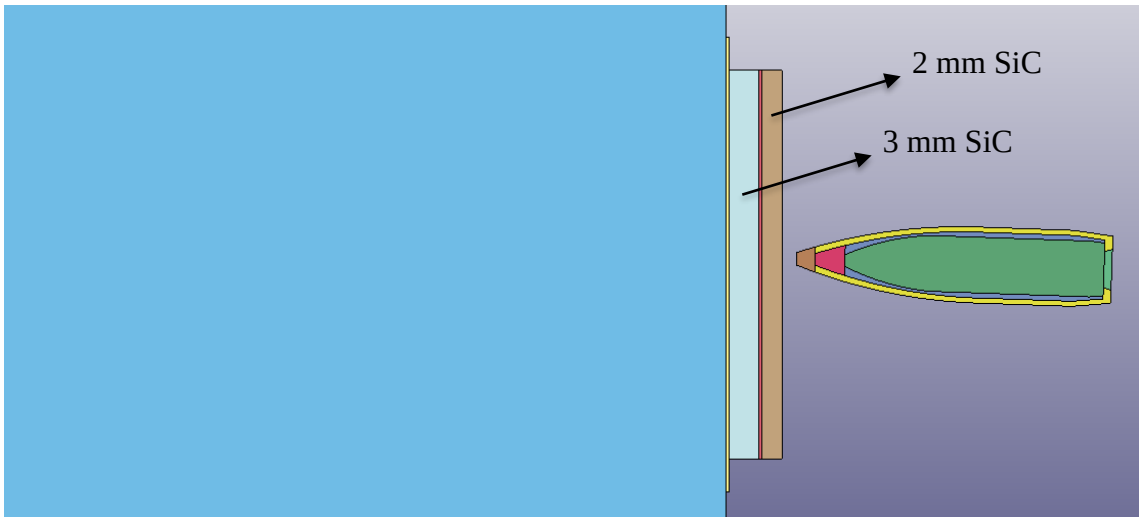

Figure 7. 14. Initial condition of Analysis #3

d) Analysis #4: Firstly, monolithic ceramic, then LCS with the same material configurations were analyzed. The following configuration is an LCS with different materials. The BC3+SiC2 configuration is compared with SiC3+SiC2 to understand the effect of the strike face B_4C ceramic. However, B_4C ceramic must be calibrated before this comparison. Due to this requirement, DoP tests of hexagonal BC3+BC2 configuration were performed. With these test data, B_4C failure strain calibration was performed. The initial condition of Analysis #4 is shown in Figure 7. 15.

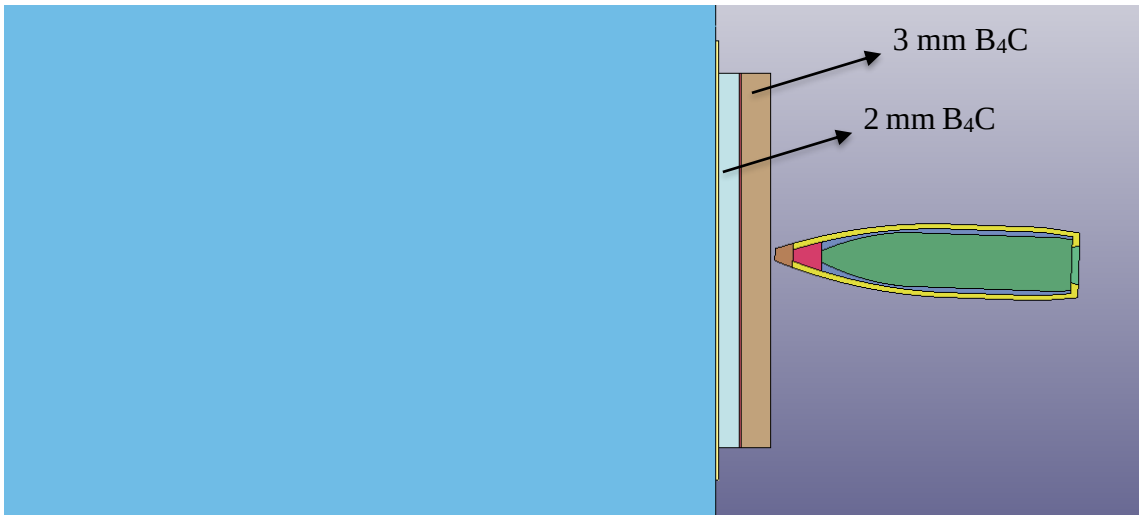

Figure 7. 15. Initial condition of Analysis #4

e) Analysis #5: Until here, the SiC and B_4C ceramics were calibrated. BC3+SiC2 analysis was performed to simulate LCS with different materials. The initial condition of Analysis #5 is shown in Figure 7. 16.

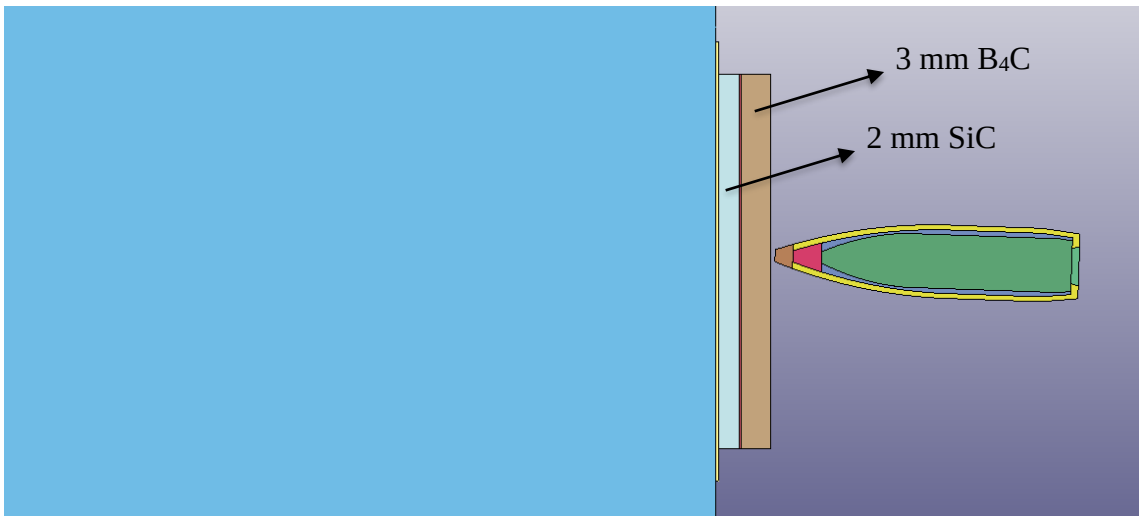

Figure 7. 16. Initial condition of Analysis #5

7.7.2. Analysis #0

Analysis #0 was developed for simulating DoP without ceramic configuration (Configuration #0). The main goal is to observe similar penetration depth in Analysis #0 with relevant ballistic DoP. In Analysis #0, the critical parts are the backing plate and the bullet's core. The backing plate was made of AA6061-T6, and the bullet's core was made of hardened steel. After several analyses, the failure strain parameters (PSFAIL) were

calibrated using ballistic DoP results. The failure strains of the Core Steel and AA6061-T6 were determined as 0.35 and 0.75 and were shown in Table 7. 3. The initial condition of Analysis #0 was shown in Figure 7. 11. The final condition of Analysis #0 can be seen in Figure 7. 17. The eroded elements and hole profile can be seen in Figure 7. 18.

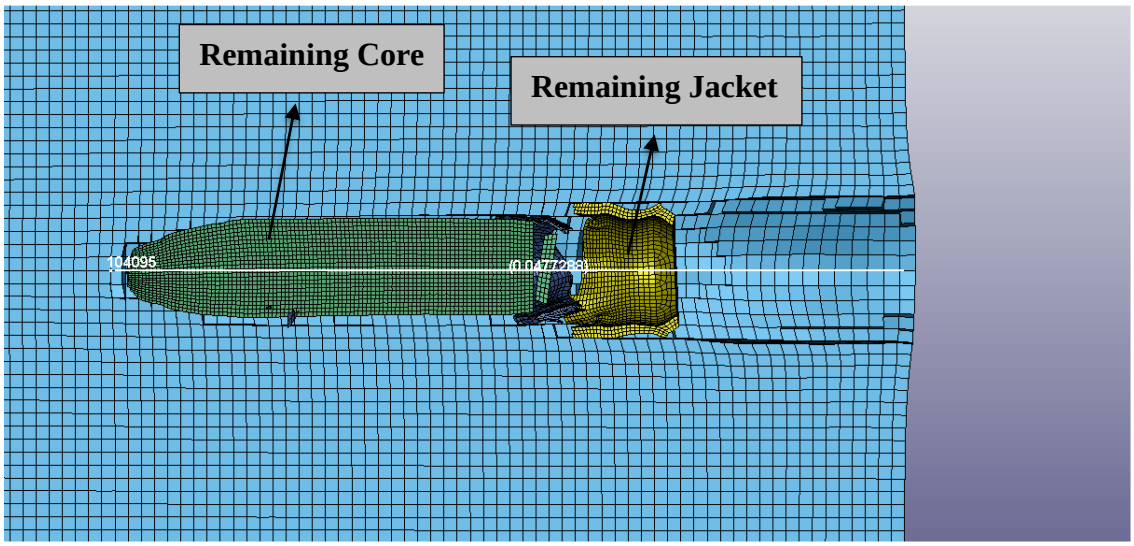

Figure 7. 17. The final condition of Analysis #0 (1)

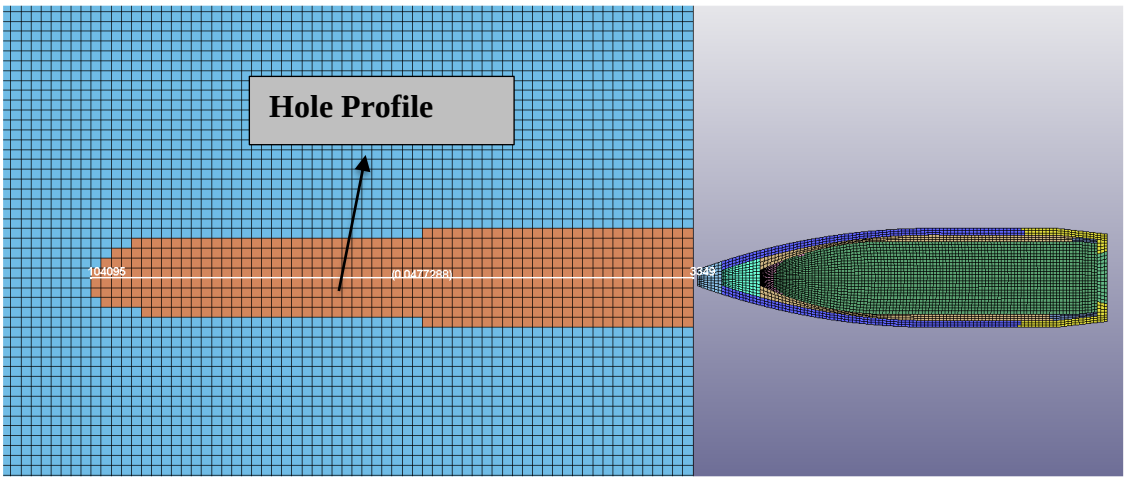

Figure 7. 18. The final condition of Analysis #0 (2).

The DoP results of the test and analysis can be seen in Table 7. 5. The penetration depth of Analysis #0 was measured on Figure 7. 18 and determined as 47.72 mm. And the average DoP result of the test was 50.81 mm. The DoP difference between the test and analysis was observed as 6.4%.

Table 7. 5. DoP results comparison of tests and Analysis #0

	Ballistic DoP Test		Avg. of the valid Ballistic DoP Test	Analysis DoP	Difference b/w. Test & Analysis
Test No:	#1	#2	#1 & #2	Analysis #0	-
DoP [mm]	51.85	49.77	50.81	47.72	6.4%

The visual comparison was conducted between the X-Ray image of Specimen #1 and the final condition of Analysis #0. The comparison image can be seen in Figure 7. 19. The X-Ray and analysis images are similar. The only difference is that; in the ballistic test, the bullet hit the backing plate with an impact angle in addition to the angle of attack. Therefore, the bullet's path was not perpendicular to the strike face.

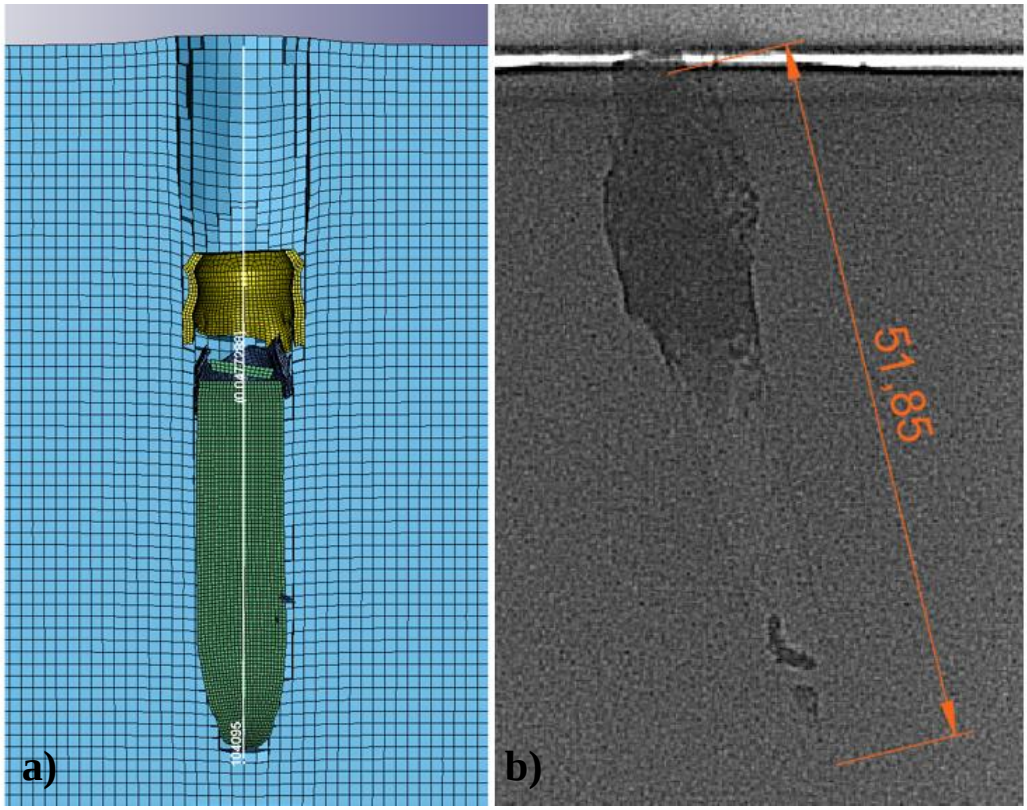

Figure 7. 19. The comparison of the final views of the analysis and test; a) Analysis #0, b) Specimen #1.

7.7.3. Analysis #1

The backing plate and bullet were calibrated in Analysis #0. Analysis #1 was developed to simulate SiC5 configuration (Configuration #1). The monolithic 5 mm SiC ceramic

and 0.3 mm adhesive layer were added to Analysis #0 then Analysis #1 was created. The ceramic thickness is an essential parameter for the DoP test. The average ceramic thickness was observed as 5.15 mm when the tested specimens were investigated. For this reason, the ceramic thickness of the SiC5 configuration was modeled as 5.15 mm.

The analysis was performed with the SiC parameters obtained from the literature. The initial condition of Analysis #1 is shown in Figure 7. 12. The final condition of Analysis #1 can be seen in Figure 7. 20. The eroded elements and hole profile can be seen in Figure 7. 21.

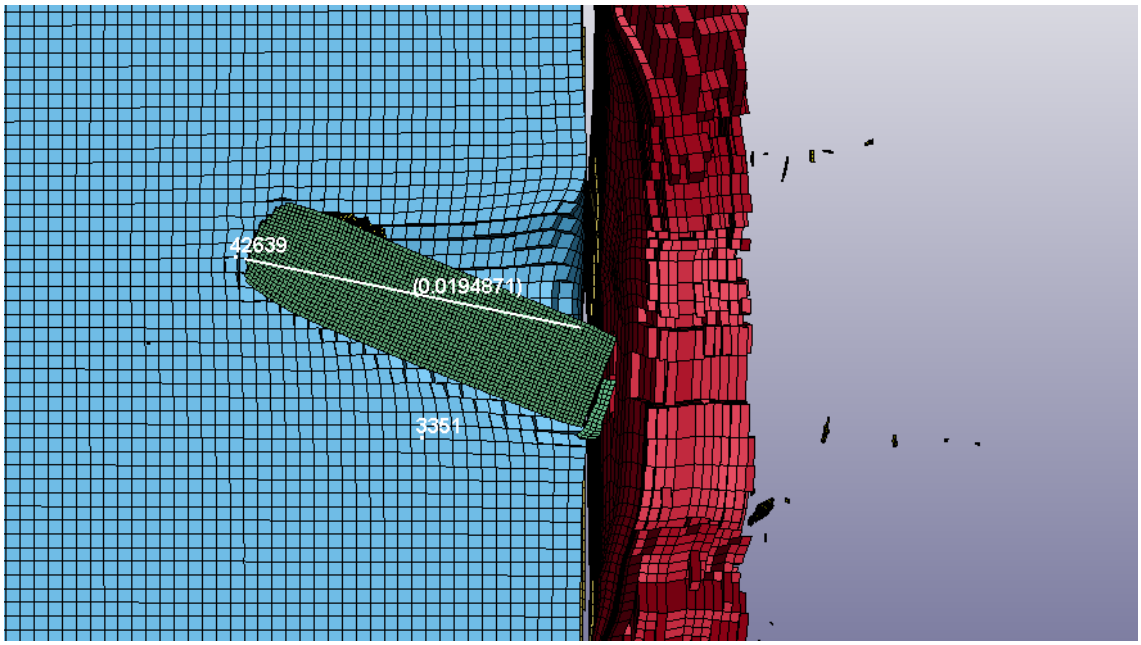

Figure 7. 20. The final condition of Analysis #1 (1)

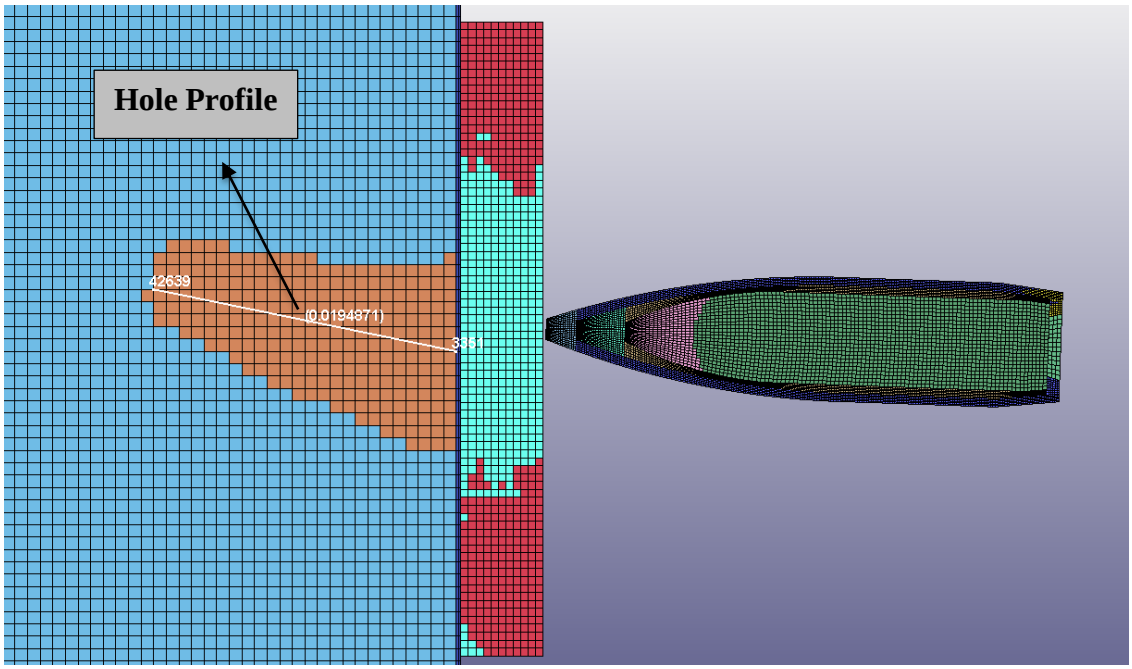

Figure 7. 21. The final condition of Analysis #1 (2)

The Ballistic Efficiencies of the test and analysis can be seen in Table 7. 6. The Ballistic Efficiency of Analysis #1 was calculated by DoP, which was measured on Figure 7. 21 (19.48 mm). The average Ballistic Efficiency of the DoP tests was 6.81. The difference between the test and analysis was observed as 32.5%.

Table 7. 6. Ballistic Efficiency comparison of tests and Analysis #1

	Ballistic DoP Test			Avg. of the valid Ballistic DoP Test	Analysis DoP Result	Difference b/w. Test & Analysis
Specimen No:	#5	#6	#18	#5 & #18	Analysis #1	-
Ballistic Efficiency Coeff.	7.55	5.22	6.58	6.81	5.14	32.5%

Although the bullet and backing plate calibration was completed successfully in Analysis #0, an obvious difference between the tests and Analysis #1 was observed. The main problem for Analysis #1 is the Johnson-Holmquist material parameters of SiC. These parameters are obtained from the literature, and it was observed that these parameters could not simulate tested ceramic material. In Figure 7. 22, a visual comparison was conducted. The X-Ray images of Specimen #6 and #18 were compared with the Analysis

#1 result. The Specimen #6 and Analysis #1 DoP results were similar. However, Specimen #6 was excluded from evaluation due to the Near-the-Edge impact location. Except for penetration depth, similar hole profiles were observed between Specimen #18 and Analysis #1. Based on this comparison, it can be said that the strength parameter of SiC was improper; however, the behavior of the SiC was similar to the tests.

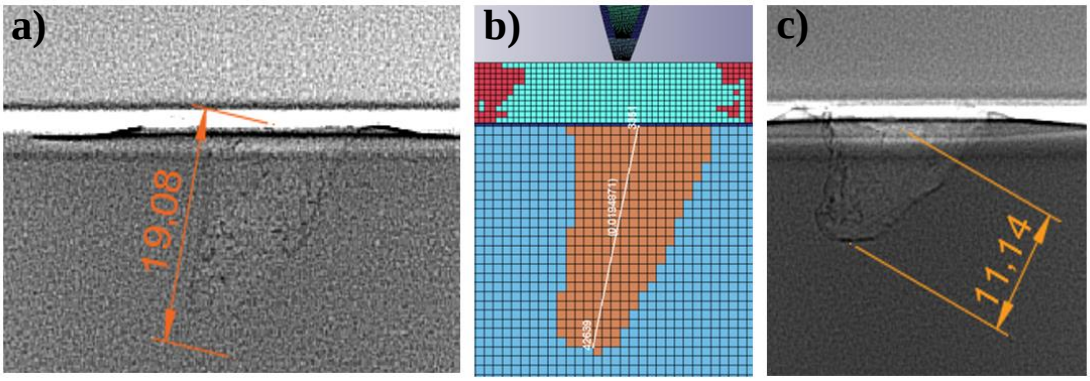

Figure 7. 22. The comparison of the final views of the test and analysis; a) Specimen #6, b) Analysis #1, c) Specimen #18.

7.7.4. Analysis #2

Analysis #2 was developed the simulate the SiC3 + SiC2 configuration. Analysis #2 was created by replacing the SiC3 + SiC2 with SiC5 ceramic in Analysis #1. In this configuration 0.3 mm adhesive layer was applied between the ceramic layers. As mentioned, ceramic thickness is critical for the DoP test & analysis. The tested ceramic's average thicknesses were 3.1 mm for SiC3 and 2.1 mm for SiC2 ceramics. Therefore, ceramics were modeled as 3.1 mm and 2.1 mm.

The initial condition of Analysis #2 is shown in Figure 7. 13. The same Johnson-Holmquist material parameters of SiC were used for Analysis #2. The final condition of Analysis #2 can be seen in Figure 7. 23. The eroded elements and hole profile can be seen in Figure 7. 24.

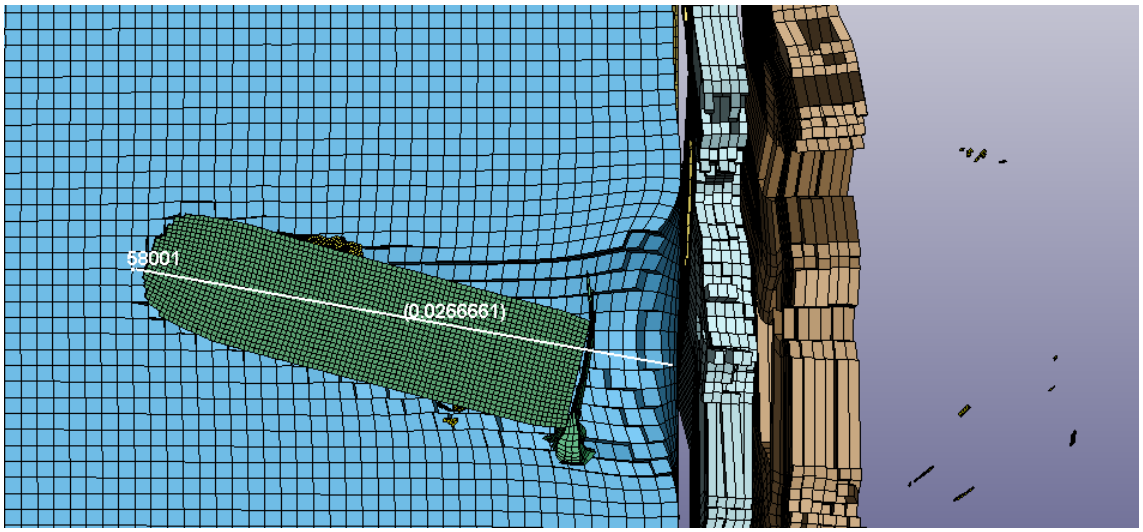

Figure 7. 23. The final condition of Analysis #2 (1)

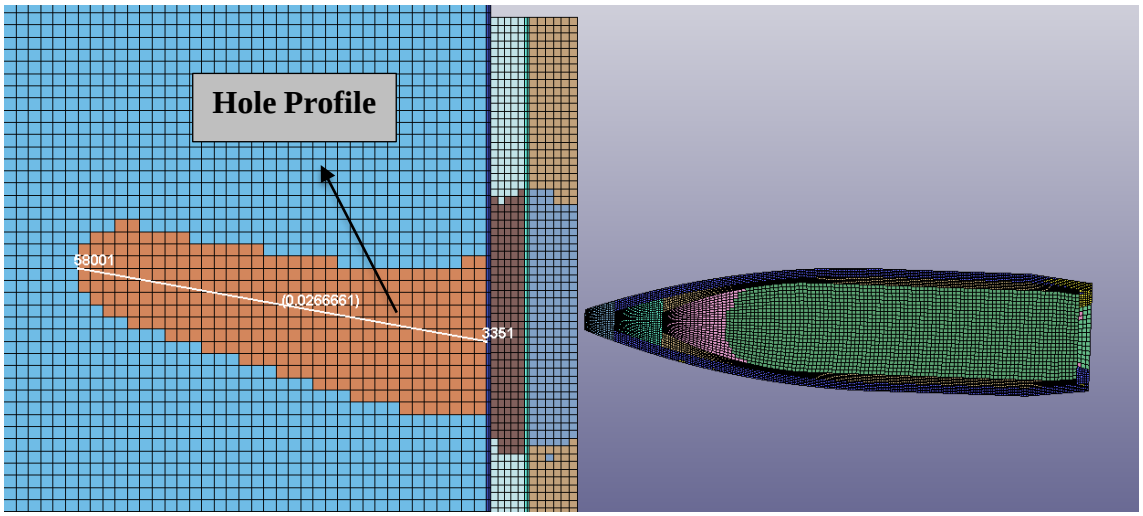

Figure 7. 24. The final condition of Analysis #2 (2)

The Ballistic Efficiencies of the test and analysis can be seen in Table 7. 7. The Ballistic Efficiency of Analysis #2 was calculated by DoP, which was measured on Figure 7. 24 (26.66 mm). The average Ballistic Efficiency of the DoP tests was 5.37. The difference between the test and analysis was observed as 35.6%.

Table 7. 7. Ballistic Efficiency comparison of tests and Analysis #2

	Ballistic DoP Test Results			Avg. of the valid Ballistic DoP Test Results	Analysis DoP Result	Difference b/w. Test & Analysis
Specimen No:	#7	#8	#19	#7, #8 & #19	-	-
Ballistic Efficiency Coeff.	5.58	5.52	5.0	5.37	3.96	35.6%

7.7.5. Analysis #3

Analysis #3 was developed the simulate the SiC2 + SiC3 configuration. Analysis #3 is very similar to Analysis #2; the only difference is the positions of the thicker and thinner ceramics. Ceramic thicknesses, adhesive thicknesses, and material parameters were the same. The initial condition of Analysis #3 is shown in Figure 7. 14. The final condition of Analysis #3 can be seen in Figure 7. 25. The eroded elements and hole profile can be seen in Figure 7. 26.

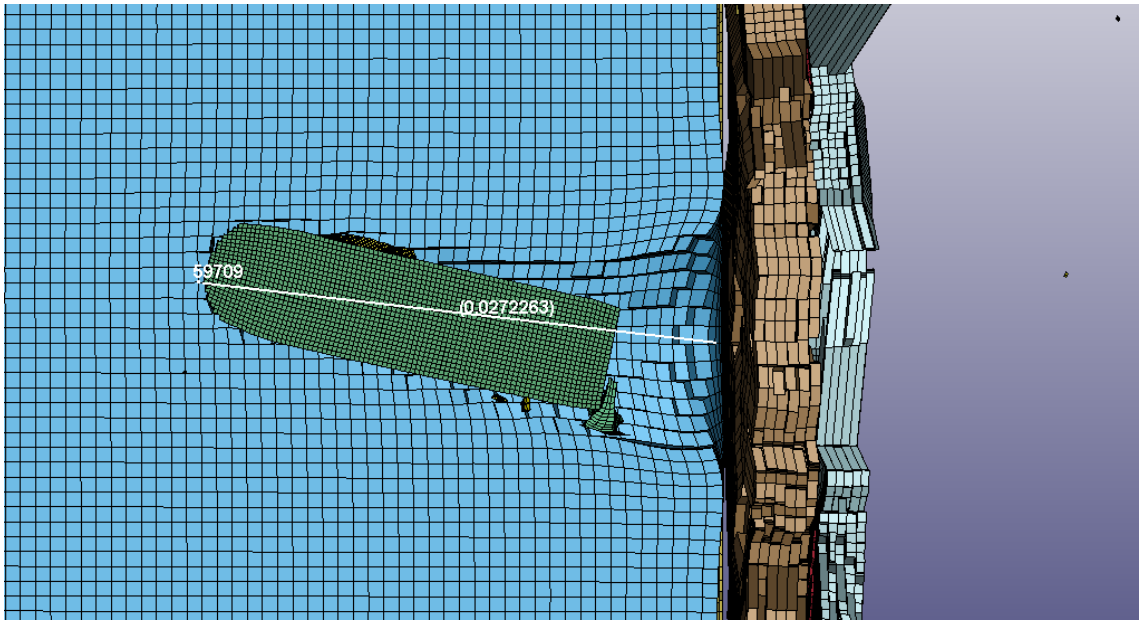

Figure 7. 25. The final condition of Analysis #3 (1)

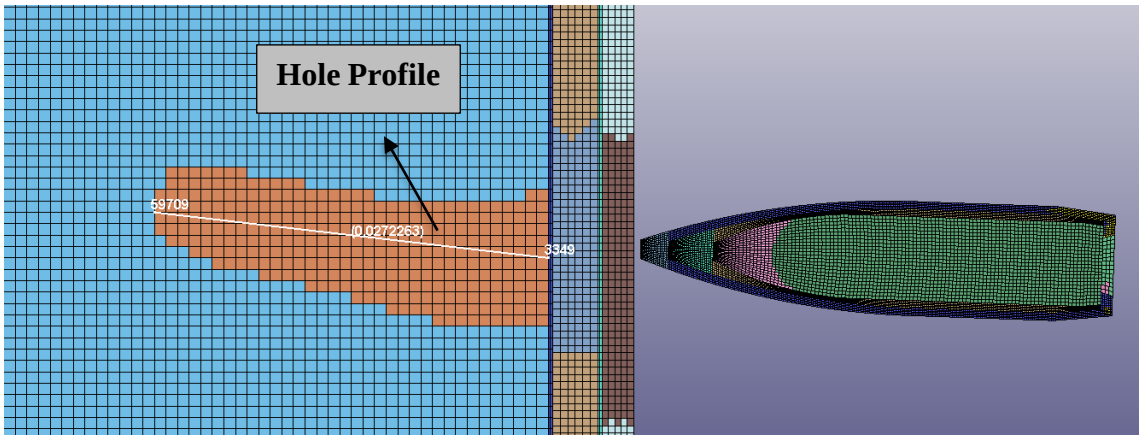

Figure 7. 26. The final condition of Analysis #3 (2)

The Ballistic Efficiencies of the test and analysis can be seen in Table 7. 8. The Ballistic Efficiency of Analysis #3 was calculated by DoP, which was measured on Figure 7. 26 (27.22 mm). The average Ballistic Efficiency of the DoP tests was 4.59. The difference between the test and analysis was observed as 18.6%.

Table 7. 8. Ballistic Efficiency comparison of tests and Analysis #3

	Ballistic DoP Test Results		Avg. of the valid Ballistic DoP Test Results	Analysis DoP Result	Difference b/w. Test & Analysis
Specimen No:	#9	#10	#9 & #10	-	-
Ballistic Efficiency Coeff.	4.68	4.49	4.59	3.87	18.6%

7.7.6. Preliminary Comparison

Until here, SiC5, SiC3+SiC2, and SiC2+SiC3 configurations were analyzed. The test and analysis results and differences are shown in Table 7. 9. Although the backing plate and bullet calibrated well, the test and analysis differences are significant. The main reason is the Johnson-Holmquist strength parameters of SiC. These parameters were obtained from the literature. The tested ceramics and used parameters are improper. There is a significant difference between test and analysis efficiency values. However, the behaviors of the configurations are consistent. In the analysis domain, the SiC5 performed the best when

compared with LCS with the same material configurations. Also, the SiC3+SiC2 configuration performed better than SiC2+SiC3, similar to ballistic test results.

Table 7. 9. Summary of preliminary results

Configuration Name	Ballistic DoP Test Results [η]	Analysis DoP Results [η]	Difference [%]
SiC5	6.81	5.14	32.5
SiC3+SiC2	5.37	3.96	35.6
SiC2+SiC3	4.59	3.87	18.6

7.7.7. Analysis #4

In Analysis #5, LCS with different materials configuration is simulated, and B_4C material is used with SiC. B_4C material must be calibrated to perform better simulation. For this reason, three ballistic DoP tests were performed with the BC3+BC2 configuration. Analysis #4 was developed to simulate BC3+BC2 configuration, which is very similar to Analysis #2. Ceramic thicknesses, adhesive thicknesses, and ceramic positions were the same. The only difference is the ceramic material, and B_4C was used instead of SiC. The initial condition of Analysis #4 is shown in Figure 7. 15. The final condition of Analysis #4 can be seen in Figure 7. 27. The eroded elements and hole profile can be seen in Figure 7. 28.

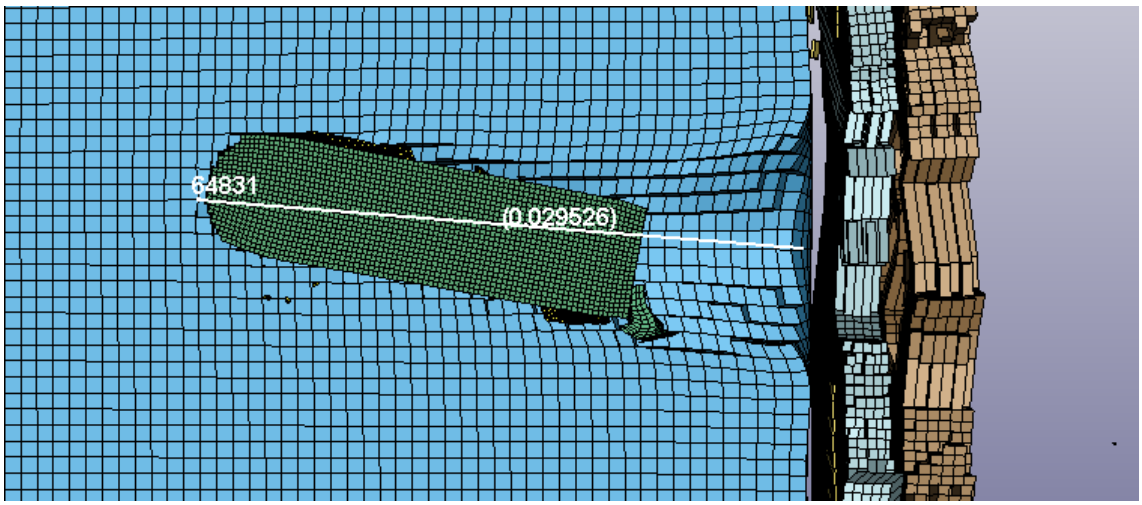

Figure 7. 27. The final condition of Analysis #4 (1)

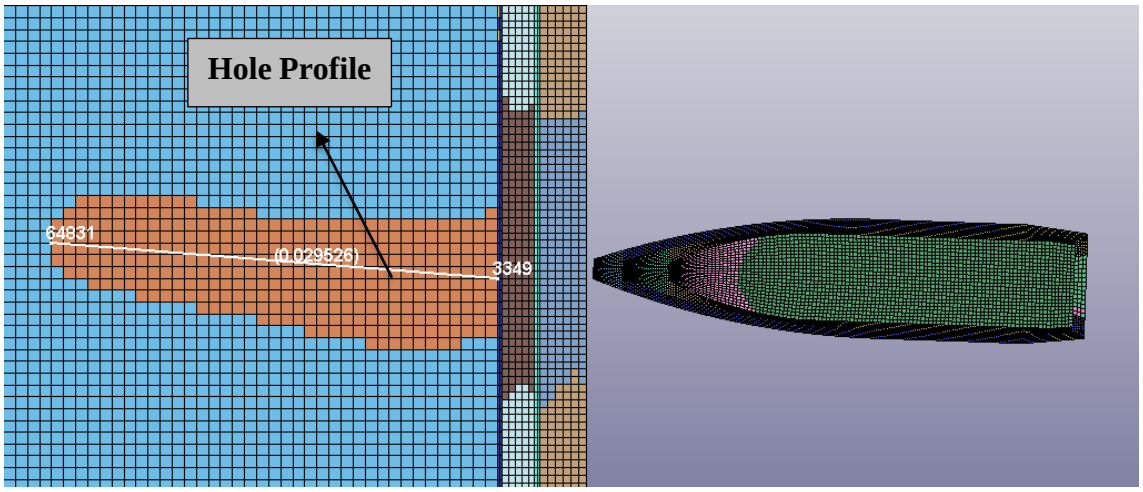

Figure 7. 28. The final condition of Analysis #4 (2)

Ballistically three DoP tests were performed, and the DoP test results are 28.96 mm, 24.08 mm, and 29.07 mm for the Non-Center Impact location test. The average of these tests is 27.37 mm. The B_4C parameters were found in the literature; however, the failure strain value was missing. Several analyses were performed, and failure strain was calibrated as FS=2.0. In Analyses #4, the DoP value is measured as 29.52 mm. The DoP difference between the test and analysis is ~7%. The Ballistic Efficiencies of tests and analysis are shown in Table 7. 10. The average Ballistic Efficiency of the DoP tests was determined as 4.69. Moreover, Analysis #4's Ballistic Efficiency was determined as 4.40, and the efficiency difference between the test and analysis was observed as 6.1%.

Table 7. 10. Test and analysis Ballistic Efficiencies of BC3+BC2 configuration and comparison of tests and Analysis #4

	Ballistic DoP Test Results			Avg. of the valid Ballistic DoP Test Results	Analysis DoP Result	Difference b/w. Test & Analysis
Specimen No:	BC3+BC2 #1	BC3+BC2 #2	BC3+BC2 #3	BC3+BC2 #1, #2 & #3	-	-
Ballistic Efficiency Coeff.	4.35	5.38	4.34	4.69	4.40	6.1%

7.7.8. Analysis #5

Analysis #5 was developed to simulate BC3+SiC2 configuration, which is very similar to Analysis #2. Ceramic thicknesses, adhesive thicknesses, and ceramic positions were the same. The only difference is the ceramic material; the strike-face ceramic was modeled as B_4C, and the rear-face ceramic was modeled as SiC. The initial condition of Analysis #5 is shown in Figure 7. 16. The final condition of Analysis #5 can be seen in Figure 7. 29. The eroded elements and hole profile can be seen in Figure 7. 30.

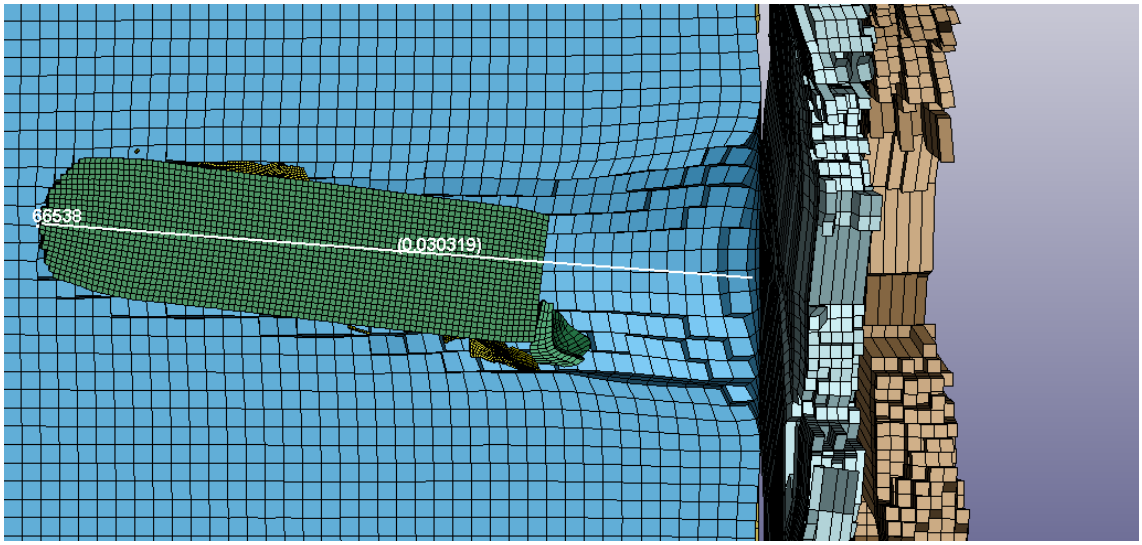

Figure 7. 29. The final condition of Analysis #5 (1)

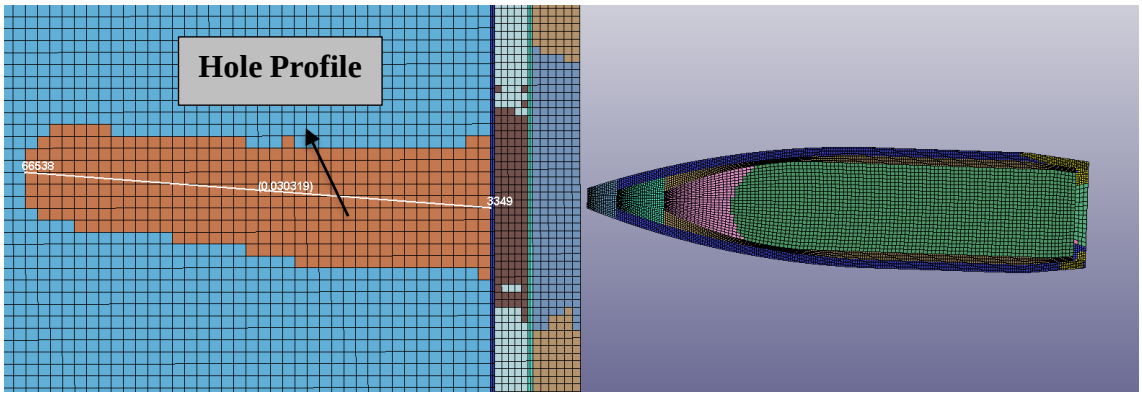

Figure 7. 30. The final condition of Analysis #5 (2)

The Ballistic Efficiencies of the test and analysis can be seen in Table 7. 11. The Ballistic Efficiency of Analysis #5 was calculated by DoP, which was measured on Figure 7. 30 (30.32 mm). The average Ballistic Efficiency of the DoP tests was 4.35. Analysis #5's

Ballistic Efficiency was determined as 3.84, and the efficiency difference between the test and analysis was observed as 11.7%. Previous analyses have shown that B4C was well calibrated and SiC was not. The test and analysis Ballistic Efficiency differences for SiC3+SiC2 and BC3+BC2 were 40.0% and 6.1%, respectively. When both materials used in Analysis #5, the test and analysis difference was dropped to 11.7%.

Table 7. 11. Ballistic Efficiency comparison of tests and Analysis #5

	Ballistic DoP Test Results		Avg. of the valid Ballistic DoP Test Results	Analysis DoP Result	Difference b/w. Test & Analysis
Specimen No:	#40	#41	#40 & #41	-	-
Ballistic Efficiency Coeff.	4.55	4.15	4.35	3.84	11.7%

7.7.9. Final Comparison

In the Preliminary Conclusion, the monolithic and LCS with the same material configurations were discussed. In the analysis domain, the monolithic SiC5 performed better than LCS with the same material configurations. Also, the SiC3+SiC2 configuration performed better than SiC2+SiC3. It has been observed that the tests and analyzes are consistent with the ceramic behavior. The details were explained in the Preliminary Conclusion.

In this section, mainly the test and analysis comparison of LCS with the same and LCS with different materials were discussed. The summary of the Ballistic Efficiency results is shown in Table 7. 12. The ballistic test results were compared in Chapter 6. SiC3+SiC2 configuration was performed better than BC3+SiC2. There is a significant difference between the test & analysis efficiency results, especially for SiC3+SiC2. However, the behaviors of the layered ceramic structures were similar. SiC3+SiC2 configuration was performed better than BC3+SiC2 in the analysis domain. It can be said that the test and analysis were consistent in terms of ceramics behaviors. With better calibration for SiC3+SiC2, consistency between test and analysis may be provided not only in terms of ceramic behaviors but also in terms of Ballistic Efficiency.

Table 7. 12. Summary of test and analysis results (LCS with the same and LCS with different materials).

Configuration Name	Ballistic DoP Test Results [η]	Analysis DoP Results [η]	Test & Analysis Difference [%]
SiC3+SiC2	5.55	3.96	35.6
BC3+SiC2	4.35	3.84	11.7

In these analyses, the calibration of bullet cores was also examined. After DoP tests, three bullet cores were found. These bullet cores are shown in Figure 7. 31. When these cores were examined, it was observed that their noses were eroded and blunted due to ceramics. The residual bullet core's lengths were measured as 23.40 mm, 22.26 mm, and 23.00 mm for cores a, b, and c, respectively; the average length is 22.88 mm. Several Ls-Dyna analyses were performed, and the average residual core length was measured as 21.6 mm. When the residual length of the test and analysis were compared, a 5.6% error was observed.

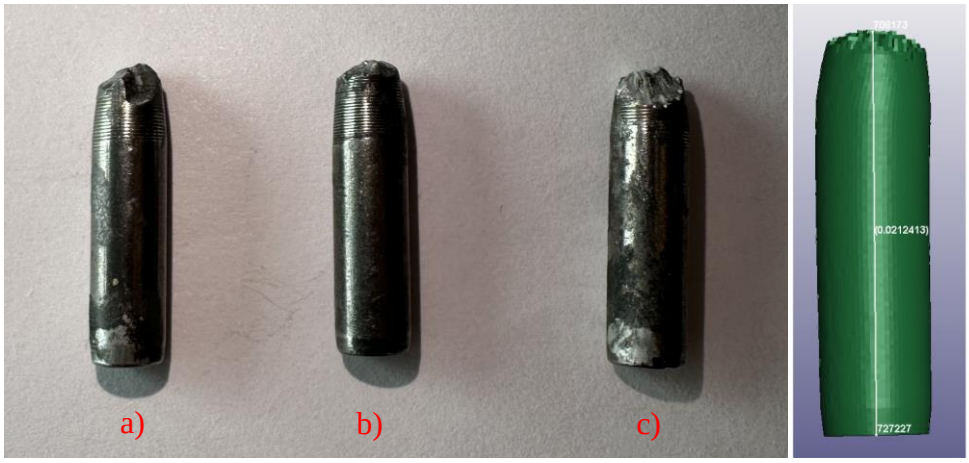

Figure 7. 31. Residual bullet cores of DoP ballistic test and numerical analysis

8. GENERAL CONCLUSION & DISCUSSION

8.1. Summary

Ceramic armors consist of two main components: ceramic tile and backing plate. In this study, monolithic and layered ceramic tiles are investigated by ballistic tests and numerical analysis. The study starts with the investigation of ceramic armor, its working principle, and the mechanical behavior of the materials. Then, a deep literature survey was conducted about previous studies about the ballistic performance of layered ceramic tiles. It was followed by an introduction to the Depth of Penetration (DoP) Test methodology, and important points were mentioned. In Chapter 5, the backing plate material selection method and adhesive material decision reasons are explained. Then a methodology was introduced for DoP test specimen preparation with details. The manufactured and tested configurations were also discussed in Chapter 5. The DoP tests were performed in the MKE's shooting range with manufactured specimens. Numerous comparisons were created, and the created comparisons evaluate the ballistic efficiency of monolithic ceramic, layered ceramics made of the same material, and layered ceramics made of different materials. In Chapter 7, the keystones of the Finite Element Analysis and some material models were mentioned. Then DoP tests with monolithic ceramic, LCS with the same material, and LCS with different materials were modeled in LS-PrePost software. In the final, modeled DoP tests were analyzed by LS-DYNA hydrocode software, and then the results of the test and analysis were compared.

8.2. General Conclusion

Several tests and analyses were performed. The summary of their conclusions is explained here:

For the ballistic DoP test,

a) The impact location of the ceramic is vital for ballistic performance. Ballistic Efficiency decreases drastically when the impact location shifts from the center to the edge.
b) In both geometries (hexagonal & square), monolithic ceramic structures and LCS with the same material were compared. The monolithic ceramic structures provide better protection than LCS with the same material in both geometries.

c) The strike face ceramic thickness was investigated on LCS with the same material in both geometries. It was observed that thicker ceramic use on the strike-face increases the ballistic efficiency.

d) LCS with the same material and LCS with different materials were investigated in both geometries. It was observed that when rear face ceramic is combined with a more efficient strike face ceramic, the total efficiency increases. In the comparison of BC3+SiC2 and SiC3+SiC2, the result was observed in the opposite. In Carton et al.'s study, it was shown that there is a critical areal density (critical thickness) for ceramics. When the areal density decrease below the critical value, the protection ability of ceramic decreases dramatically. The SiC3+SiC2 configuration has ~16.8 kg/m^2 areal density, and the BC3+SiC2 configuration has ~13.67 kg/m^2 areal density. The reason for the unexpected Ballistic Efficiency results of the BC3+SiC2 might be low areal density.

For DoP FE analysis:

e) Monolithic and LCS with the same material were compared by analyzing SiC5, SiC3+SiC2, and SiC2+SiC3 configurations. Material parameters were obtained from literature studies. The backing plate, bullet, and B4C ceramic failure strains were calibrated well. However, SiC parameters ceramic calibration was problematic; the strength parameters were incompatible. Therefore, significant differences were observed between the test and analysis of efficiency results of SiC5, SiC3+SiC2, and SiC2+SiC3. However, the behaviors of these configurations are consistent. The monolithic ceramic structure provides better protection than LCS with the same material in the analysis domain, similar to the ballistic test.

f) SiC3+SiC2 and SiC2+SiC3 were also compared in the analysis domain to investigate the thickness effect of the strike-face ceramic. There is a significant difference between the test and analysis efficiency values due to the SiC material parameters. However, the behaviors of the configurations are consistent with ballistic tests. In the analysis domain, the Ballistic Efficiency of SiC3+SiC2 is higher than the SiC2+SiC3 configuration, similar to the ballistic tests.

g) LCS with the same material and LCS with different materials were compared by analyzing BC3+SiC2 and SiC3+SiC2 configurations. Although the SiC

calibration was poor, similar efficiency values were obtained between the test and analysis for BC3+SiC2 due to the good calibration of B_4C. In the analysis domain, SiC3+SiC2 has higher Ballistic Efficiency than BC3+SiC2. This result is consistent with the ballistic test.

8.3. Discussion

In this study, it has been shown by the test and analysis that LCS with the same material has less efficiency than monolithic ceramic. Also, it was observed that when rear-face ceramic is combined with a more efficient strike-face ceramic, the efficiency of LCS with different materials higher than LSC with the same material.

There are few studies about LCS with the same material in the literature. These studies were grouped and investigated in Chapter 3. While some of these studies argue that LCS with the same material has higher Ballistic Efficiency than monolithic ceramic (Group 1), others argue the opposite (Group 2). It has been observed that relatively thick layer ceramics are used in Group 1 studies. The ceramic layer thicknesses are 5 mm, 12.7 mm, and 14 mm, as shown in Table 8. 1. In Group 2 studies, relatively thin ceramic layers are used; these are 2 mm, 3 mm, 3.5 mm, 6.35 mm, and 7 mm as shown in Table 8. 2.

The efficiency of the ceramic decreases dramatically when the ceramic thickness is under a specific value. This value is called a critical thickness. When the literature results and the results of this study are considered together, it is understood that the efficiency of LCS is related to the ceramic layer thickness. The LCS is more efficient than monolithic ceramic if the layers' thickness is above the critical value. Also, it was shown that with this study, LCS with different materials has higher Ballistic Efficiency than LCS with the same material.

To sum up, LCS with different materials have more Ballistic Efficiency than LCS with the same material. If the ceramic layer thicknesses of LCS are thicker than the critical thickness, LCS with different materials might have higher Ballistic Efficiency than monolithic ceramic.

Table 8. 1. Ceramic thicknesses of Group 1 studies.

Study	Monolithic Ceramic	LCS with the Same Material
Yadav and Ravichandran's study [5]	38.1 mm AlN	3 × 12.7 mm AlN
Weiss et al.'s study [4]	40 mm Al_2O_3	3 × 14 mm Al_2O_3
Gao et al.'s study [1]	10 mm TiB_2-B_4C	2 × 5mm TiB_2-B_4C

Table 8. 2. Ceramic thicknesses of Group 2 studies.

Study	Monolithic Ceramic	LCS with the Same Material	
Yadav and Ravichandran's study [5]	38.1 mm AlN	6 × 6.35 mm AlN	
Carton et al.'s study [3]	10 mm SiC	7 mm SiC + 3.5 mm SiC	
	7 mm SiC	3.5 mm SiC + 3.5 mm SiC	
Polla et al.'s study [7]	6 mm Al_2O_3	2 × 3 mm Al_2O_3	3 × 2 mm Al_2O_3

8.4. Future Work

Based on the findings and outcomes of the study, the following recommendations are shown for future research:

1) The critical thickness of the ceramics must be considered when creating the layered ceramic structure. For this reason, a critical thickness determination study can be performed for various ceramic materials.
2) The type and thickness of the adhesive affect the ballistic efficiency. Previous studies investigated adhesive thickness between the ceramic and the backing plate. However, the effect of adhesive thickness between layered ceramics is a subject that needs clarification.
3) TiB_2 is one of the most famous armor ceramics. This work can be extended using TiB_2. A more efficient LCS can be created, especially in combination with B_4C.

9. REFERENCES

[1] Y. Gao, W. Zhang, P. Xu, X. Cai, and Z. Fan, "Influence of epoxy adhesive layer on impact performance of TiB2-B4C composites armor backed by aluminum plate," *International Journal of Impact Engineering,* vol. 122, pp. 60-72, 2018.

[2] R. C., "Ceramic materials for lightweight armour applications.," in *Proceedings of the Combat Vehicle Survivability Symposium*, Cranfield University, RMCS, Shrivenham, UK, 8-10 December 2004.

[3] E. Carton, G. Roebroeks, J. Weerheijm, A. Diederen, and M. Kwint, "Tno's research on ceramic based armor," in *Advances in Ceramic Armor XI: A Collection of Papers Presented at the 39th International Conference on Advanced Ceramics and Composites*, 2015: John Wiley & Sons, Inc. Hoboken, NJ, USA, pp. 1-18.

[4] A. Weiss, A. Borenstein, G. B.-M. STAN, M. Ravid, and N. Shapira, "Ballistic performance of ceramic targets against 25mm APDS-T projectile," in *30th international symposium on ballistics*, 2017.

[5] S. Yadav and G. Ravichandran, "Penetration resistance of laminated ceramic/polymer structures," *International Journal of Impact Engineering,* vol. 28, no. 5, pp. 557-574, 2003.

[6] P. Chabera, A. Boczkowska, A. Morka, T. Niezgoda, A. Oziębło, and A. Witek, "Numerical and experimental study of armour system consisted of ceramic and ceramic-elastomer composites," *Bulletin of the Polish Academy of Sciences: Technical Sciences,* no. 4, 2014.

[7] M. B. Polla, D. Fabris, A. D. Noni, and O. Montedo, "Desempenho balístico de estruturas multicamadas à base de alumina/epóxi," *Cerâmica,* vol. 65, pp. 207-215, 2019.

[8] W. A. Gooch, "An overview of ceramic armor applications," *Ceramic transactions,* vol. 134, pp. 3-21, 2002.

[9] I. Crouch, *The science of armour materials*. Woodhead Publishing, 2016.

[10] Coorstek. Advanced Alumina Materials & Manufacturing Processes [Online] Available: https://www.coorstek.com/media/1715/advanced-alumina-brochure.pdf

[11] T. Vogler, W. Reinhart, and L. Chhabildas, "Dynamic behavior of boron carbide," *Journal of applied physics,* vol. 95, no. 8, pp. 4173-4183, 2004.

[12] A. Ruys, "11 - Alumina in lightweight body armor," in *Alumina Ceramics*, A. Ruys Ed.: Woodhead Publishing, 2019, pp. 321-368.

[13] P. J. Hazell, *Armour: materials, theory, and design*. CRC press, 2015.

[14] A. Bhatnagar, *Lightweight ballistic composites: military and law-enforcement applications*. Woodhead Publishing, 2016.

[15] L. Gilson, A. Imad, L. Rabet, and F. Coghe, "On analysis of deformation and damage mechanisms of DYNEEMA composite under ballistic impact," *Composite Structures,* vol. 253, p. 112791, 2020.

[16] M. Grujicic, B. Pandurangan, and B. d'Entremont, "The role of adhesive in the ballistic/structural performance of ceramic/polymer–matrix composite hybrid armor," *Materials & Design,* vol. 41, pp. 380-393, 2012/10/01/ 2012, doi: https://doi.org/10.1016/j.matdes.2012.05.023.

[17] M. Übeyli, R. O. Yıldırım, and B. Ögel, "Investigation on the ballistic behavior of Al2O3/Al2024 laminated composites," *Journal of Materials Processing Technology,* vol. 196, no. 1-3, pp. 356-364, 2008.

[18] R. Zaera, S. Sánchez-Sáez, J. L. Pérez-Castellanos, and C. Navarro, "Modelling of the adhesive layer in mixed ceramic/metal armours subjected to impact," *Composites Part A: Applied Science and Manufacturing,* vol. 31, no. 8, pp. 823-833, 2000.

[19] K. J. Doherty, "The effect of metal-ceramic bonding on ballistic impact," *Ceramic transactions,* vol. 134, pp. 635-642, 2002.

[20] P. J. Hazell, C. J. Roberson, and M. Moutinho, "The design of mosaic armour: The influence of tile size on ballistic performance," *Materials & Design,* vol. 29, no. 8, pp. 1497-1503, 2008.
[21] J. López-Puente, A. Arias, R. Zaera, and C. Navarro, "The effect of the thickness of the adhesive layer on the ballistic limit of ceramic/metal armours. An experimental and numerical study," *International Journal of Impact Engineering,* vol. 32, no. 1, pp. 321-336, 2005/12/01/ 2005, doi: https://doi.org/10.1016/j.ijimpeng.2005.07.014.
[22] A. Prakash, J. Rajasankar, N. Anandavalli, M. Verma, and N. R. Iyer, "Influence of adhesive thickness on high velocity impact performance of ceramic/metal composite targets," *International Journal of Adhesion and Adhesives,* vol. 41, pp. 186-197, 2013/03/01/ 2013, doi: https://doi.org/10.1016/j.ijadhadh.2012.11.008.
[23] V. B. Harris AJ, Yeomans JA, Smith PA, Burnage ST. , "Surface preparation of alumina for improved adhesive bond strength in armor applications," presented at the Advanced Ceramic Armor VIII Florida, 22.06.2012, 2012.
[24] K. B. Lausund, B. B. Johnsen, D. B. Rahbek, and F. K. Hansen, "Surface treatment of alumina ceramic for improved adhesion to a glass fibre-reinforced polyester composite," *International Journal of Adhesion and Adhesives,* vol. 63, pp. 34-45, 2015/12/01/ 2015, doi: https://doi.org/10.1016/j.ijadhadh.2015.07.015.
[25] S. Noormohammed, C. Li, G. Toussaint, and J. Ilse, "New Generation Surface Treatment Techniques for Enhanced Adhesively Bonded Ceramic-Based Composite Armour Systems," 2019.
[26] W. Chen and G. Ravichandran, "Static and dynamic compressive behavior of aluminum nitride under moderate confinement," *Journal of the American Ceramic Society,* vol. 79, no. 3, pp. 579-584, 1996.
[27] D. Sherman and T. Ben-Shushan, "Quasi-static impact damage in confined ceramic tiles," *International Journal of Impact Engineering,* vol. 21, no. 4, pp. 245-265, 1998.
[28] Y. Bao, S. Su, J. Yang, and Q. Fan, "Prestressed ceramics and improvement of impact resistance," *Materials Letters,* vol. 57, no. 2, pp. 518-524, 2002.
[29] A. H. Gassman *et al.*, "Effect of Pre-stressing on the Ballistic Performance of Alumina Ceramics: Experiments and Modeling," *Advances in Ceramic Armor IX,* pp. 31-40, 2013.
[30] R. Chi, A. Serjouei, I. Sridhar, and T. E. Geoffrey, "Pre-stress effect on confined ceramic armor ballistic performance," *International Journal of Impact Engineering,* vol. 84, pp. 159-170, 2015.
[31] M. J. Normandia and W. A. Gooch, "An overview of ballistic testing methods of ceramic materials," *Ceramic transactions,* vol. 134, pp. 113-138, 2002.
[32] D. Sherman and D. Brandon, "The ballistic failure mechanisms and sequence in semi-infinite. supported alumina tiles," *Journal of materials research,* vol. 12, no. 5, pp. 1335-1343, 1997.
[33] Z. Rosenberg, Y. Ashuach, Y. Yeshurun, and E. Dekel, "On the main mechanisms for defeating AP projectiles, long rods and shaped charge jets," *International journal of impact engineering,* vol. 36, no. 4, pp. 588-596, 2009.
[34] B. James, "Practical issues in ceramic armour design," *Ceramic transactions,* vol. 134, pp. 33-44, 2002.
[35] T. J. Moynihan, S.-C. Chou, and A. L. Mihalcin, "Application of the depth-of-penetration test methodology to characterize ceramics for personnel protection," ARMY RESEARCH LAB ABERDEEN PROVING GROUND MD, 2000.
[36] M. Bolduc *et al.*, "Ballistic evaluation of nanocomposite ceramic," in *Proceedings of Personal Armour Systems Symposium PASS*, 2016, pp. 19-23.
[37] "Geschossstabilisierung (İng. Bullet Spin-Stabilisation)." https://de.wikipedia.org/wiki/Geschossstabilisierung (accessed.

[38] I.-D. Popa and F. Dobriţa, "Considerations on dop (depth of penetration) test for evaluation of ceramics materials used in ballistic protection," *Acta Universitatis Cibiniensis. Technical Series,* vol. 69, no. 1, pp. 162-166, 2017.
[39] M. Vural, Z. Erim, B. Konduk, and A. Ucisik, "Ballistic performance of alumina ceramic armors," 2001.
[40] P. Woolsey, D. Kokidko, and S. A. Mariano, "Alternative test methodology for ballistic performance ranking of armor ceramics," ARMY LAB COMMAND WATERTOWN MA MATERIAL TECHNOLOGY LAB, 1989.
[41] D. L. Logan, *A first course in the finite element method*. Cengage Learning, 2016.
[42] "Autodyn [Computer Software]. (2016)http://www.ansys.com/products/structures/ANSYS-Autodyn." (accessed.
[43] LS-DYNA, *Keyword User's Manual Volume II, Material Models (R13)*. 2021.
[44] J. O. Hallquist, *LS-DYNA, Theory Manual*. 2006.
[45] LS-DYNA, *Keyword User's Manual Volume I (R13)*. 2021.
[46] T. Børvik, S. Dey, and A. Clausen, "Perforation resistance of five different high-strength steel plates subjected to small-arms projectiles," *International Journal of Impact Engineering,* vol. 36, no. 7, pp. 948-964, 2009.
[47] G. R. Johnson and W. H. Cook, "Fracture characteristics of three metals subjected to various strains, strain rates, temperatures and pressures," *Engineering fracture mechanics,* vol. 21, no. 1, pp. 31-48, 1985.
[48] R. Campilho and T. Fernandes, "Comparative evaluation of single-lap joints bonded with different adhesives by cohesive zone modelling," *Procedia Engineering,* vol. 114, pp. 102-109, 2015.
[49] *AUTODYN, Material Library, Epoxy Resin.*
[50] D. S. Cronin, K. Bui, C. Kaufmann, G. McIntosh, T. Berstad, and D. Cronin, "Implementation and validation of the Johnson-Holmquist ceramic material model in LS-Dyna," in *4th European LS-dyna users conference*, 2003, vol. 1, pp. 47-60.

10.APPENDICES

APPENDIX I – POST - TEST CONDITION OF TEST SPECIMENS

Specimen number is written on test specimen

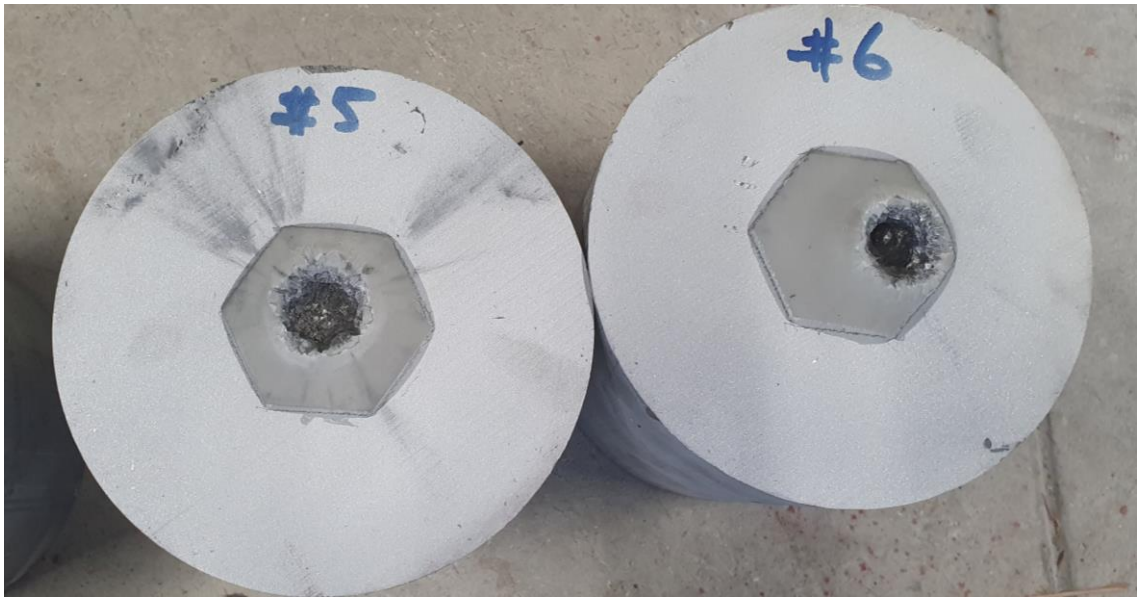

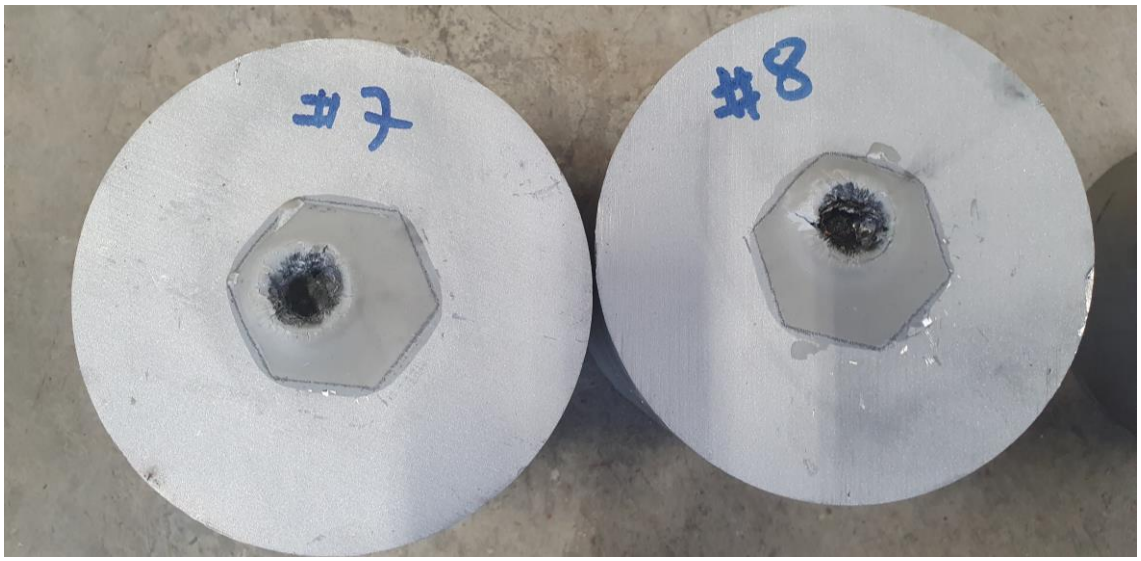

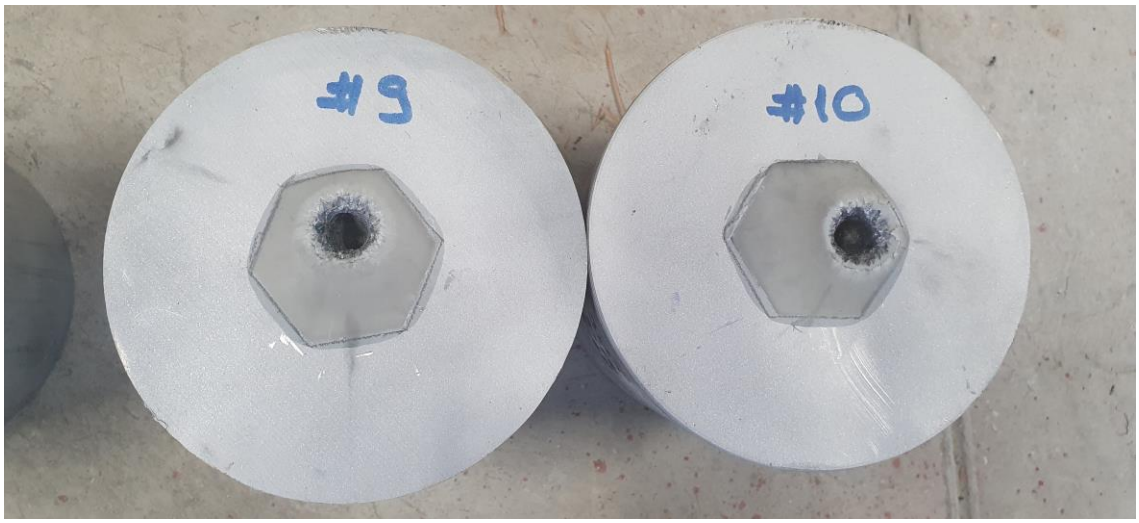
#9
#10

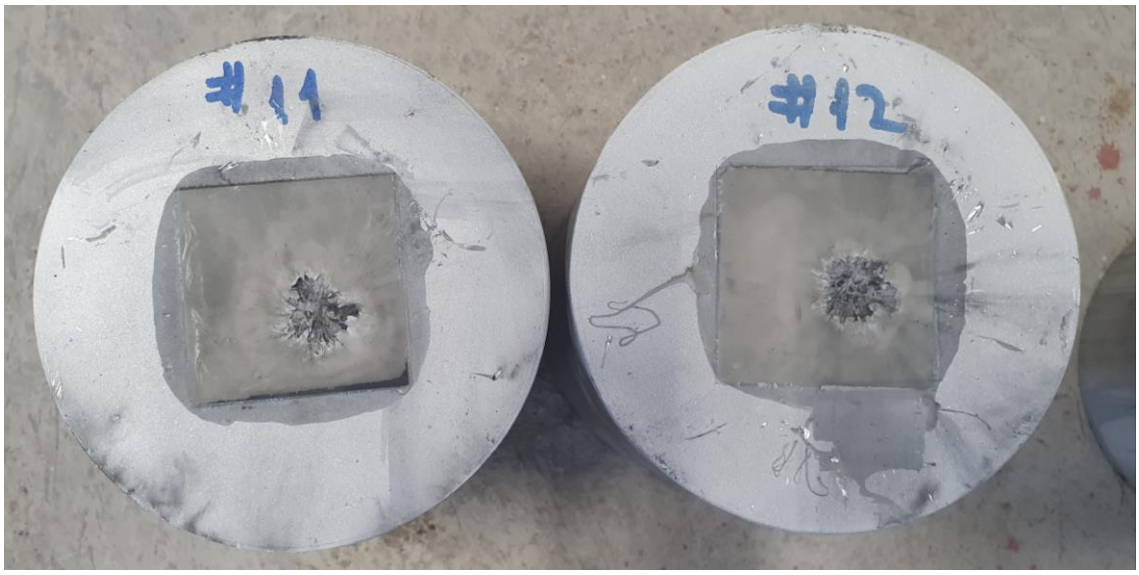
#11
#12

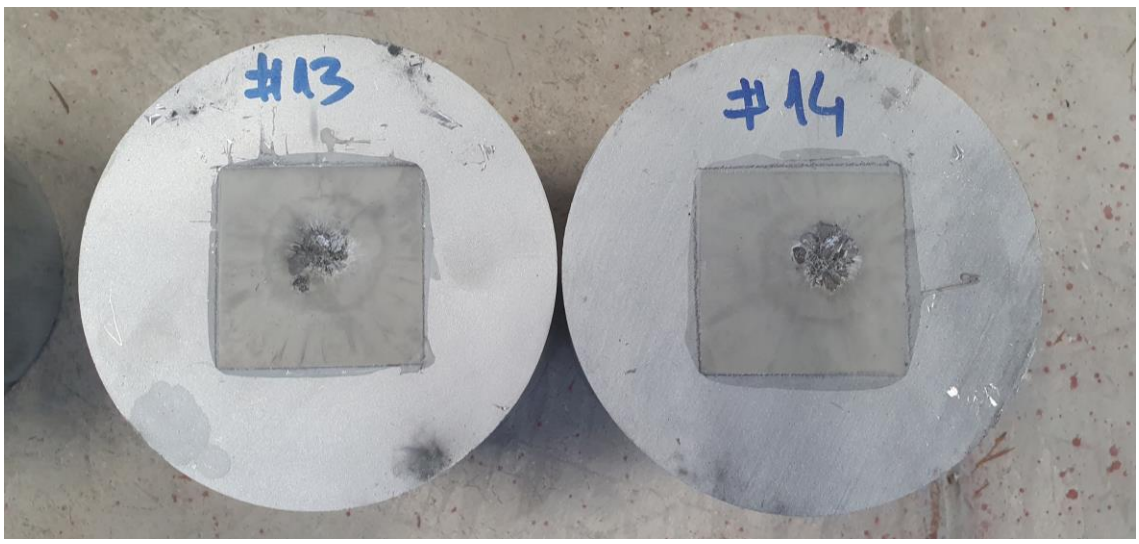
#13
#14

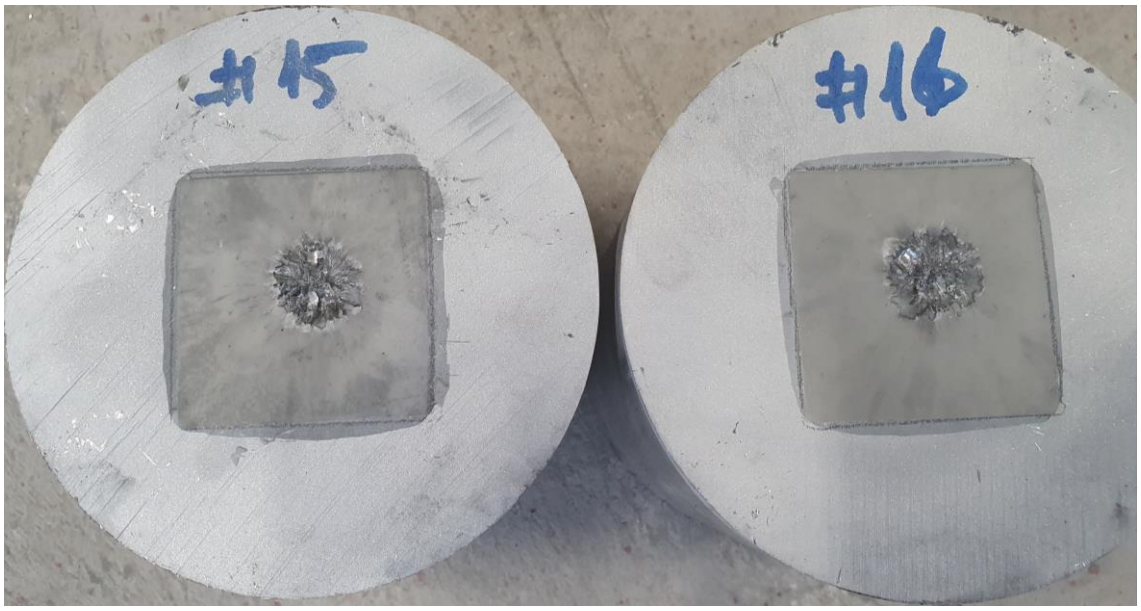
#15
#16

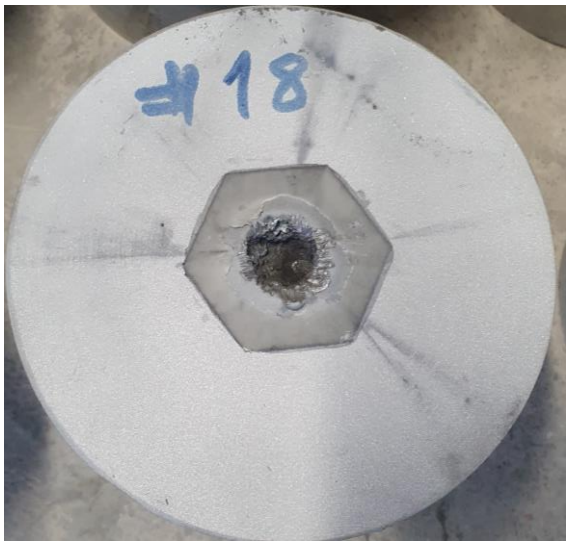
#18

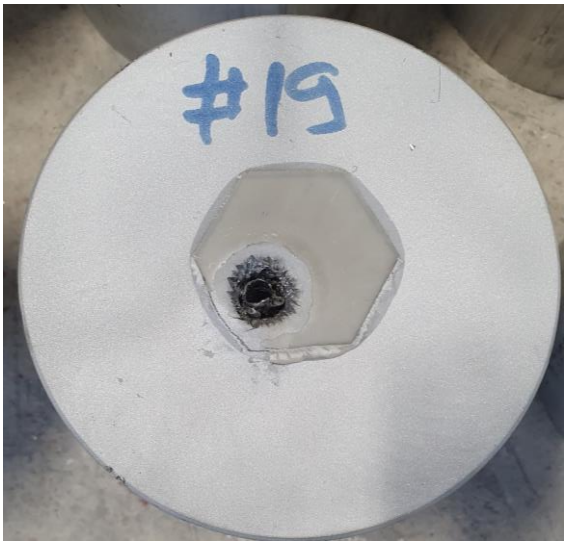
#19


#27


#28

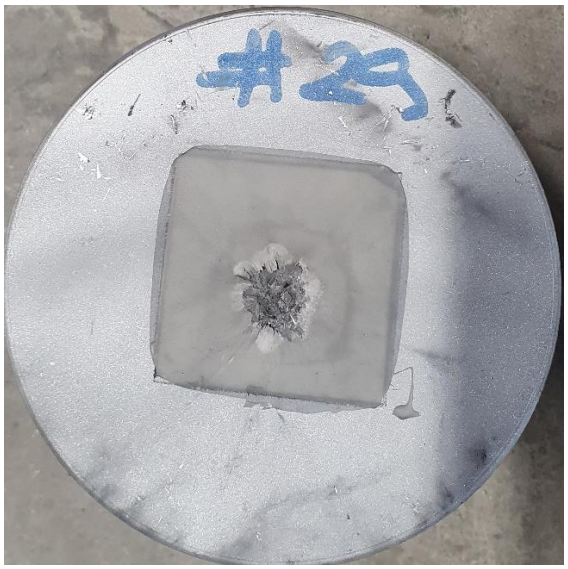
#29


#30


#32


#31


40


41

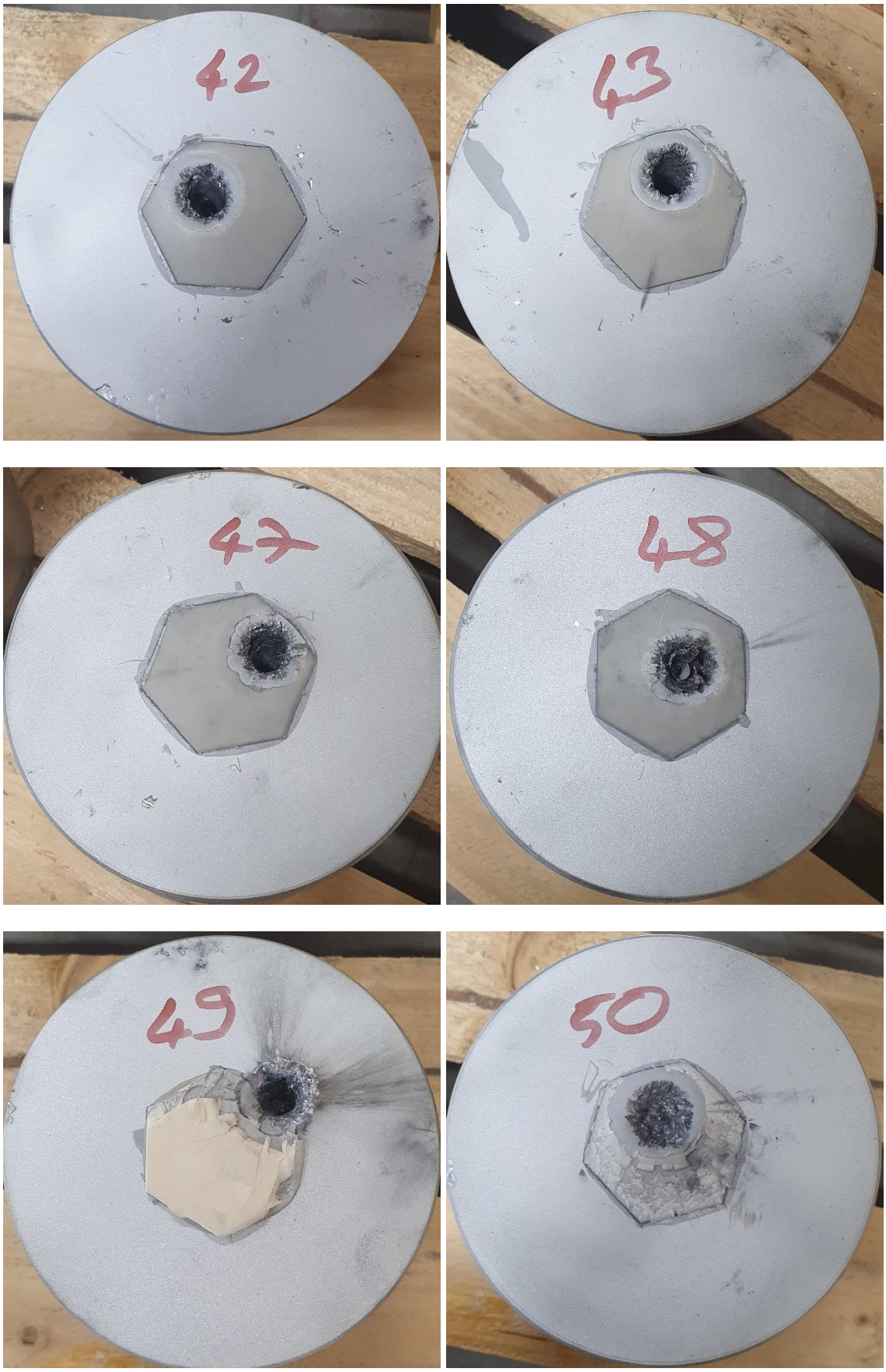
42
43
47
48
49
50

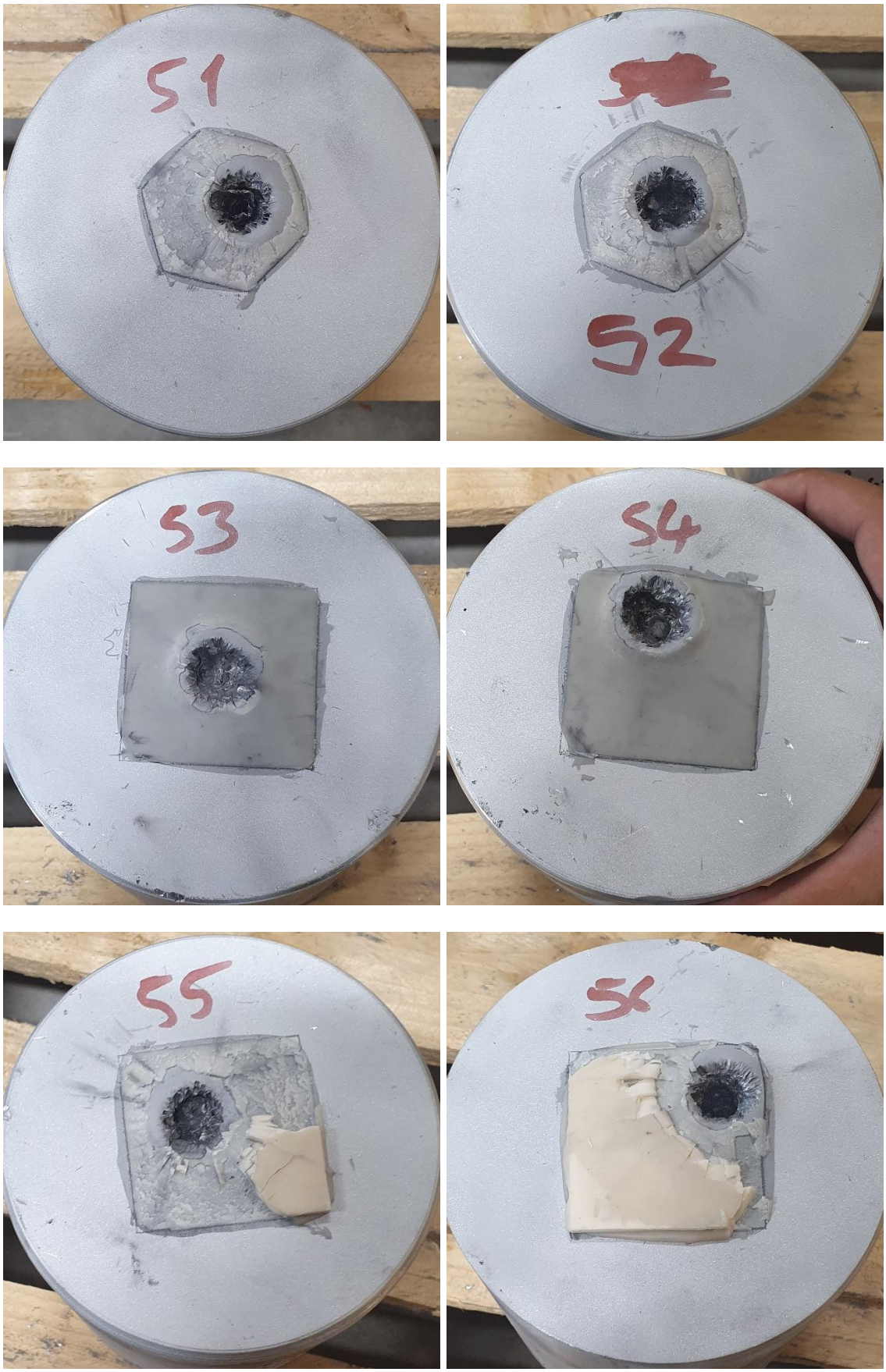
S1
S2
S3
S4
S5
S6

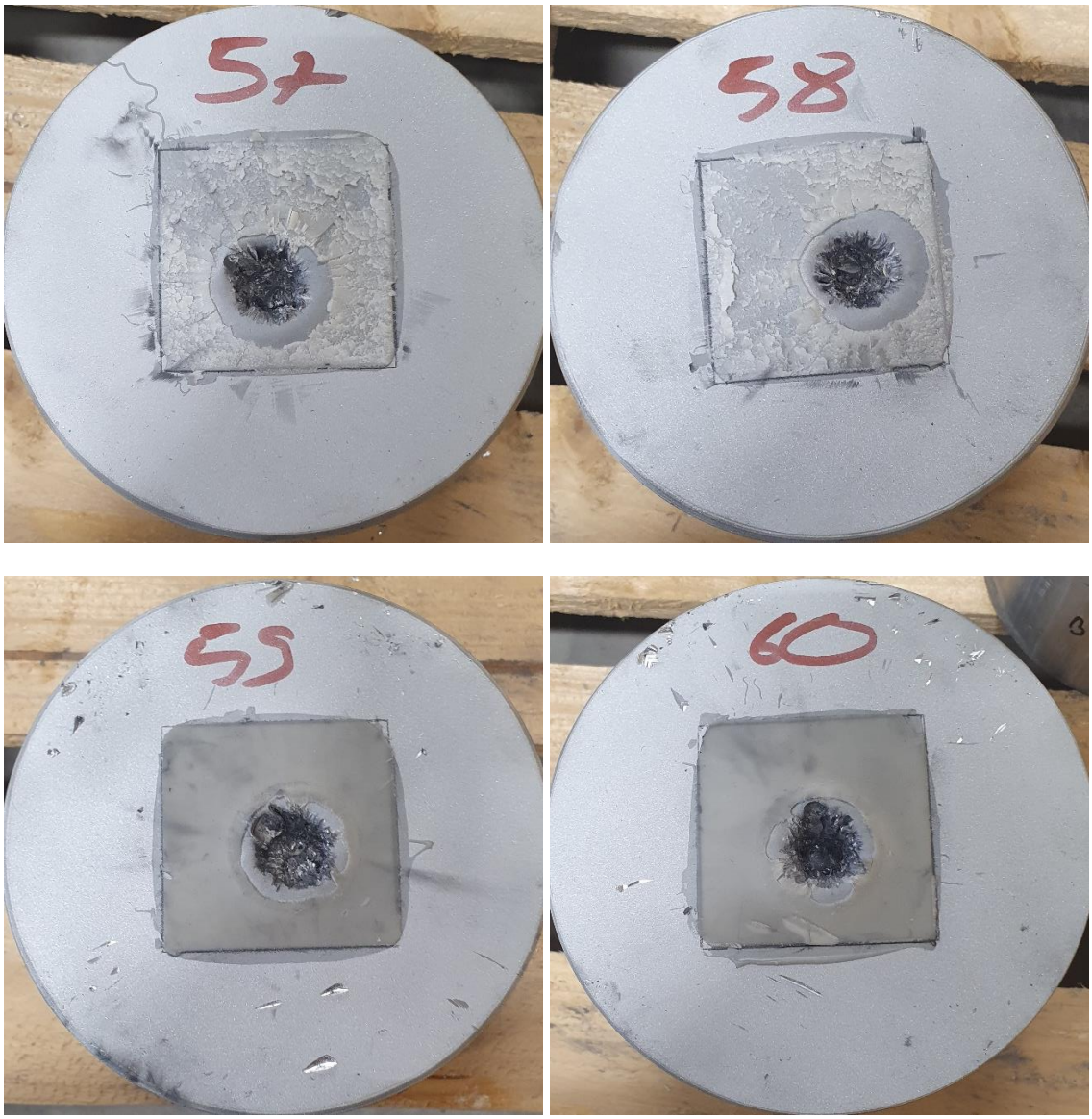
57
58
59
60

APPENDIX II - DOP X-RAY IMAGES

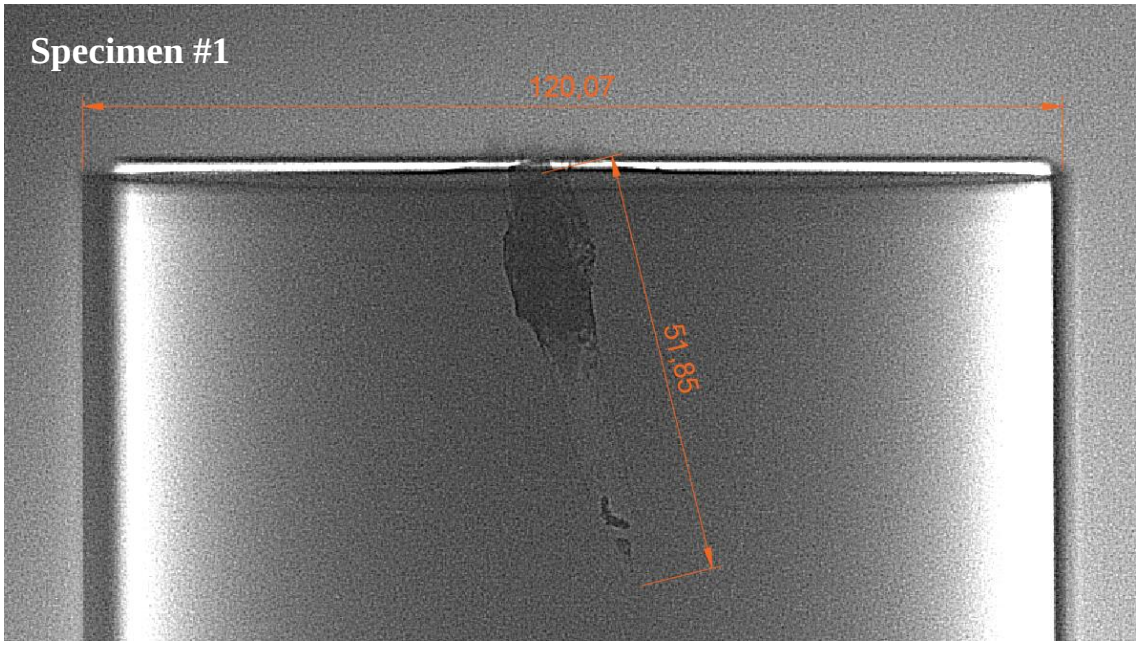

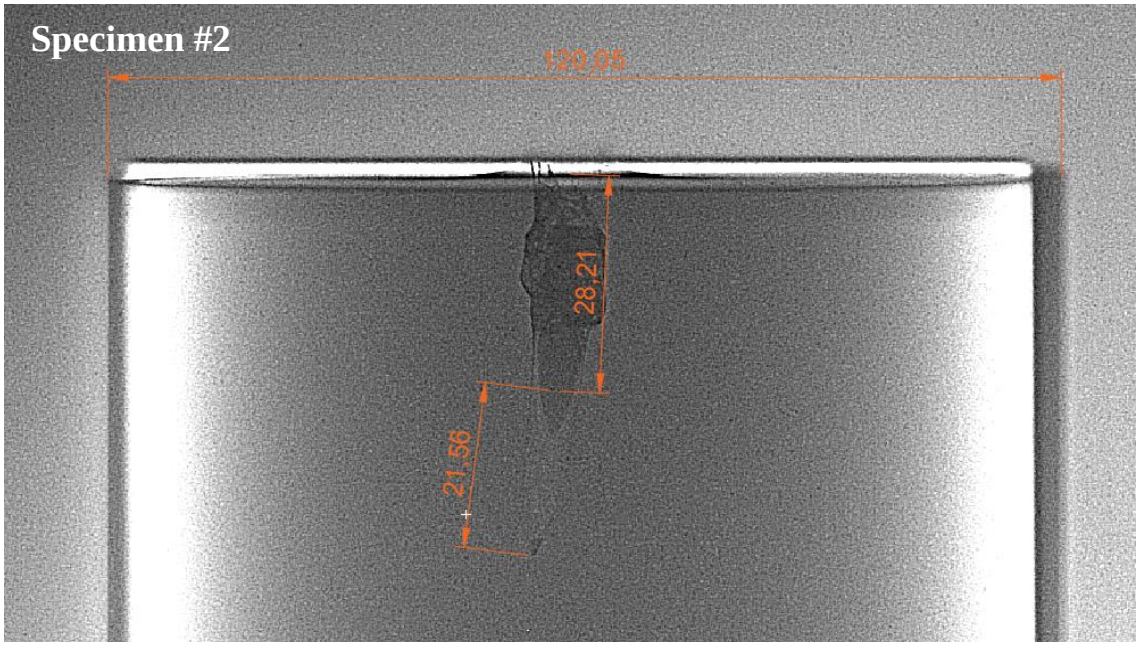

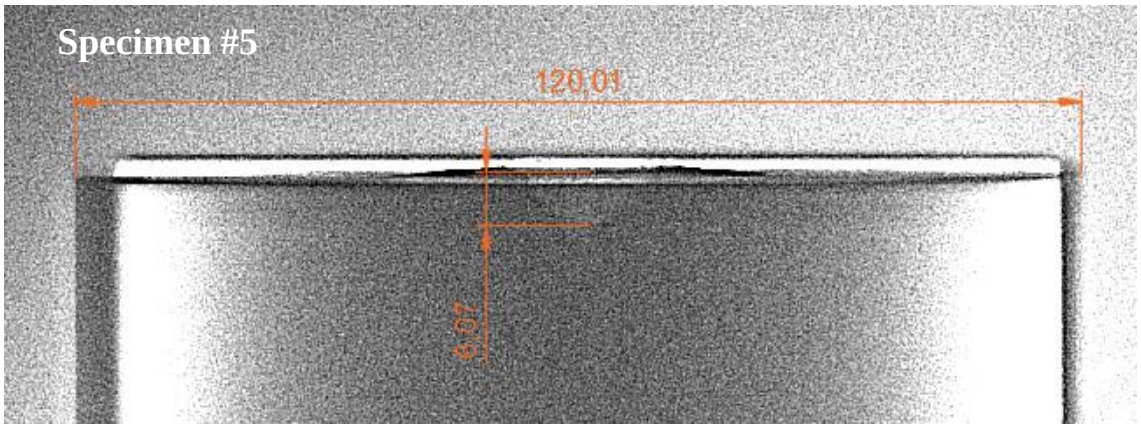

Important Note: The X-Ray image of the Specimen #5 is not clear to measure. For this reason, DoP measurement for Specimen #5 is performed by caliper.

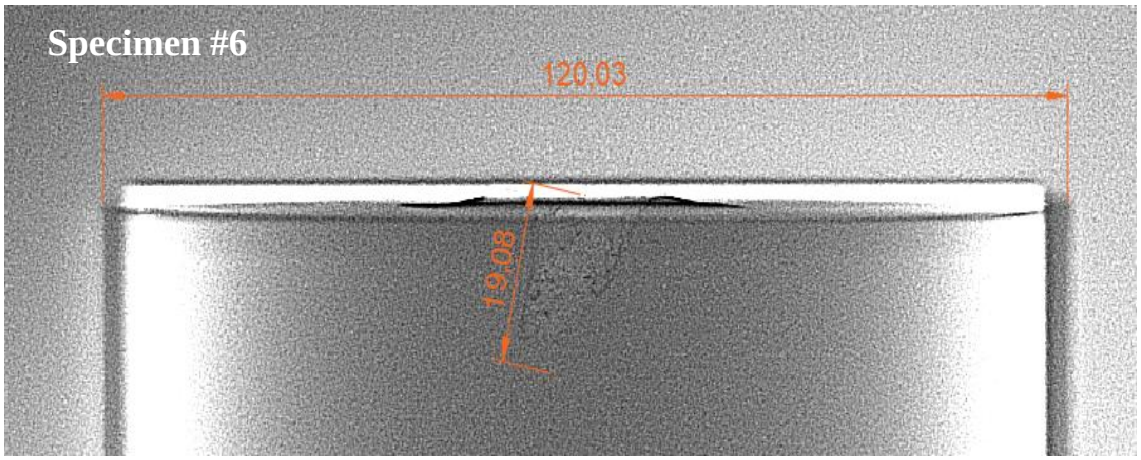

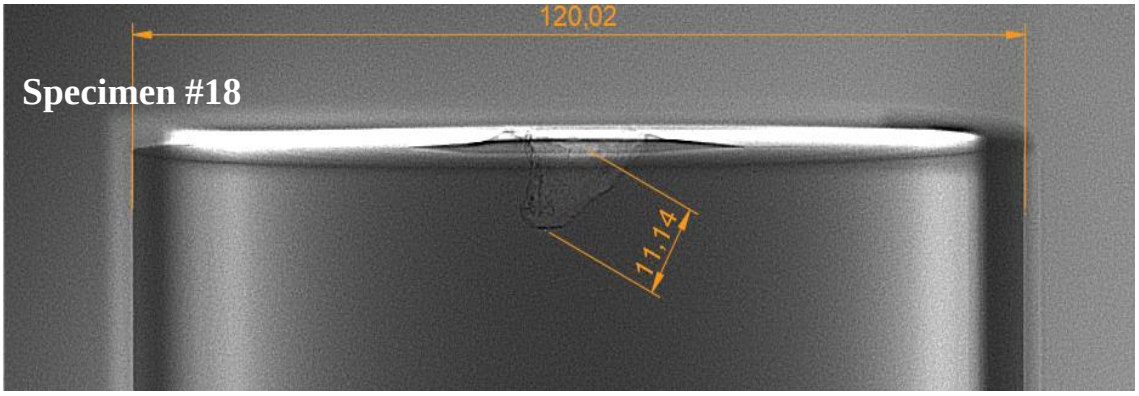

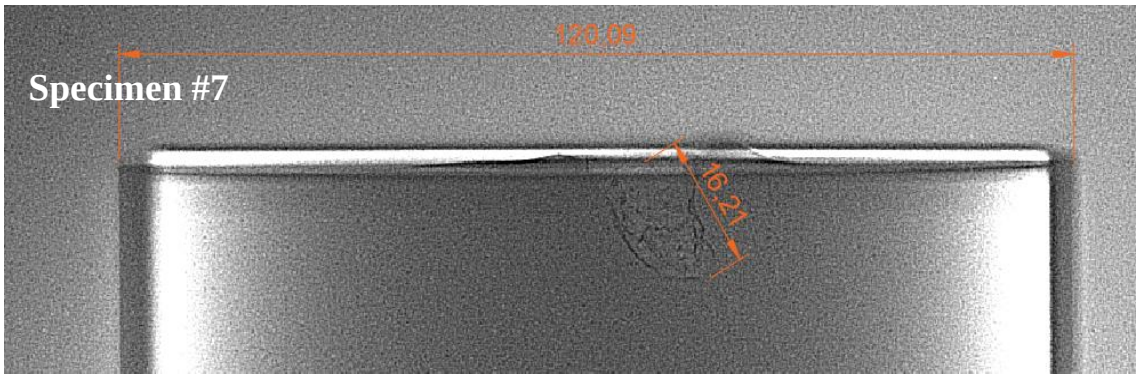
Specimen #7
120,09
16,21

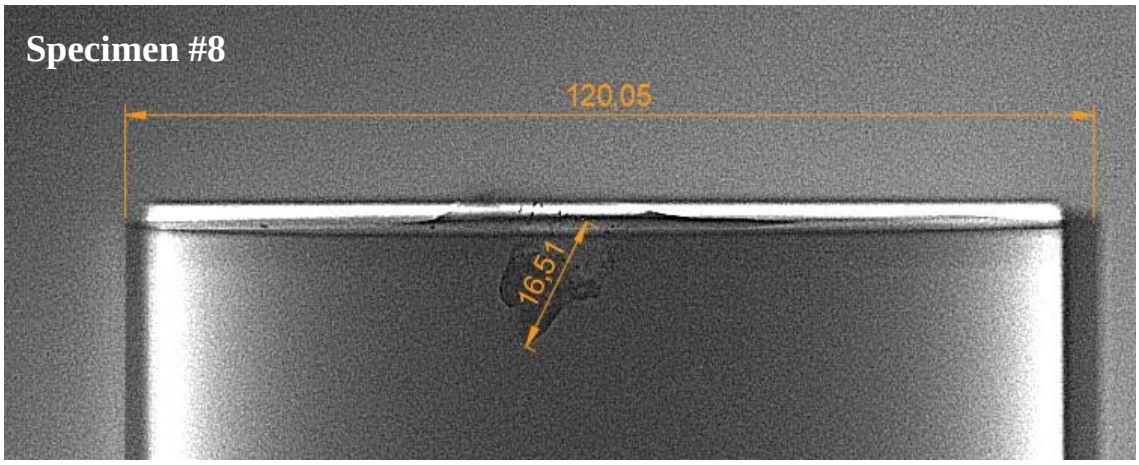
Specimen #8
120,05
16,51

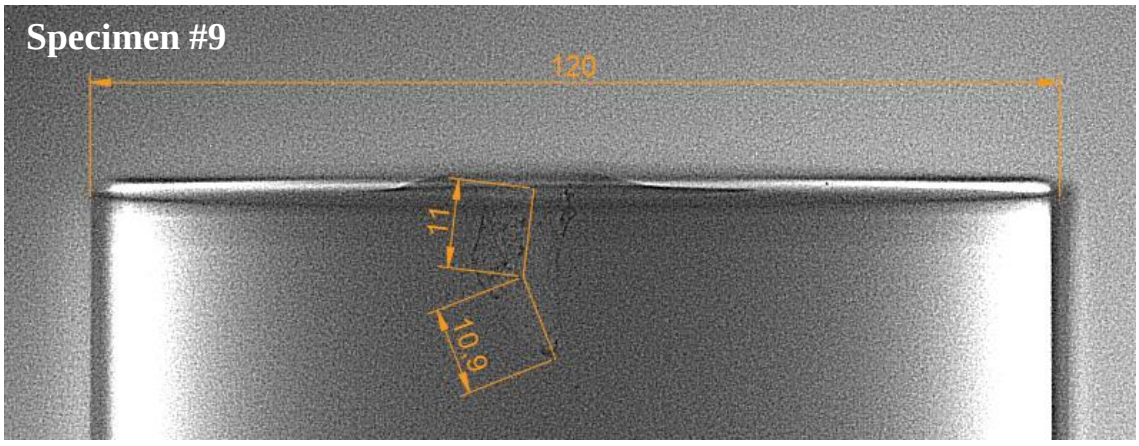
Specimen #9
120
11
10,9

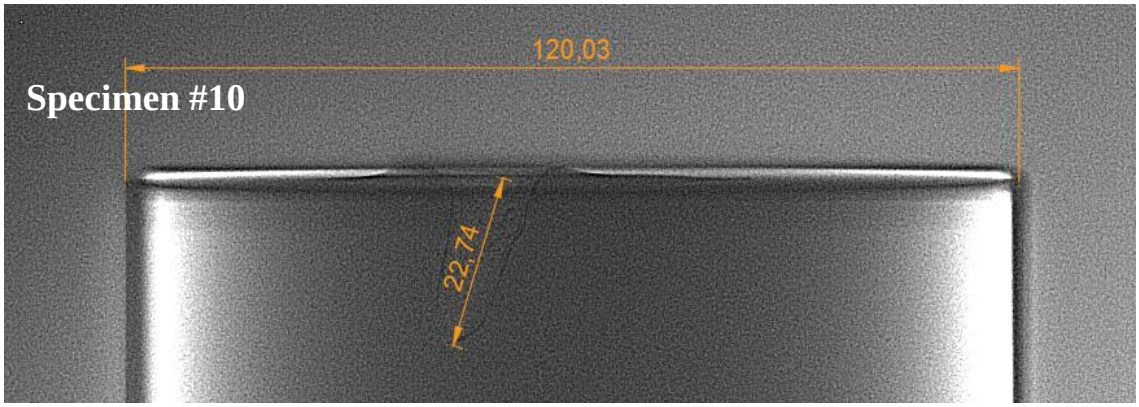
Specimen #10
120,03
22,74

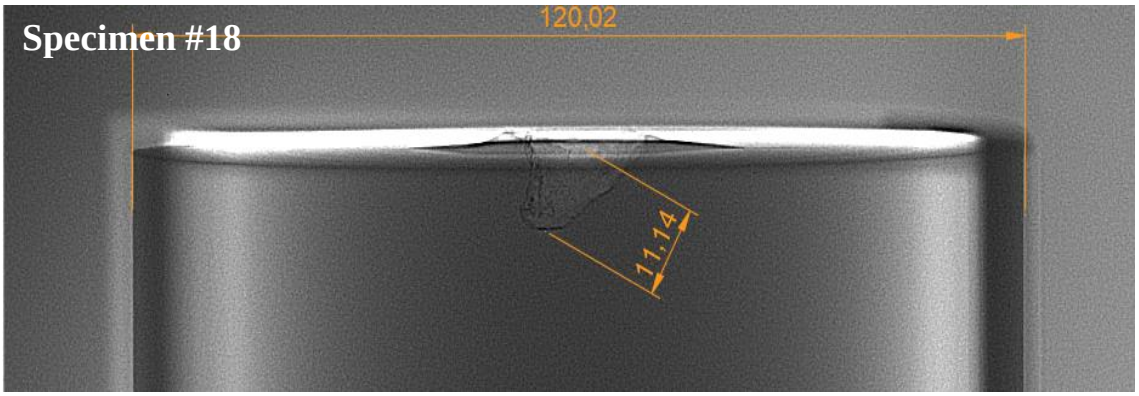
Specimen #18
120,02
11,14

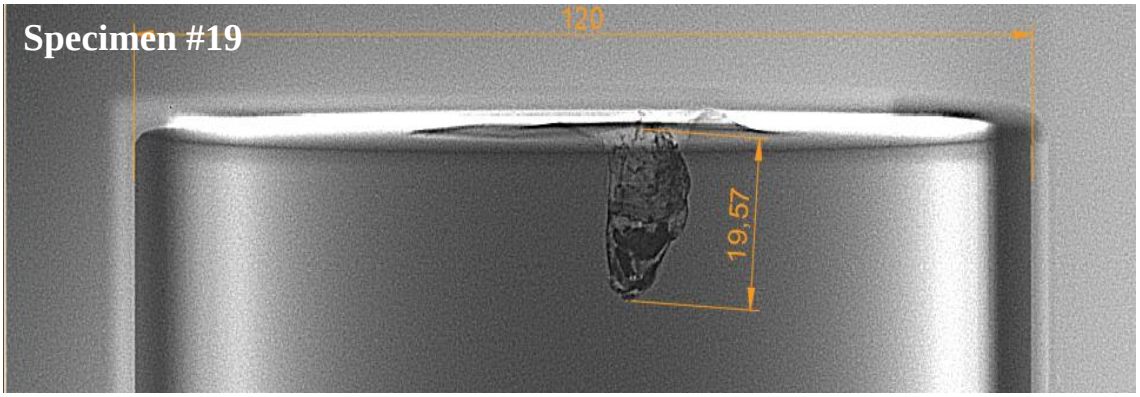
Specimen #19
120
19,57

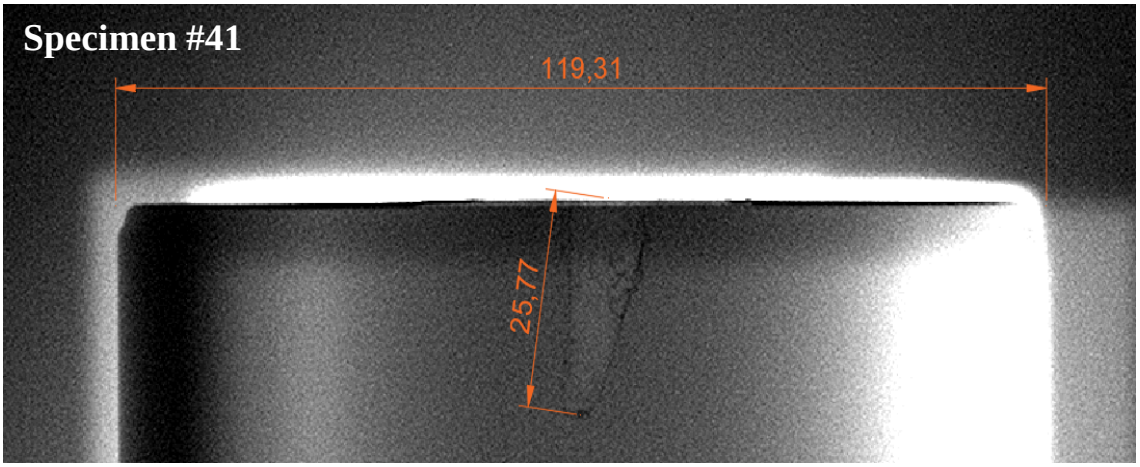
Specimen #41
119,31
25,77

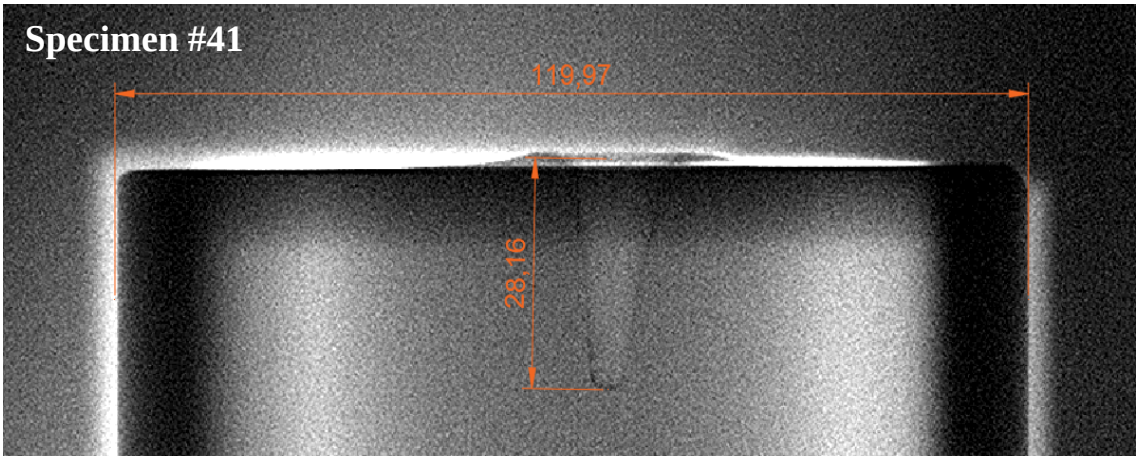
Specimen #41
119,97
28,16

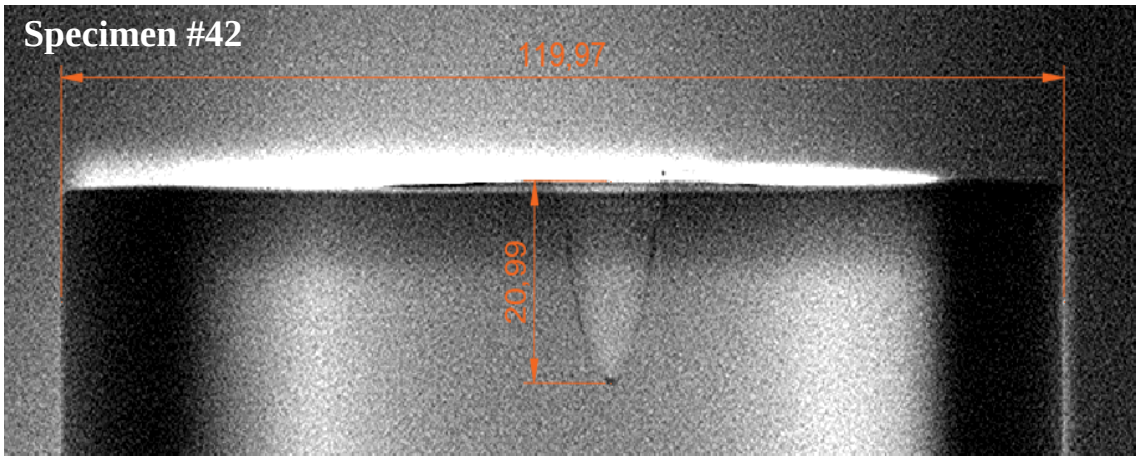
Specimen #42
119.97
20.09

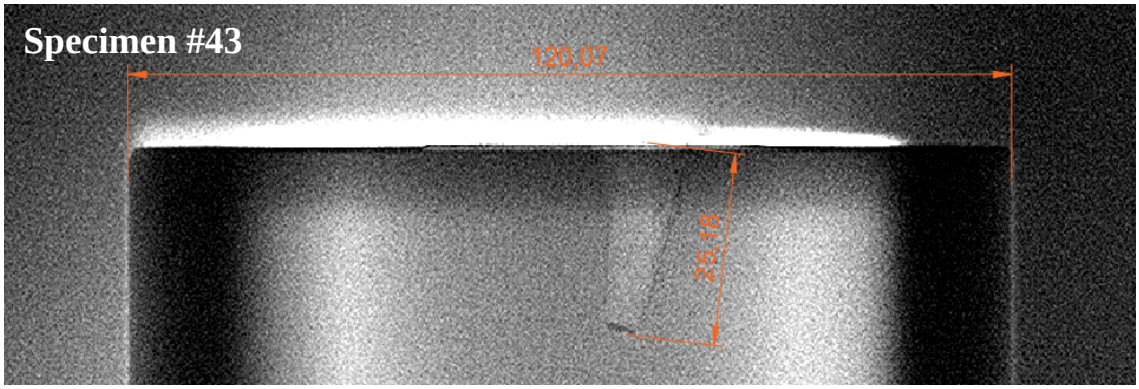
Specimen #43
120.07
25.18

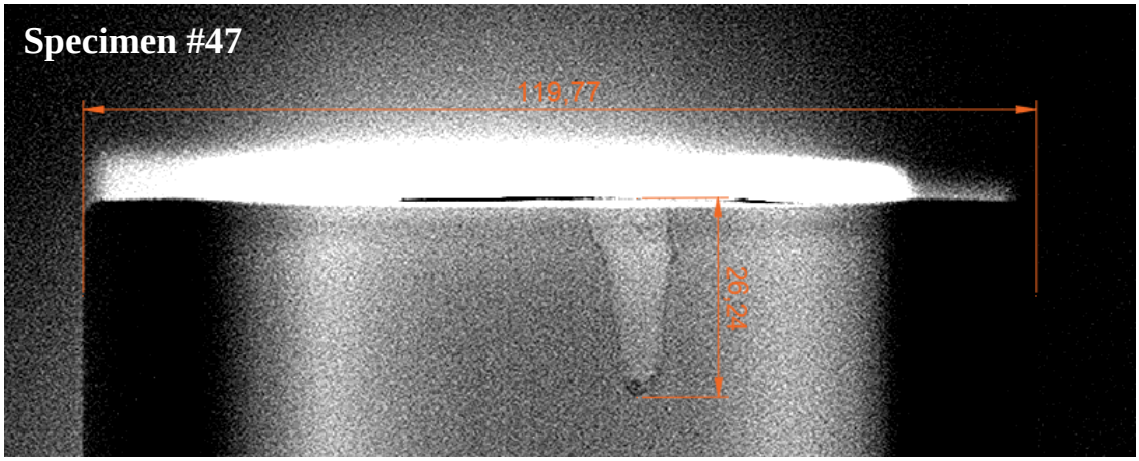
Specimen #47
119.77
20.24

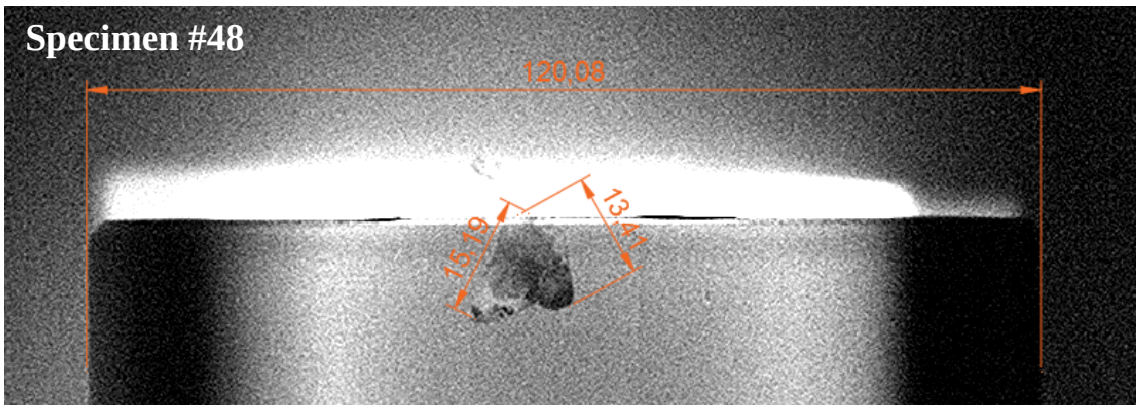
Specimen #48
120.08
15.19
13.41

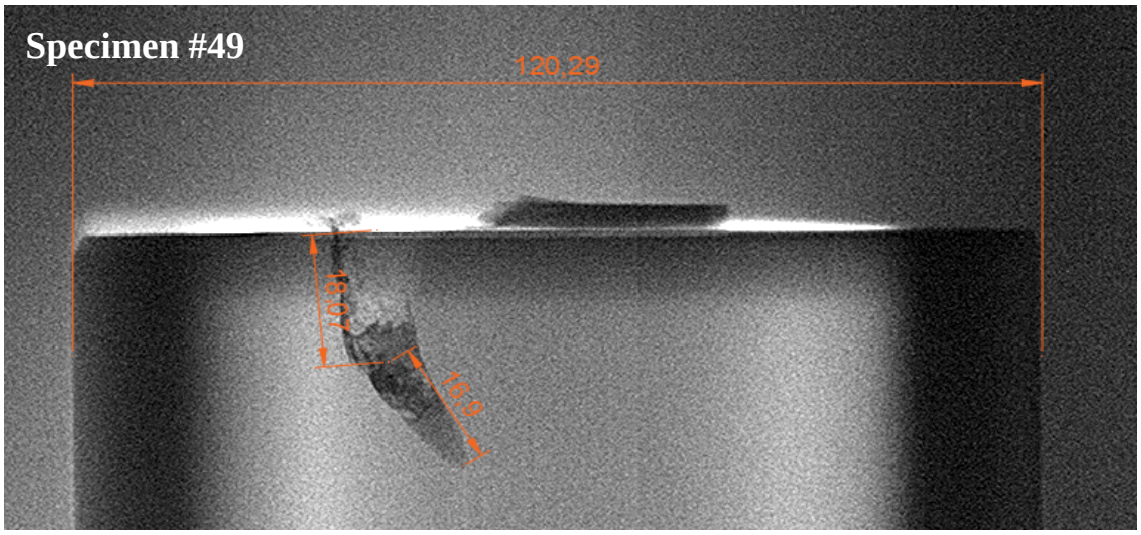
Specimen #49
120,29
18,07
16,9

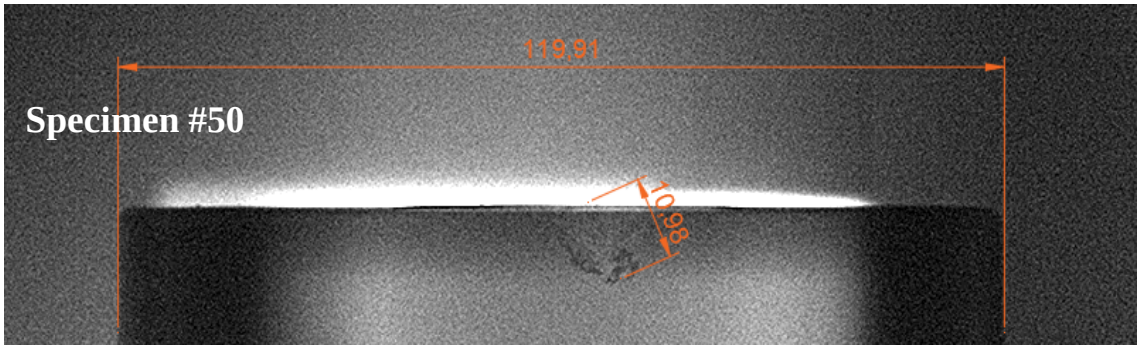
119,91
Specimen #50
10,98

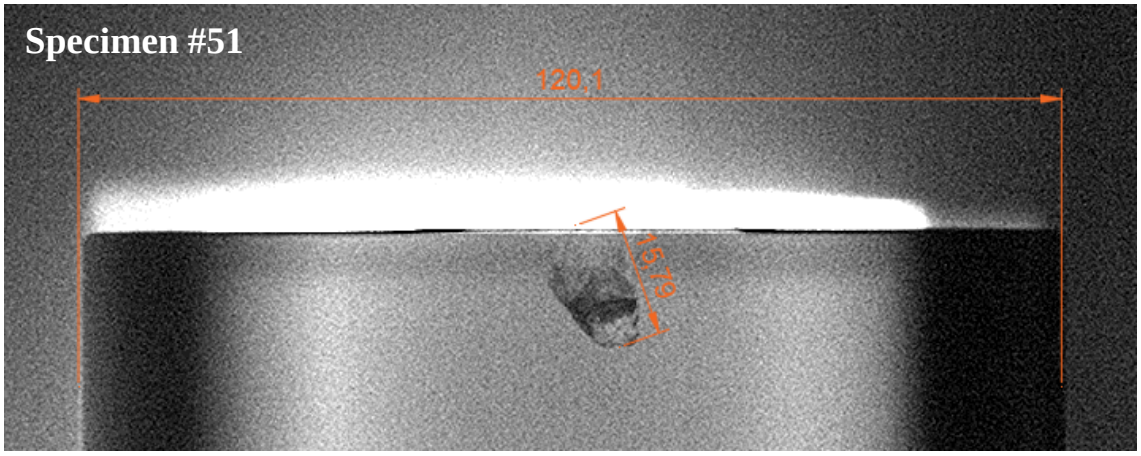
Specimen #51
120,1
15,19

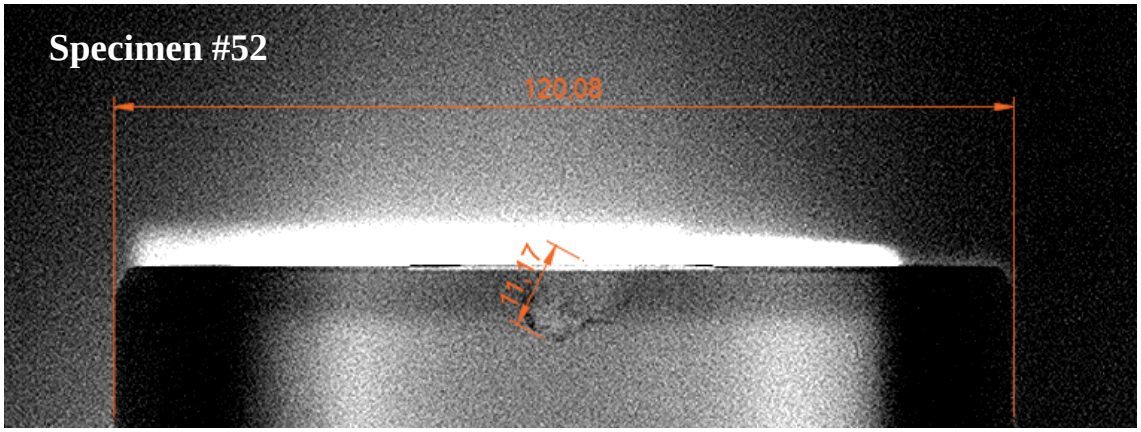
Specimen #52
120,08
11,17

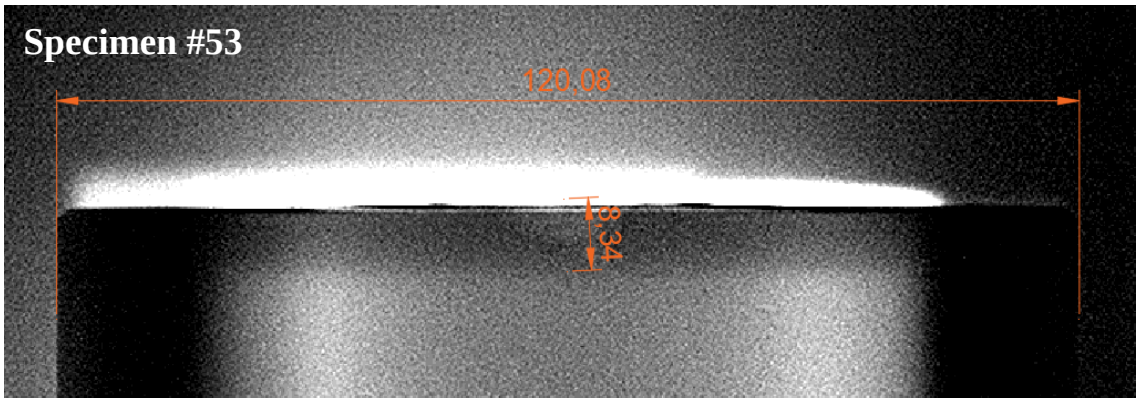
Specimen #53
120,08
3,43

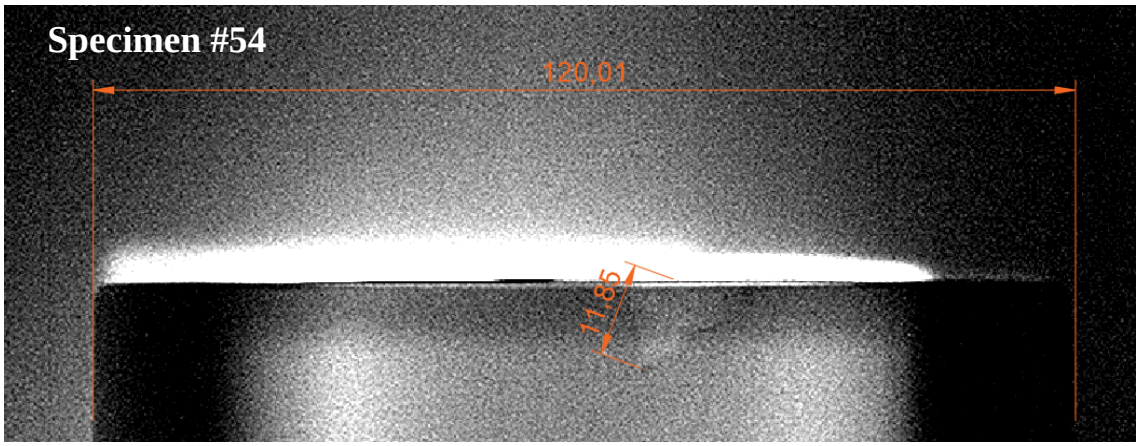
Specimen #54
120,01
11,85

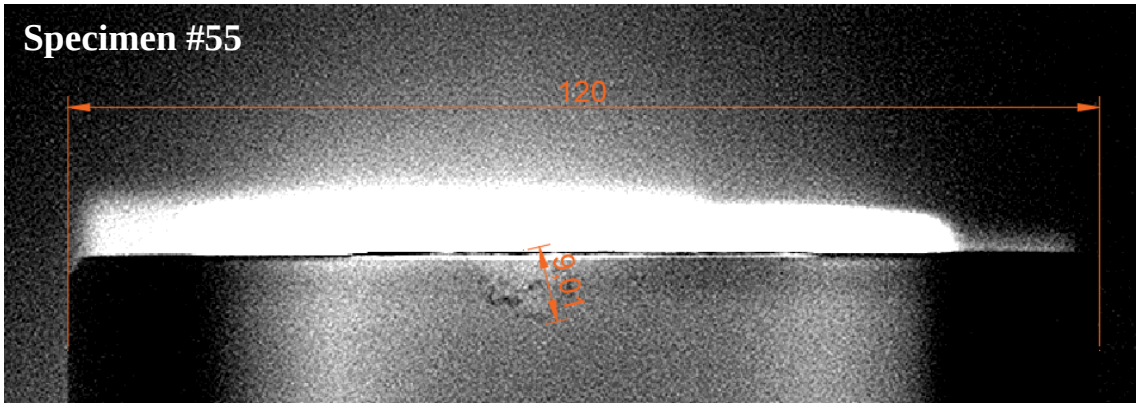
Specimen #55
120
6,13

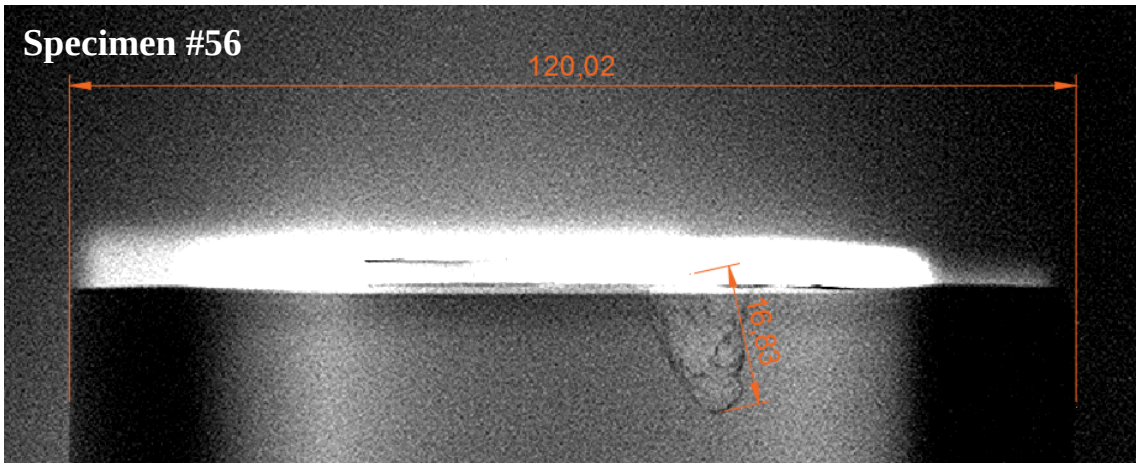
Specimen #56
120,02
16,83

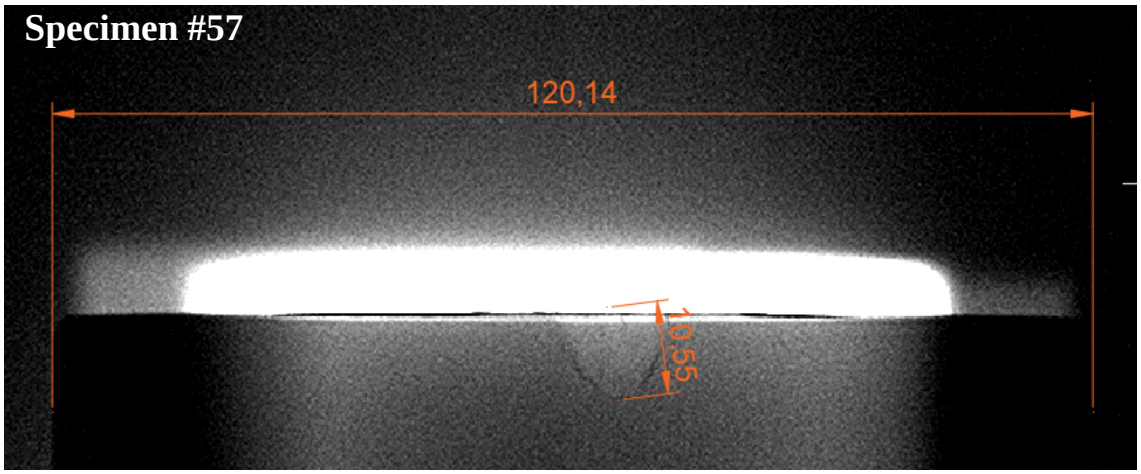
Specimen #57
120,14
10,55

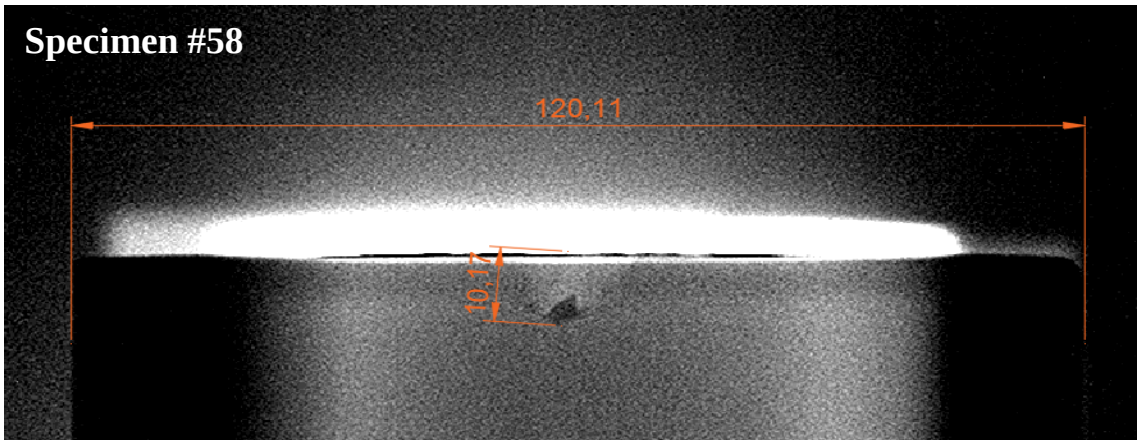
Specimen #58
120,11
10,17

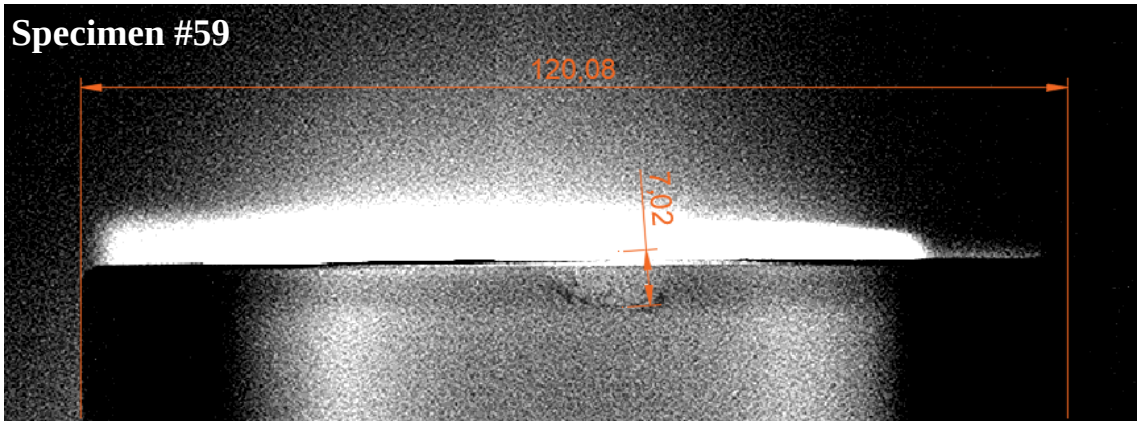
Specimen #59
120,08
7,02

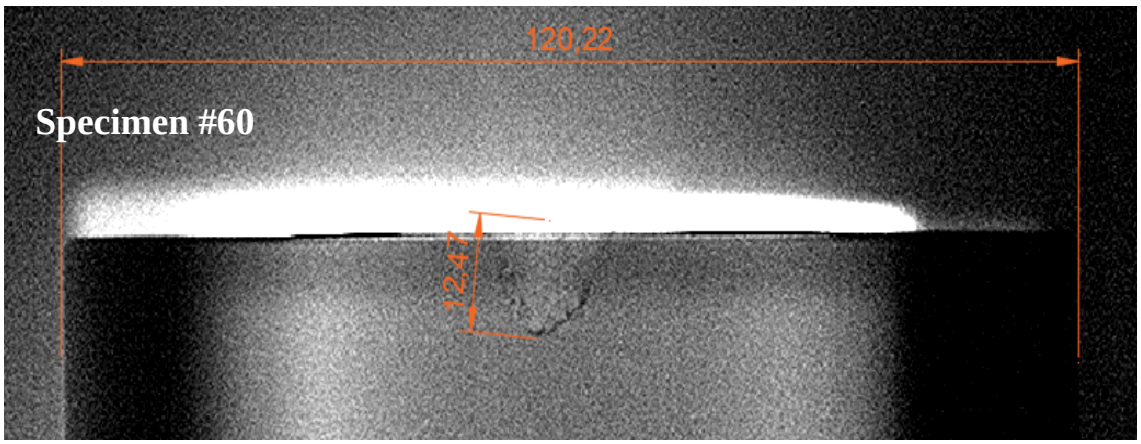
120,22
Specimen #60
12,47

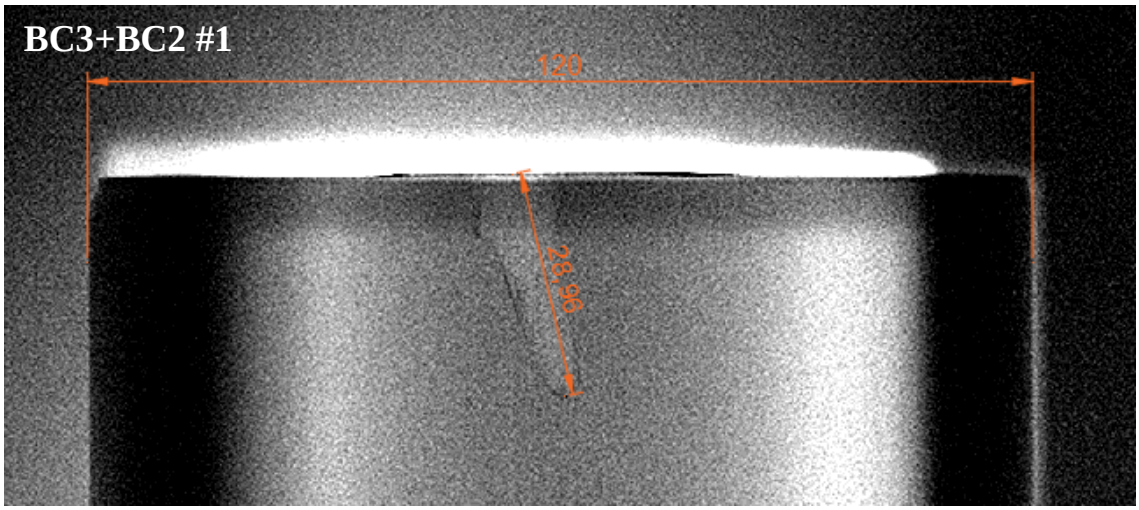
BC3+BC2 #1
120
28,96

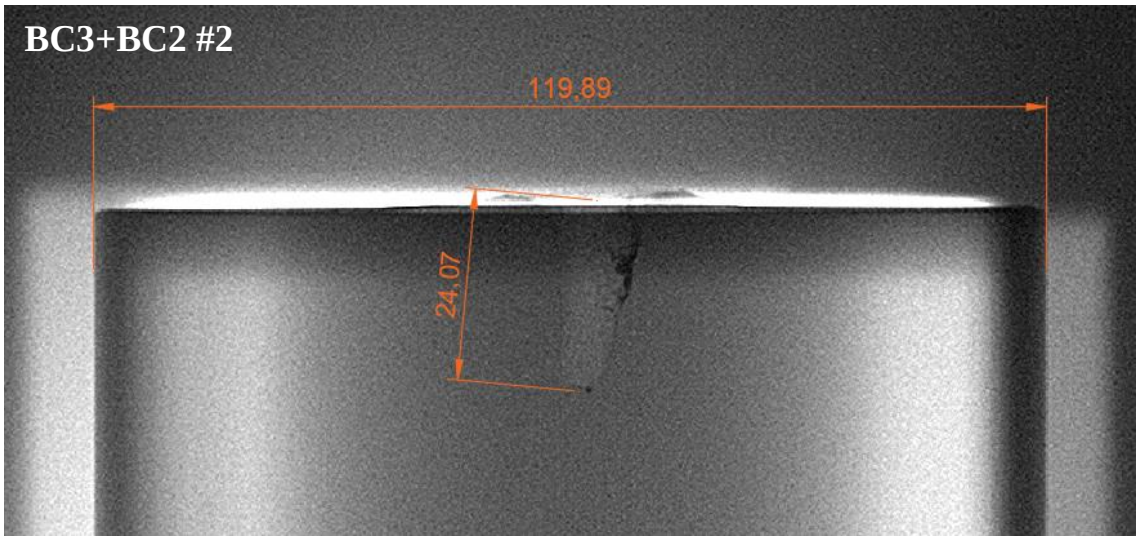
BC3+BC2 #2
119,89
24,07

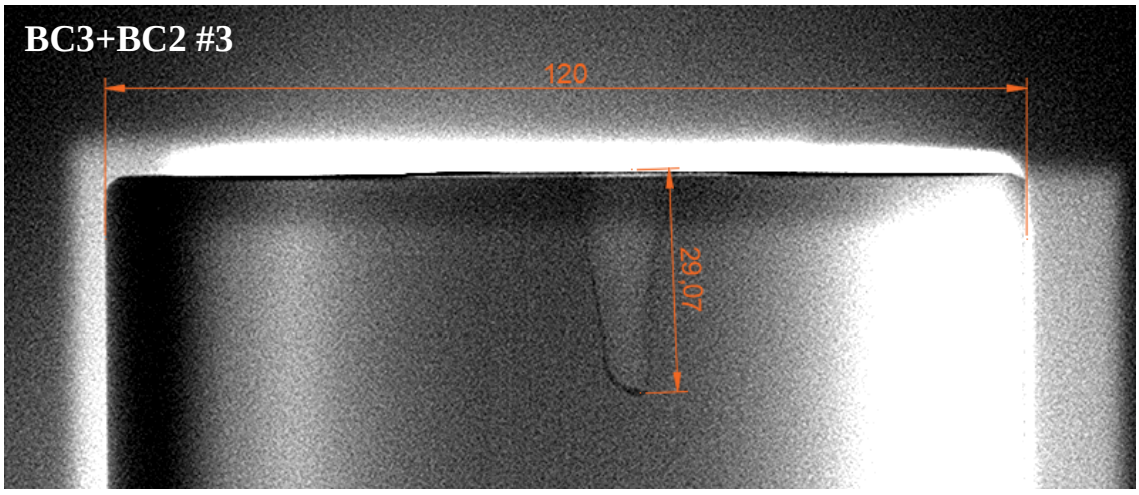
BC3+BC2 #3
120
29,07